71-12,630

WITTENBACH, Alice June, 1937-
A LIGHT AND ELECTRON MICROSCOPE STUDY OF INULEAE (COMPOSITAE) POLLEN.

The University of Oklahoma, Ph.D., 1970
Botany

University Microfilms, A XEROX Company, Ann Arbor, Michigan

THIS DISSERATION HAS BEEN MICROFILMED EXACTLY AS RECEIVED

Downloaded from SHAREOK. Persistent Handle URL: https://hdl.handle.net/11244/2983

THE UNIVERSITY OF OKLAHOMA

GRADUATE COLLEGE

A LIGHT AND ELECTRON MICROSCOPE STUDY OF INULEAE (COMPOSITAE) POLLEN

A DISSERTATION

SUBMITTED TO THE GRADUATE FACULTY

in partial fulfillment of the requirements for the

degree of

DOCTOR OF PHILOSOPHY

BY

ALICE JUNE WITTENBACH

Norman, Oklahoma

1970

A LIGHT AND ELECTRON MICROSCOPE STUDY

OF INULEAE (COMPOSITAE) POLLEN

APPROVED BY

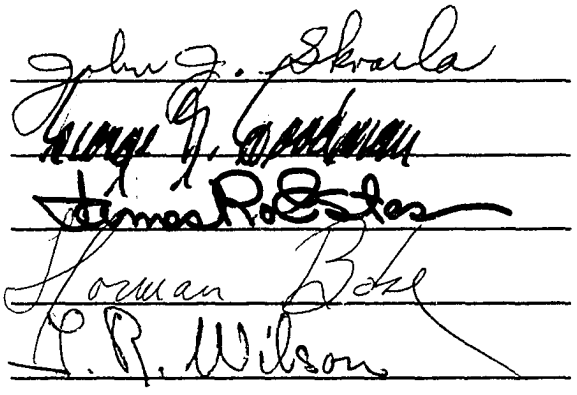

DISSERTATION COMMITTEE

To Dad

--who truly celebrated life--

in fond and grateful memory

ACKNOWLEDGEMENTS

I am especially and deeply grateful to Dr. John J. Skvarla for his suggestion of the problem, for his collection of initial pollen samples, for the EM work, and for his generous help throughout the course of this investigation.

I would also like to thank Drs. George J. Goodman, Norman H. Boke, L. R. Wilson and James R. Estes for their constructive criticism of the manuscript.

My gratitude extends further to my Congregation of Dominican Sisters for the time to spend pursuing this research, and for their combined concern and interest.

Financial support for this work was provided in part through a NSF Academic Year Institute, a departmental assistantship, and NSF grant GB-6768 to Dr. John J. Skvarla.

Finally, special thanks go to my fellow graduate students--particularly the "Herbarium Therapy Group," and to my deeply understanding and loving family and friends--for without their hope and their laughter, their humanity and their warmth, life here would not have been such a tremendous and invigorating experience.

TABLE OF CONTENTS

		Page
LIST OF TABLES		vii
LIST OF FIGURES		viii
Chapter		
I.	INTRODUCTION	1
II.	MATERIALS AND METHODS	5
III.	RESULTS	9
	Tarchonantheae	22
	Plucheineae	24
	Filagineae	33
	Gnaphalieae, Series 1	41
	Gnaphalieae, Series 2	55
	Angiantheae	72
	Relhanieae	81
	Athrixieae	88
	Inulineae	93
	Buphthalmeae	102

Page

IV. DISCUSSION 180

Light Microscopy 180

Key to Light Microscope Surface Features .. 186

Electron Microscopy 195

Key to Wall Patterns as Interpreted with Electron Microscopy 196

Techniques 215

Phylogenetic Implications 216

V. CONCLUSIONS AND SUMMARY 226

LITERATURE CITED 227

LIST OF TABLES

Table		Page
1.	Genera and species studied, with averaged specific characteristics	111-122
2.	A summary of types within subtribes as elucidated by light microscopy	191-192
3.	A summary of types within subtribes as elucidated by electron microscopy	199-200

LIST OF FIGURES

Figure		Page
1.	Terminology applied to light microscope characteristics	11
2.	Non-caveate exines	12-13
3.	Caveate exines	12-13
4.	Basic stratification layers in Compositae pollen walls	15
5.	Variations in exines without caveae	17-18
6.	Variations in exines with caveae	19-21
7-25		123-124
26-36		125-126
37-48		127-128
49-68		129-130
69-88		131-132
89-106		133-134
107-124		135-136
126-133		137-138
134-152		139-140
153-170		141-142
171-182		143-144

Figure	Page
183-202	145-146
203-222	147-148
223-234	149-150
235-248	151-152
249-259	153-154
260-265	156-157
266-270	158-159
271-280	160-162
281-289	163-165
290-300	166-168
301-308	169-171
309-316	172-174
317-323	175-176
324-331	177-179

A LIGHT AND ELECTRON MICROSCOPE STUDY OF INULEAE (COMPOSITAE) POLLEN

CHAPTER I

INTRODUCTION

The tribe Inuleae (Compositae) is cosmopolitan. Approximately 2600 species are distributed into 175 genera, many of which are monotypic (Bentham, 1873; Hoffman, 1897; deDalle Torre and Harms, 1907; Willis, 1957, 1966). It is comprised mainly of herbs and shrubs, along with climbers, and, more rarely, trees (Humbert, 1923). The tribes (characterized by the double character of style branches without terminal appendages, and of tailed anthers) is divided into nine fairly distinct subtribes: Tarchonantheae, Plucheineae, Filagineae, Gnaphalieae, Angiantheae, Relhanieae, Athrixieae, Inulineae, and Bupthalmeae (Bentham, 1873; Hoffman, 1897). Of these, the Plucheineae, Filagineae, and Gnaphalieae, though most numerous in the Old World, range also over the New; the remaining six are limited to the Old World. The Tarchonantheae and Relhanieae are exclusively South African, the Angiantheae almost exclusively Australian, the Athrixieae South African

with one or two northern species, the Inulineae and Buphthalmeae African, European, and more sparingly Asiatic (Bentham, 1873).

Since composite pollen was first investigated by Fischer (1890) a number of studies have appeared. The family became best known through the extensive investigations of Wodehouse (1926-1935), which emphasized morphologic and phylogenetic trends primarily concerned with the taxonomy of hayfever groups. Wodehouse emphasized the great diversity of pollen forms occurring in the family and recognized the basic tricolporate character of the pollen. Inuleae were not extensively studied by Wodehouse; rather, they were mentioned as indicating a reduction of spine length. The tendency toward spine reduction was considered a character denoting advancement in the family (Wodehouse, 1928). Erdtman (1952) surveyed 400 species from 155 composite genera; information relative to Inuleae was restricted to 4 genera and 6 species and consisted of a discussion of size relationships and drawings of aperture and wall patterns, as well as spine types. The investigations of both Wodehouse and Erdtman were accomplished with light microscopy of whole pollen mounts.

Individual groups of Compositae have received detailed attention by Pausinger-Frankenburg (1951) on Cichorieae, Wagenitz (1955) on Centaurea (Cynareae) and by Carlquist (1957a, 1963) in a series of studies on Fitchia (Heliantheae), and Mutisieae (1957b).

In recent years Stix (1960) broadly surveyed the entire Compositae.

Her approach had an advantage over previous work in that methacrylate embedded sections of pollen 0.5-1μ thick were examined with ultraviolet light. This work served to indicate that highly refined variations in pollen wall morphology were apparent even though external morphology appeared similar. Of 225 species investigated approximately 45 pollen wall patterns were distinguished. Thirteen genera of Inuleae were included in this study and 3 pollen types were established. Stix's general conclusions can be summarized as follows: (1) exine stratification is a constant character and is important in the separation and classification of pollen wall types; (2) a pollen type may characterize tribes; more commonly, a pollen type may be limited to several subtribes, although, rarely, it may delimit a single subtribe or genus; (3) neither the apertures, nor the shape and size, which vary greatly with a species are considered as useful in delimiting pollen wall types.

Phase-contrast examination of 0.5-1μ sections of Inulinae and Buphthalminae pollen by Leins (1969) indicate a profusion of pollen types. For the Inulinae, 13 pollen types were found; for the Buphthalminae, 10. These types were differentiated by the criteria of Stix (1960) but little correlation was evident between the two studies.

Electron microscopy of 1/40μ sectioned pollen walls has been carried out in a series of studies by Skvarla and Larson (1965a, 1965b) and by Skvarla and Turner (1966a, 1966b, 1969). These studies, which are considered to be extensions of the light microscope work, have the

advantage of permitting more precise interpretation of the wall morphology. Although the ultrastructural results tentatively substantiate the morphological diversity outlined by Stix and Leins, considerably fewer pollen types have been recognized. The reason is that it appears more accurate to consider small variations as expanding the morphological parameters rather than as evidence for establishing new types (Skvarla and Turner, 1966b). In depth EM studies in the Inuleae have yet to be made. However, the four genera examined (Skvarla and Turner, 1966b), indicate that there are subtle morphological differences which can only be resolved by eiectron microscopy. The present study is directed toward this end. In this study, in which both light and electron microscope techniques are incorporated and their respective observations correlated, basic questions considered were: (1) can the tribe and its subtribes be separated on the basis of pollen morphology in the same way they are separated by floral characteristics; (2) can various genera and species be separated; (3) can evidence be found for intraspecific and interspecific variation; and (4) what information can Inuleae pollen morphology bring to bear on phylogeny within the Compositae?

CHAPTER II

MATERIALS AND METHODS

Pollen collections were made through the cooperation of several herbaria: Bebb Herbarium of the University of Oklahoma, Norman, Oklahoma (OKL), East African Herbarium, Nairobi, Kenya, East Africa (EA), Michigan State University Herbarium, East Lansing, Michingan (MSC), Missouri Botanical Garden, St. Louis, Missouri (MO), New York Botanical Garden, New York, New York (NY), U.S. National Museum (Dept. of Botany), Washington, D. C. (US), University of Texas Herbarium, Austin, Texas (TEX), and the private collection of Dr. B. L. Turner at the University of Texas (BLT). For purposes of citation of specific material studied the letters designating the particular institution are used. It should be noted that pollen was removed from herbarium sheets which were identified by their respective collectors. Each specimen was not checked for correct identification as a part of this study.

Buds containing mature pollen were removed from herbarium sheets and placed in appropriately labeled glassine envelopes. Subsequently, the buds were transferred to tapered test tubes and acetolyzed according to the method of Erdtman (1960). The residue (viz., pollen

and insoluble bud debris) was passed through 1000-mesh copper screens in order to remove as much extraneous material as possible. The sample was then divided into portions for light and electron microscope study.

For light microscopy a portion of the pollen concentrate was rinsed in distilled water, pipetted (using disposable Pasteur pipettes) onto small drops of glycerine jelly on glass microscope number 0 or 1 coverslips which were then inverted onto glass microscope slides (adapted from Wilson and Goodman, 1964). The slides were placed on a drying plate until the glycerine jelly was water free, and the coverslips were then sealed with clear nail polish. The remaining pollen was stored in 10% glacial acetic acid for future reference. All pollen specimens are stored in the Samuel Roberts Noble laboratory of electron science at the University of Oklahoma. In addition, slides of specimens from each herbarium are on file at the respective institutions, and the whole plants sent from East Africa are now in the Bebb Herbarium at the University of Oklahoma. Slides were examined in transmitted light with a Leitz Ortholux microscope. Size measurements were made on 10 grains in the polar view (Fig. 1), with the exception of spine measurements, for which equatorial views were used. Photomicrographs were made under oil immersion with a 100x objective lens on Kodak Panatomic-X film.

In an effort to determine the most effective and efficient processing

techniques for electron microscopy the acetolyzed pollen was treated in a variety of ways. Some of the samples were stained in 1-2% solutions of OsO_4 buffered in either phosphate or cacodylate at pH's ranging 7.0-7.4. Staining time ranged from 2-8 hrs and staining was done at room temperature. Pollen was then given several rinses in distilled water followed by centrifugation until all traces of stain were removed. A secondary stain, 0.5% aqueous uranyl acetate, was applied for 2-8 hrs under room temperature conditions. Following removal of the stain by water rinses and centrifugation, a small quantity of warmed, viscous 1.5% agar (Difco) was added to the test tube. The pollen and agar were quickly stirred with a wood applicator and then immediately centrifuged (Skvarla, 1966). After approximately 5 min of centrifugation the agar solidified and the pellet was then removed from the test tube. Thin slices were cut perpendicular to the tip with a razor and then diced into small cubes. Before allowing the cubes to become dehydrated they were placed in 70% ethanol. This solution can be used as a "holding stage" for forthcoming embedding or it can be considered as the first step in dehydration. In the latter event the 70% ethanol is decanted after 15 min and replaced by 2 successive 15 min changes of absolute ethanol. The pollen is then rinsed in transitional solvent, either propylene oxide or reagent grade acetone (2 treatments for 15 min each) and embedded through graded concentrations in Araldite-Epon resin (Skvarla, 1966).

Variations in the above technique involved both fixatives and

embedding. Some acetolyzed exines were not treated with OsO_4 or uranyl acetate stains. Instead, they were incorporated directly into agar and processed as already described. The second variation involves drastic shortening of the embedding schedule by omission of ethanol dehydration and reduction of embedding from 3 steps to 1 (Skvarla and Kelley, 1968).

Thin sectioning of polymerized Araldite-Epon resin was done with diamond knives on a Porter-Blum MT-2 ultramicrotome (Skvarla and Pyle, 1968). Sections approximately 250-600 Å thick, estimated from interference colors, (Peachey, 1958) were collected on uncoated 300-mesh copper grids (Skvarla and Pyle, 1968). Various stains were employed to enhance inherent exine contrast under the electron beam. For exines previously stained with OsO_4 and uranyl acetate this consisted of a 5-10 min application of lead citrate (Venable and Coggeshall, 1965). For exines not previously stained, one of the following treatments was applied: (1) uranyl acetate-lead citrate, (2) OsO_4. Exines were examined with a Philips electron microscope model 200. Thin foil apertures of 60 or 20u were used with an accelerating voltage of 60KV. Photographs were made with 35mm Kodak Fine Grain Positive Release film.

CHAPTER III

RESULTS

Whole mounts of Inuleae pollen examined by light microscopy can be generally described as highly variable in size, radially symmetrical and isopolar, oblate-spheroidal in shape, usually tricolporate with variable pore diameters, and with an exine ornamented with elongate or markedly reduced spines. In median-optical section the overwhelming majority of taxa show separations termed "caveae", (Iversen and Troels-Smith, 1950) between wall layers in mesocolpial areas which impart a bladder-like appearance to the pollen. Although the above description characterizes pollen of the Inuleae, considerable latitude exists in the morphology. Therefore, light microscope analyses are presented for each taxon studied. The characters considered are (1) size, (2) symmetry, (3) polarity, (4) shape, (5) aperture configurations and dimensions, (6) sculptural patterns and (7) presence or absence of caveae.

Taxa descriptions include the range of size variability; size variations along the polar axis (P) are represented in the first number set, the second notes the equatorial axis (E). Specific averages are not included in the text unless the variation indicates differences in size not referable to

harmomegathi (Wodehouse, 1935), chemical treatment or embedding media (Cushing, 1961; Faegri-Iversen, 1964), and, as such, is indicative of interspecific or intraspecific variation. The averages for each sample, computed from the measurement of the axes, and the basis for placing the pollen in one of the shape classes (Erdtman, 1952, are listed in Table 1 (pp. 111-122) as well as average sizes for pore and spine characteristics. Genera described are grouped according to the 9 subtribes outlined by Bentham, 1873. When more than one collection is listed, or more than one species, the description takes this into account; in those cases where significant intra- or interspecific variation occurs descriptions are accordingly supplemented. Figure 1 illustrates the basic descriptive terms. Terminology essentially follows Erdtman, 1952. Specific descriptive terms have also been adapted from Dahl (1952), Faegri (1956), Stix (1960), Stuchlik (1967) and Leins (1969) in an effort to promote a uniformity of light microscope analysis.

Pollen types are arranged in plates to illustrate common morphological characteristics to be discussed later. Figure 2 and Fig. 3 summarize exine surface patterns discernible from light microscopy. Magnification for all grains pictured is x3200.

Immediately following the light microscope descriptions, observations are presented from electron microscopy. Since a considerable amount of data is available on composite ultrastructure (Skvarla and Turner, 1966b) an attempt has been made to utilize this in order to obtain

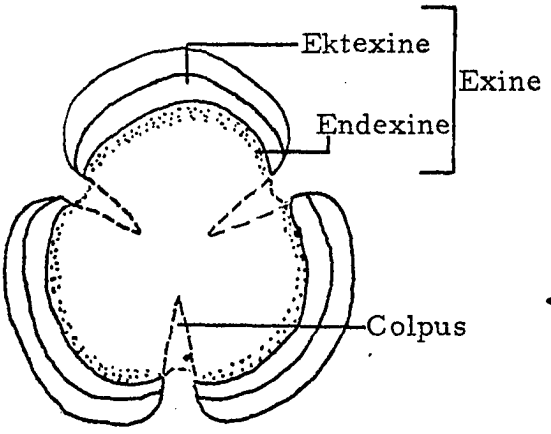

Polar View: without cavus, and with smooth exine surface

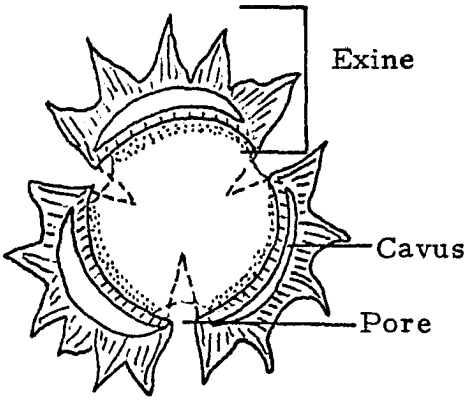

Polar View: with cavus, and with spinose exine

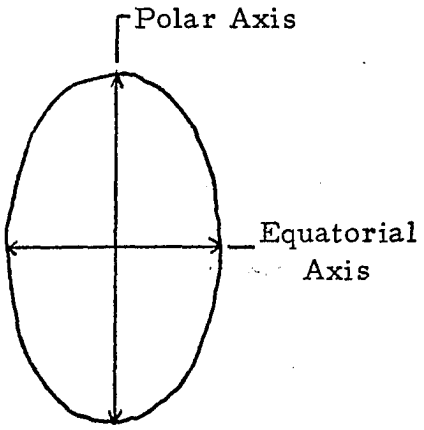

Equatorial View

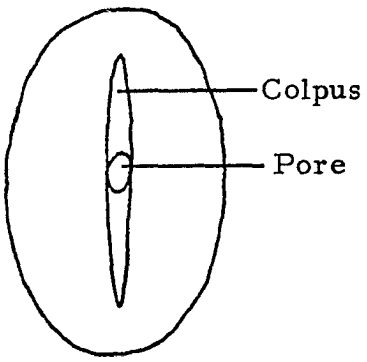

Equatorial View

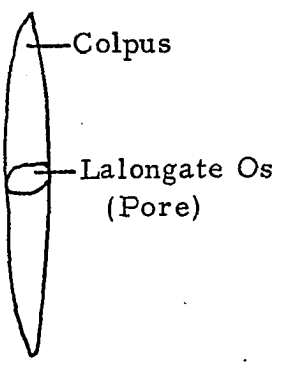

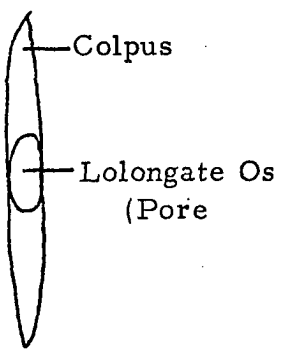

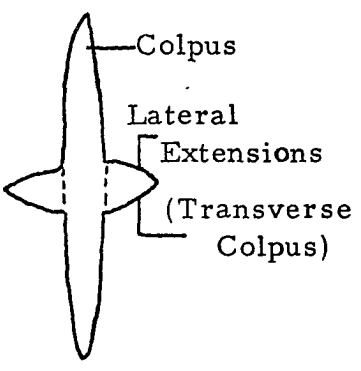

Fig. 1 Terminology applied to light microscope characteristics

Figure 2. Non-caveate exines. Fig. 2A depicts a smooth to subspinulose exine surface. Fig. 2B shows a spinose (2.5-3.0u) exine surface, and Fig. 2C shows a non-caveate exine with the longest spines (3+u).

Figure 3. Caveate exines. Fig. 3A depicts an exine surface with spinules 1+ or less, densely massed. Fig. 3B is spinulose, 1+-3.0u, the spines widely spaced. Fig. 3C is similar to Fig. 3B, with the spines densely massed. Fig. 3D is spinose, 3+-4.5u, not dense. Fig. 3E shows the same spine length, the spines having blunted tips, and wide bases. Fig. 3G is densely spinose (spines 4.5-6.0u), the spines with narrow bases. Fig. 3H represents the same spine length as Fig. 3G, the spines having wide bases. Fig. 3I depicts wide based, bluntly tipped spines. Fig. 3J has narrow based conical spines. Fig. 3K depicts a wide based, inverted funnelform spine type which is finely tipped. Fig. 3L has wide bases and gradually tapering spines with fine tips.



Figure 2. Non-caveate exines.

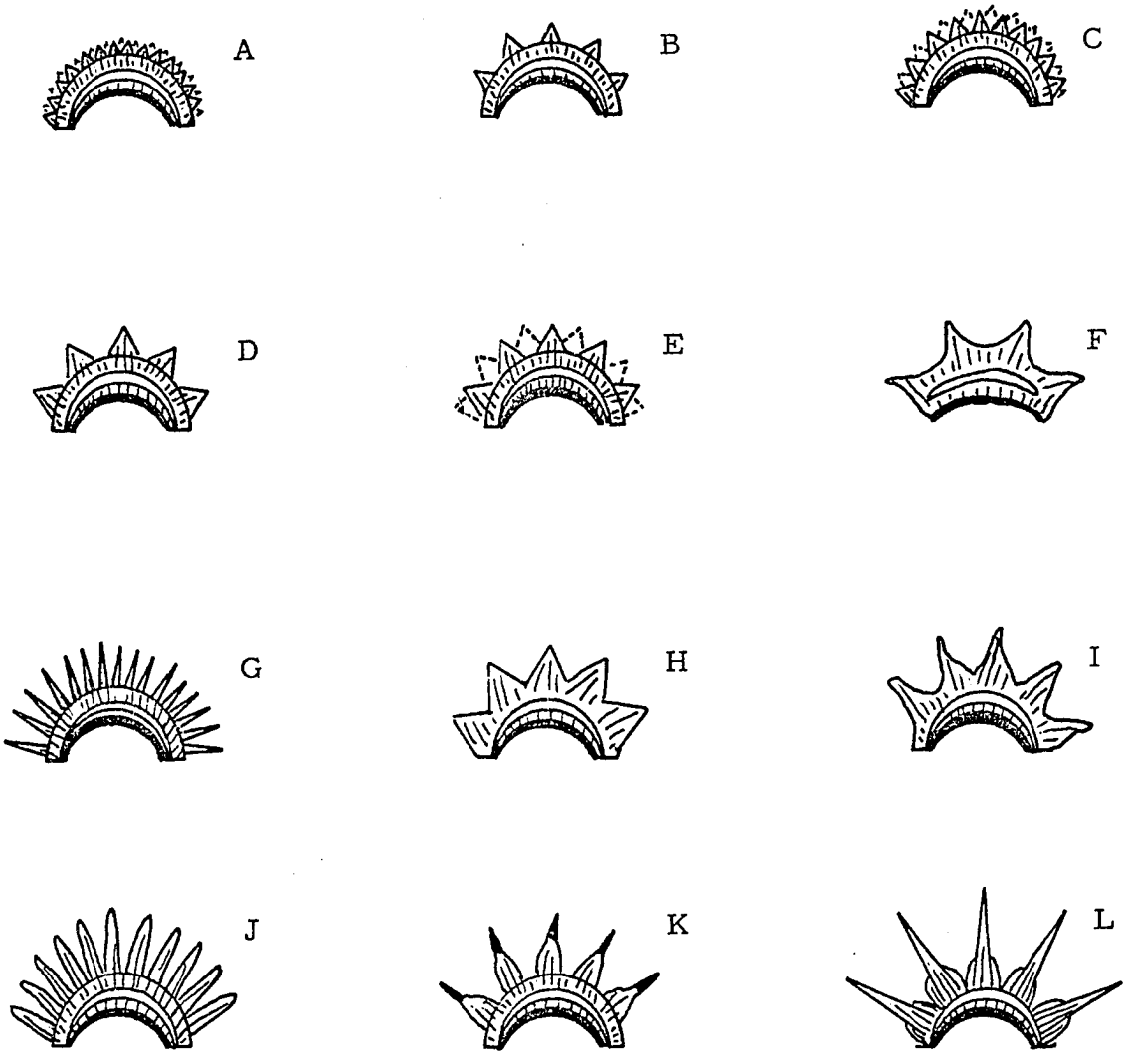

Figure 3. Caveate exines.

a consistency of interpretation and better integration of observations. The current studies indicate that although a variety of pollen wall patterns exist at the ultrastructural level, all have the common feature of a bilayered electron image. The least complex layer morphologically is generally unipartite, varies in degree of thickness and homogeneity, is disrupted along its inner margin, is less dense to electrons, and is always located at the inside of the pollen wall. This layer is the endexine (Faegri, 1956). The second, more complex layer, the ektexine (Faegri, 1956), consists of several units. The first unit, the foot layer, is directly above the endexine and in apposition with it; occasionally, fine lamellae are interbedded with endexine. In individual taxa the foot layer is of uniform thickness but among taxa and subtribes it is highly variable. This variability is useful in taxonomic distinctions. When compared with the endexine the thickness ratio can be in the order of 1:8, 1:2 or 1:1. Perpendicular extensions from the foot layer constitute the second unit, the columellae. This unit is the most variable and, therefore, of paramount importance in morphological distinctions. Columellae can range in length and width among taxa; terminal extremities (both basal and distal) can be straight and sharp, rounded or club-shaped, or more commonly forked or bifurcate. The latter are often highly ramified. When forked distally it is termed digitate (Iversen and Troels-Smith, 1950), when forked basally, it is termed conjunctate. Lateral branches generally project from the bifurcate columellae. These branches also can

project along midlengths of columellae. Fusion of the lateral branches basally results in the formation of a layer termed supporting membrane (Stix, 1960) which is considered part of the sexine (Stix, 1960) or columellae-foot layer (Skvarla and Turner, 1966b); fusion along midlengths forms the internal tectum (Skvarla and Turner, 1966b) and fusion distally forms the tectum (Faegri, 1956). The tectum also can result from fusions of the rounded or club-shaped distal ends. As a rule tecta are often perforated or broken, depending upon degree of fusion of lateral branches. Spinules of varying sizes protrude from the tectum. Text-figure 4 summarizes the more salient exine features described above.

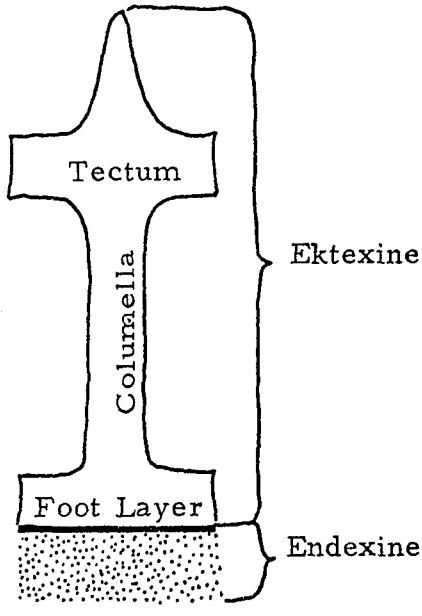

Fig. 4 Basic stratification layers in Compositae pollen walls.

Columellae and tectum are further characterized in many taxa by the presence of holes, termed internal foramina (Skvarla and Larson, 1965a) and which are recognizable only by electron microscopy. In profile view

they can range from roughly circular to highly elongate and occasionally are filled with electron dense particles. Internal foramina can be so common that they impart a honeycomb appearance to columellae and tectum or so sparse that they are difficult, if not impossible to differentiate from normal biological effects of oxidation or sample processing. Generally, internal foramina occur in columellae, however, they are also common in some taxa in the tectum. While they can occur exclusively in the columellae, the converse is not so.

Caveae are seen to occur between columellae and foot layer along intercolpial (mesocolpial) areas. At the colpus margins columellae and foot layer are united. Caveae can vary from narrow to broad but this character is difficult to accurately determine due to possible disturbances during processing.

The above description, like that given for light microscopy, is generalized and the variations of patterns can be subdivided into two major categories: (1) those exines lacking caveae, and (2) those possessing caveae.

1. Exines without caveae. In this category differences in exine patterns are distinguished principally on the basis of variations in columellae morphology and involve (1) type of lateral branching and (2) formation of a layer or layers of internal tecta. These features, as well as changes in footlayer: endexine ratios are combined to form the three distinctive variations in wall patterns as depicted in text-figure 5. No

Figure 5. Exines without caveae. In Fig. 5A the endexine is thick (approximately equal to the foot layer) and mainly homogeneous in composition. Extending from the foot layer are thick columellae which, at their upward extremity, become digitate, with resultant lateral branches. These form a thick internal tectum. Short, thickened columellae extend from the internal tectum to form a thick, imperforate "outer" tectum.

Figure 5B has a foot layer: endexine ration of 1:1, but it is thinner than that shown in Fig. 5A. The lateral branches are fine and form layers of internal tecta. A second layer of columellae, somewhat longer and and narrower than depicted in Fig. 5A, extends from the internal tecta to form a thin, slightly perforate "outer" tectum.

Figure 5C has a foot layer: endexine ratio of approximately 2:1. While thickened columellae extend the entire length of the ektexine and form a thin, nearly imperforate "outer" tectum, fine lateral branches extend from the upper 2/3 of the columellae to form multiple layers of internal tecta.

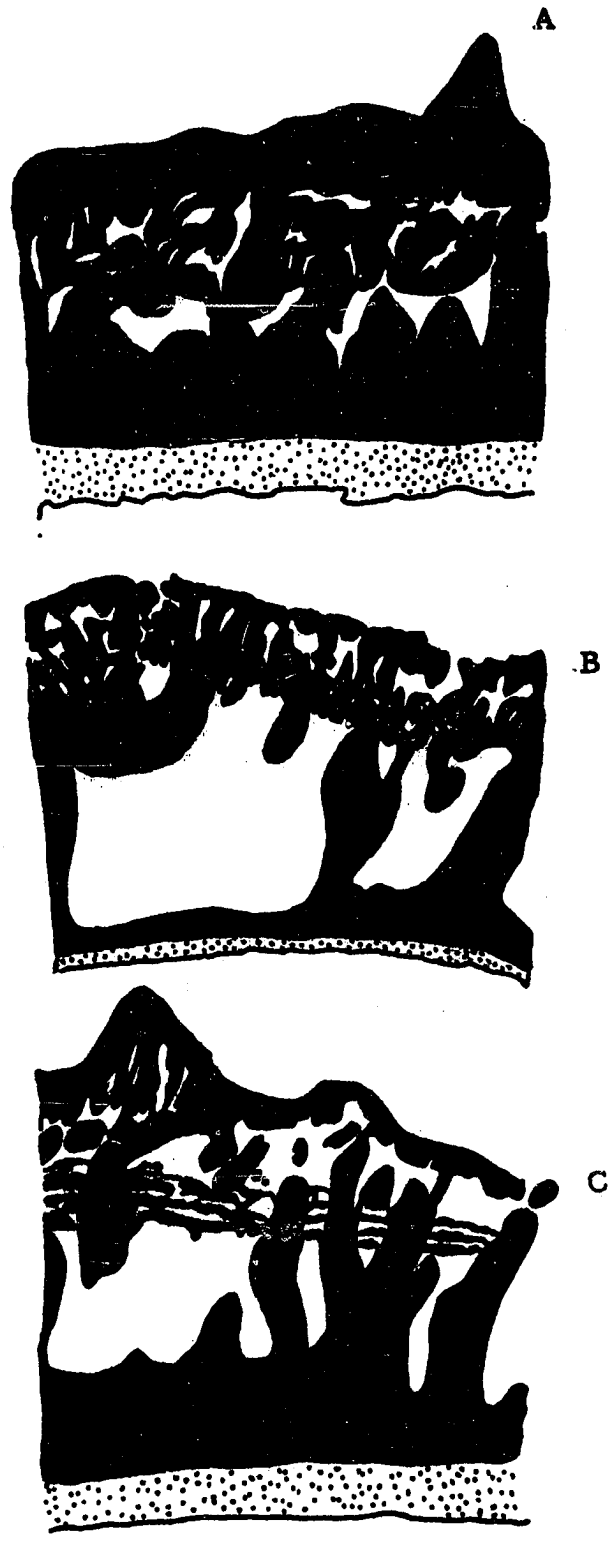

Fig. 5 Variations in exines without caveae.

Figure 6. Variations in exines with caveae. In Fig. 6A irregular perforations, possibly vestiges of internal formaina, are scattered throughout the single-layered columellae. Columellar bases are connected, while the tectum is perforate. The footlayer: endexine ratio is approximately 1:4, the endexine being somewhat disrupted.

Figure 6B is similar to Fig. 6A with small, irregularly shaped internal foramina scattered throughout the entire structure.

Figures 6C through 6E depict double-layered columellae patterns with internal tecta, and endexines which are disrupted throughout their entirety. More specifically, in Fig. 6C the lower 2/3 of the columellae is complexly ramified and only intermittently fused at the base, while the upper 1/3 is less complex, capped by a thick, perforate tectum. Internal foramina are difficult to establish with certainty.

In Fig. 6D the basal columellae vary from 1/2 to 2/3 the total columellae pattern; the bases are thick, and the thin tectum is perforate. Irregularly shaped internal foramina are common in columellae and tectum.

Figure 6E depicts a pattern in which the lower 1/2 of the columellae are complexly ramified, the columellae are thin, the tectum is perforate and the internal foramina are extremely elongate.

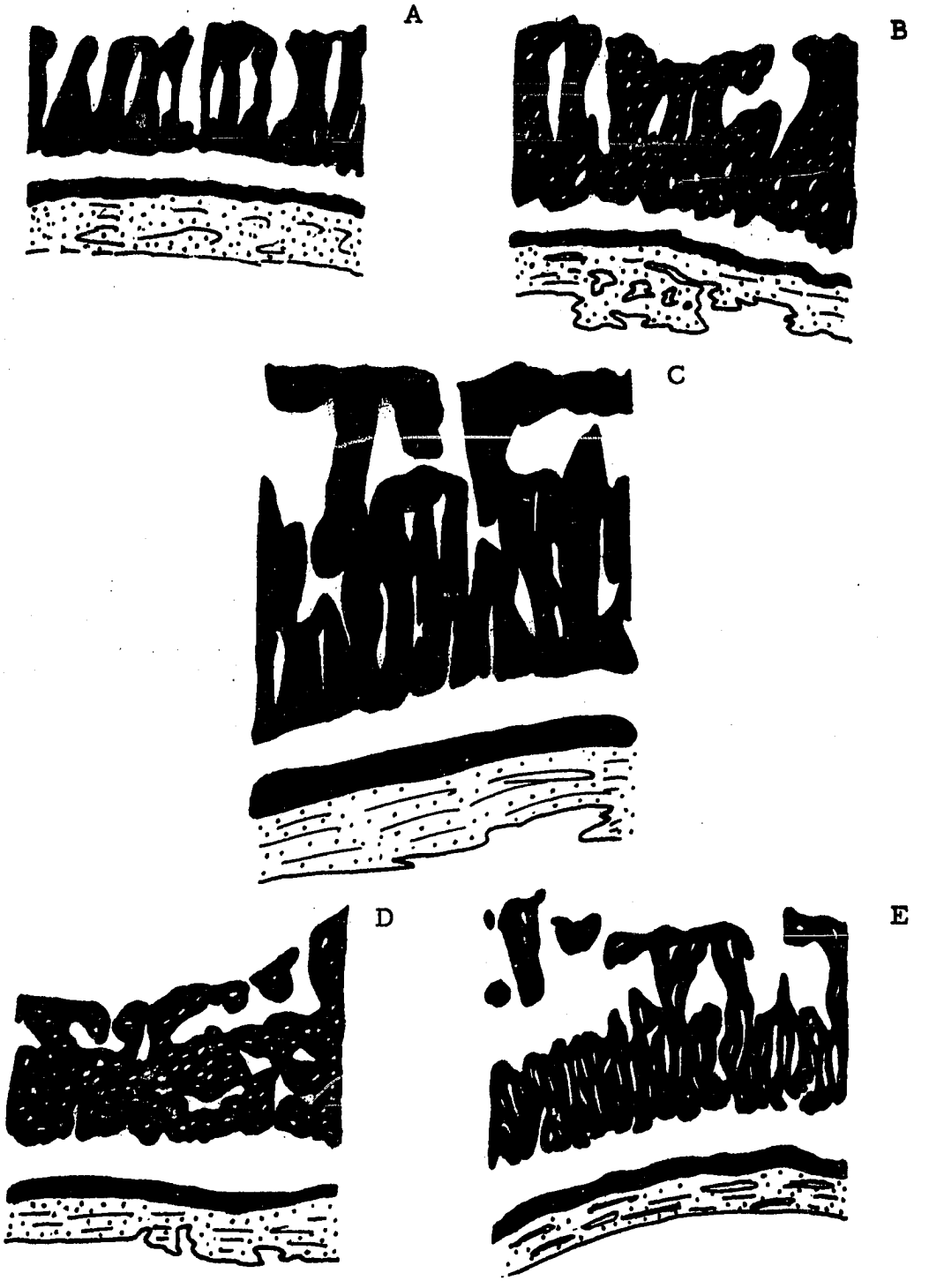

Fig. 6 Variations in exines with caveae.

internal foramina are present.

2. Exines with caveae. Inuleae are most commonly represented by exines in this category and five basic variations (Fig. 6) are in evidence. The primary variation again centers about columellae morphology and involves (1) the changes from a simple rod to complex ramifications, and (2) the presence or absence of foramina. These features, as well as changes in foot layer: endexine ratios combine to form the variation noted.

I. TARCHONANTHEAE

This subtribe consists of two genera and approximately 30 species.

Brachylaena R. Brown Fig. 7-16, 18.

Grains radially symmetrical and isopolar, prolate-spheroidal to subprolate, 24-32 x 23-30μ; tricolporate, more rarely, tetracolporate; ora 2-4μ maximum diameter when conspicuous in equatorial view, congruent with colpi, to not well defined; colpi equidistant in diameter the full length of the polar axis, thin-margined, ± distinctly constricted in equatorial view, to less elongate; exine surface: subspinulose, almost knobby, to a smooth or finely granular surface; caveae not present.

Interspecific variation. Two species (B. elliptica and B. hutchinsii have a predominant tetracolporate morphology, although both also include the tricolporate form. B. hutchinsii is granular as opposed to the sub-

spinulose condition of the remaining species.

Intraspecific variation. B. hutchinsii and B. nereifolia display many grains with a short colpus, as opposed to the predominant form which spans the full length of the polar axis.

Electron microscopy (Fig. 260-262, 264). B. elliptica, B. nereifolia, and B. rotundata are similar to Fig. 5A, but with the exception of a thinner, perforate tectum. B. hutchinsii is similar to Fig. 5A.

Species examined. B. discolor DC. (US #2137819); B. elliptica Less. (US #924); B. hutchinsii Hutch. (EA #4); B. hutchinsii Hutch. (US #1373483); B. nereifolia R. Br. (US #1579501); B. rhodesiana S. Moore (US); B. rotundata S. Moore (MO #1712310); B. transvaalensis Hutch. ex Phil. et Schw. (US #2272123); B. uniflora Harv. (US #633396).

Tarchonanthus L. Fig. 17, 19-25.

Grains radially symmetrical and isopolar, prolate-spheroidal, 24-33 x 21-30μ; tricolporate; ora circular to rectangular in outline (2-4μ maximum diameter) when conspicuous in equatorial view, congruent with colpi or with ± pointed lateral extensions, to not well-defined; colpi extending total length of the polar axis ± distinctly constricted at equator, to less elongate; exine surface subspinulose (almost knobby) to smooth or very finely granular; caveae not present.

Intraspecific variation. T. camphoratus has both types of colpi

present. All three species have lalongate ora, either congruent with the colpi, or having lateral extensions ± pointed.

Electron microscopy (Fig. 263, 265). T. camphoratus and T. angustissimus are similar to Fig. 5A except that columellae are longer and tectum is thinner and more perforate.

Species examined. T. angustissimus DC. (US #1170025); T. camphoratus L. (MO # 1646623); T. camphoratus L. (EA #9047, US #2247074, US #2247291); T. minor Less. (NY).

II. PLUCHEINEAE

This subtribe consists of approximately twenty genera and 250 species.

Blumea DC. Fig. 72; 191, 202.

Grains radially symmetrical and isopolar, oblate-spheroidal, 22-34 x 23-34μ; tricolporate; ora lalongate (4-5μ maximum diameter) with lateral extensions when conspicuous in equatorial view, to not well defined; colpi wide and smoothly outlined, extending full length of the polar axis, ± distinctly constricted at equator; exine surface: spinose, spines 3-5μ in length; caveae present.

Interspecific variation. Spines in B. ambigua are shorter (3μ), narrower, having an inverted funnelform shape, and more crowded than B. laciniata and B. mollis. Spines in the latter species are longer

(4-5μ), with a wider base, more triangular in shape, and much less dense in number.

Electron microscopy (Fig. 273). B. mollis is similar to Fig. 6A but has a highly disrupted endexine; B. laciniata is similar to Fig. 6A.

Species examined. B. ambigua DC. (MSC #80617); B. laciniata (Roxb.) DC. (MO #885362); B. mollis (G. Don) Merr. (MSC #80619).

Denekia Thunb. Fig. 134, 145.

Grains radially symmetrical and isopolar, oblate-spheroidal, 22-26 x 23-27μ; tricolporate; ora lalongate (3μ maximum diameter) with lateral extensions; colpi wide, smoothly outlined, extending full length of the polar axis, ± distinctly constricted at the equator; exine surface: spinose, spines 3μ in length; short, wide (3μ) base, with a finely pointed tip; dense; caveae present.

Electron microscopy. D. copensis is similar to Fig. 6A, although the presence or absence of foramina is difficult to establish.

Species examined. D. copensis Thunb. (MO #1751254).

Epaltes Cass. Fig. 108.

Grains radially symmetrical and isopolar, oblate-spheroidal, 17-27 x 19-27μ; tricolporate; ora lalongate, rectangular in outline (3-5μ maximum diameter), with lateral extensions when conspicuous in equatorial view, to not well defined; colpi wide, smoothly outlined, extending full

length of the polar axis, ± constricted at the equator; exine pattern: spinulose (3μ in length), to spinose, spines 3-4μ in length, wide based, gradually tapering to a slightly obtuse tip; not dense; caveae present.

Electron microscopy. E. mexicana is similar to Fig. 6A, with no internal foramina.

Species examined. E. cunninghamii (Hook.) Benth. (NY); E. mexicana Less. (MO #778746).

Laggera Sch. Bip. ex Hochst. Fig. 198, 204.

Grains radially symmetrical and isopolar, oblate-spheroidal, 24-32 x 24-34μ; tricolporate, ora lalongate, rectangular to elliptical in outline (5-8μ maximum diameter), with lateral extensions and thickened margins; colpi wide, thin-margined, extending full length of the polar axis, ± constricted at the equator, appearing less deeply sunken than in other grains; exine surface: spinose, spines 4-5μ in length, long, wide-based, tapering to a finely rounded apex; not dense; caveae present.

Intraspecific variation. Ora in some grains of L. alata are very large, circular to irregular in outline, have thicker margins, appearing to be either without colpi or to be reduced colpi.

Electron microscopy (Fig. 280). L. alata is similar to Fig. 6A.

Species examined. L. alata Sch. Bip. (MO #1760160); L. brevipes Oliv. et Hiern. (NY).

Nanothamnus T. Thoms. Fig. 44-46.

Grains radially symmetrical and isopolar, oblate-spheroidal, 32-37 x 34-40μ; tricolporate; ora lalongate, rectangular to elliptical in outline, 5-7μ maximum diameter), congruent with colpi, margins so thickened as to make the total structure appear raised in equatorial view; colpi very wide, thin margined, extending full length of the polar axis, ± constricted at the equator, appearing less deeply sunken than in other grains; exine surface: spinose, spines 5-7μ in length, wide-based, gradually tapering to a finely rounded apex, not dense; caveae present.

Electron microscopy. N. sericeus is similar to Fig. 6A, without internal foramina.

Species examined. N. sericeus T. Thoms. (MO).

Pluchea Cass. Fig. 187, 211, 221.

Grains radially symmetrical and isopolar, oblate-spheroidal, 26-32 x 26-34μ; tricolporate, ora lalongate, rectangular to elliptical to slit-like in outline (2.5-6μ maximum diameter), lateral extensions ± pointed, margins thickened; colpi wide to very narrow, thin-margined, extending the full length of the polar axis, ± distinctly constricted in equatorial view to less elongate, appearing deeply sunken in some grains to superficial or almost lacking in others; exine surface: spinose 3.5-6μ in length, wide based, gradually tapering to a finely rounded apex, to narrow based, thin, solid, not dense; caveae present.

Interspecific variation. Only very narrow, deeply sunken colpi

appear in P. odorata, as does the narrow based, thin, spine type.

Intraspecific variation. Ora vary as described in all three species examined. Colpi vary as above in P. camphorata and P. foetida.

Electron microscopy. P. camphorata is similar to Fig. 6A with no internal foramina.

Species examined. P. camphorata (L.) DC. (OKL); P. foetida (L.) DC. (OKL); P. odorata Cass. (OKL #17111).

Pterigeron Gray Fig. 237.

Grains radially symmetrical and isopolar, oblate-spheroidal, 28-35 x 28-36μ; tricolporate; ora lalongate, elliptical in outline (2.5-4μ maximum diameter), equatorial margins thickened, when conspicuous in equatorial view, to not well defined; colpi wide, extending full length of the polar axis, ± distinctly constricted at the equator, deeply sunken; exine surface: spinose, spines 4.5-6μ in length, wide based, tapering to a finely rounded tip; caveae present.

Electron microscopy. P. liatroides is similar to Fig. 6A.

Species examined. P. liatroides Benth. (BLT #5385).

Pterocaulon Ell. Fig. 109, 114; 139; 242.

Grains radially symmetrical and isopolar, oblate-spheroidal to prolate spheroidal, 22-31 x 22-31μ; tricolporate; ora lalongate, rectangular to slit-like in outline (3-4μ maximum diameter), lateral extensions

± pointed, margins thickened when conspicuous in equatorial view, to not well defined; colpi mostly narrow, thin margined, ± distinctly constricted at the equator, deeply sunken, to wide, extending full length of the polar axis, ± distinctly constricted in the equatorial view, more superficial in some grains; exine surface: spinose, spines 2.5-4μ in length, equilaterally triangular in outline, with blunt apex, to spines 4-6μ in length, conical, with blunt apex; caveae present.

Interspecific variation. P. interruptum has the narrow colpus type only; P. sphacelatum and P. virgatum have the variation described above; P. undulatum has the wide type only. P. undulatum and P. virgatum have longer, more conical spines, whereas the other two species have the shorter, more triangular form.

Electron microscopy. P. virgatum is similar to Fig. 6A.

Species examined. P. interruptum DC. (MSC #140245); P. sphacelatum (Labill.) Benth. et Hook. (MSC #187662. MSC #214577); P. undulatum (Walt) C. Mohr (OKL); P. virgatum (L.) DC. (OKL #46357).

Rhodogeron Griseb. Fig. 240-241.

Grains radially symmetrical and isopolar, oblate-spheroidal, 33-40 x 34-42μ; tricolporate; ora lalongate, rectangular to elliptical in outline (4-6μ maximum diameter), either congruent with colpi or with lateral extensions ± pointed, margins thickened; colpi wide at os region, immediately tapering to a very narrow constriction, becoming pointed in equa-

torial view, thin margined, deeply sunken; exine surface: spinose, spines 5-6.5μ in length, wide based, tapering becoming conical with blunt apex; not dense; caveae present.

Electron microscopy. R. coronopifolius is similar to Fig. 6A with two exceptions: thinner columellae, and a highly disrupted endexine.

Species examined. R. coronopifolius Griseb. (US #1559510).

Sachsia Griseb. Fig. 186, 229.

Pollen grains radially symmetrical and isopolar, oblate-spheroidal, 30-35 x 32-38μ; tricolporate; ora lalongate, rectangular--frequently irregular--in outline, (4-7μ maximum diameter), either congruent with colpi or with lateral extensions ± pointed, margins thickened; colpi wide at pore region, immediately tapering, becoming pointed even in polar view, seeming very reduced in length, thin-margined, superficial; exine surface: spinose, spines 4-5μ in length, wide-based, gradually tapering to a blunt apex, not dense; caveae present.

Electron microscopy. S. polycephala is similar to Figure 6A.

Species examined. S. polycephala Griseb. (MO #1110277).

Sphaeranthus Vaill. ex L. Fig. 183, 192.

Grains radially symmetrical and isopolar, oblate-spheroidal, 24-26 x 25-27μ; tricolporate; ora lalongate, rectangular to irregular in outline (4-7 maximum diameter), lateral extensions ± pointed, margins thicken-

ed; colpi mostly wide as os region, immediately tapering, ± distinctly constricted in equatorial view, deeply sunken, to, rarely, very narrow; exine surface: spinose, spines 4-5μ in length, with narrow base, thin projections tapering to finely rounded apex, not dense; caveae present.

Electron microscopy (Fig. 327). S. sp. is similar to Fig. 6D.

Species examined. S. africanus L. (US #852876, US #435043); S. sp. (TEX #224212).

Stenachenium Benth. Fig. 179; 257-259.

Grains radially symmetrical and isopolar, oblate-spheroidal to prolate spheroidal, 32 x 35μ to 48 x 47μ; tricolporate, rarely tetracolporate; ora lalongate, rectangular to elliptical in outline (4-8u maximum diameter, either congruent with colpi or with very long lateral extensions (3-4μ in length), ± pointed, margins thickened; colpi wide, either extending the whole length of the polar axis at this width, or gradually tapering, deeply sunken to superficial, to wide, tapering immediately and less elongate; exine surface: spinulose, spinules 2-3.5μ in length, conical with blunt apex to spinose, spines 4.5-6μ long, wide-based, gradually sloping to blunt apex, dense; caveae present.

Interspecific variation. S. campestre is oblate-spheroidal, 32 x 35μ; S. riedelii is prolate-spheroidal, 48 x 47μ. S. campestre displays the shorter spine type.

Intraspecific variation. Tetracolporate grains are in S. campestre.

This species also has ora both with and without lateral extensions. S. riedelii frequently displays a shorter colpus and, in rare cases, the os and the colpus appear to coincide, the consequent thickening displaying a raised aperture type.

Electron microscopy Fig. 327). S. campestre is similar to Fig. 6C.

Species examined. S. campestre Baker (US #2102032); S. riedelii Baker (US #1591335).

Tessaria Ruiz et Pav. Fig. 195-196.

Grains are radially symmetrical and isopolar, oblate-spheroidal, 26-28 x 29-32μ; tricolporate, ora lalongate, elliptical to irregular in outline, (4-6; 5μ maximum diameter), congruent with colpi, margins thickened; colpi margins difficult to trace, either very superficial, or reduced and almost exactly coinciding with positions of ora, to, more rarely, wide, thin margined, deeply sunken, becoming ± constricted in equatorial view; exine surface: spinose, spines 4-5.5μ long, wide based, tapering to blunt apex, not dense; caveae present.

Electron microscopy (Fig. 278). T. integrifolia is similar to Fig. 6A but appears to be without internal foramina.

Species examined. T. integrifolia Ruiz et Pav. (US #2516071).

Thespidium F. Muell. Fig. 77.

Grains radially symmetrical and isopolar, oblate-spheroidal, 22-27 x 25-30μ; tricolporate; ora lalongate, rectangular to elliptical in outline (3-7.5μ maximum diameter), large and gaping, mostly congruent with colpi, rarely with lateral extensions, margins thickened; colpi wide, thin margined, deeply sunken, immediately tapering, to superficial, hard to trace, ± distinctly constricted in equatorial view; exine surface: spinulose, spinules ca. 2.5μ in length, as widely based, equilaterally triangular, with blunt apex, very dense; caveae present.

Electron microscopy. T. basiflorum is similar to Fig. 6A with no internal foramina.

Species examined. T. basiflorum F. Muell. (US #2094844).

Triplocephalum O. Hoffm. Fig. 190, 203.

Grains radially symmetrical and isopolar, oblate-spheroidal, 23-27 x 25-32μ; tricolporate; ora lalongate, rectangular in outline, (4-6.5μ maximum diameter), lateral extensions ± pointed, margins somewhat thickened; colpi wide, thin-margined, sunken, ± distinctly constricted in polar view; exine surface: spinose, spines 4μ long, widely based, gradually tapering to blunt apex, not dense; caveae present.

Electron microscopy. No data available.

Species examined. T. holtsii O. Hoffm. (NY)

III. FILAGINEAE

This subtribe consists of approximately 14 genera and 110 species.

Athroisma DC.

Grains radially symmetrical and isopolar, oblate-spheroidal, 26-31 x 28-32μ; tricolporate, ora lalongate, rectangular to elliptical in outline (3-6μ maximum diameter), lateral extensions ± pointed, when conspicuous in equatorial view, margins thickened to not well defined; colpi wide, thin margined, sunken, full length of polar axis, ± distinctly constricted in polar view; exine surface: spinose, spines 3-4μ long, wide based, tapering to a finely rounded apex, dense; caveae present.

Electron microscopy (Fig. 281). A. laciniatum is similar to Fig. 6B.

Species examined. A. laciniatum DC. (US #1669133).

Blepharispermum Wight. ex DC.

Grains radially symmetrical and isopolar, prolate-spheroidal, 22-25 x 20-23μ; apertures: either acetolysis process was too harsh for this particular specimen or the natural development of this pollen was irregular, causing the germinal areas to be so distorted that nothing definite could be ascertained about ora or colpi. Exine surface: spinulose, spinules 1-2μ, sometimes little more than knob-like projections, wide based, blunt apices, not dense; caveae present.

Electron microscopy (Fig. 283). B. zanquebaricum is similar to Fig. 6B.

Species examined. B. zanquebaricum D. et H. (US #633527).

Cylindrocline Cass. Fig. 158.

Grains radially symmetrical and isopolar, oblate-spheroidal, 27-30 x 30-34μ; tricolporate, ora lalongate, rectangular to elliptical in outline (3-5μ maximum diameter), lateral extensions ± pointed, margins thickened; colpi wide, sunken, thin margined, extending full length of the polar axis, ± distinctly constricted in polar view, to wide, very shallow, almost not defined or so reduced that ora and colpi are as one aperture; exine surface: spinose, spines 3-4μ long, wide based, funnelform, terminating in a finely rounded apex; dense; caveae present.

Electron microscopy (Fig. 271-272). C. commersoni is similar to Fig. 6B but internal foramina are difficult to determine.

Species examined. C. commersoni Cass. (US #2155737).

Evax Gaertn. Fig. 53, 55.

Grains radially symmetrical and isopolar, oblate-spheroidal to prolate spheroidal, 20-25 x 21-26μ; tricolporate; ora lalongate rectangular to circular in outline (2-4μ maximum diameter), congruent with colpi or with lateral extensions ± pointed when conspicuous in equatorial view, to ora lolongate, rectangular to elliptical in outline (2-4μ maximum length), congruent with colpi or with lateral extensions, ± pointed, margins thickened, to inconspicuous; colpi mostly narrow, thin margined,

deeply sunken, tapering at equator, ± distinctly constricted in polar view, to (rarely) wide, equidistant in diameter the full length of the polar axis, ± distinctly constricted in polar view; exine surface: spinulose, spinules less than 2μ in length, present in great numbers, impossible to measure individually, at times appearing more as tiny, ± pointed knobs; caveae present.

Interspecific variation. E. prolifera is the only species with lolongate ora. E. rotundata is the only species with conspicuously wide colpi. All other species examined have lalongate to circular ora with essentially narrow colpi.

Electron microscopy. E. multicaulis is similar to Fig. 6B with the exception that internal foramina are much larger.

Species examined. E. candida Gray (MSC #80623); E. multicaulis DC. (OKL #295, TEX #150585, MSC #80626); E. prolifera Nutt. (OKL #4309, MSC # 80628); E. rotundata Moris (MSC #193402).

Filago L. Fig. 52.

Grains radially symmetrical and isopolar, oblate-spheroidal to prolate spheroidal, 21-28 x 22-29μ; tricolporate, ora lalongate (4μ maximum diameter), or, more frequently, lolongate (3-4μ maximum length), rectangular to elliptical in outline, congruent with colpi, or, more rarely, ± pointed with lateral extensions, to inconspicuous; colpi mostly narrow, thin margined, sunken, tapering immediately from ora, becom-

ing ± distinctly constricted while yet in equatorial view, to, rarely, wide, equidistant in diameter the full length of the polar axis, ± distinctly constricted in polar view; exine surface: spinulose, spinules mostly less than 2μ in length, to spinose, spines ca. 3μ in length, finely tipped, densely spaced; caveae present.

Interspecific variation. F. arizonica appears to have only lalongate ora and wide colpi. The other species have lolongate ora with narrow colpi.

Electron microscopy. No data available.

Species examined. F. arizonica Gray (OKL #11567); F. arvensis L. (MSC #191495); F. californica Nutt. (OKL); F. germanica (L.) Huds. (OKL); F. logopus Parl. (MSC #186336); F. montana L. (MSC #80640).

Ifloga Cass.

Grains radially symmetrical and isopolar, oblate-spheroidal, 19-21 x 20-22μ; tricolporate, ora lalongate, rectangular in outline (2-3μ maximum diameter), lateral extensions ± pointed, margins thickened, to inconspicuous; colpi narrow, deeply sunken, tapering immediately and forming distinct constrictions while yet in polar view; exine surface: spinulose, spinules less than 2μ in length, finely tipped, dense; caveae present.

Electron microscopy (Fig. 292). I. seriphioides is similar to Fig. 6D.

Species examined. I. fontanesii Cass. (NY); I. seriphioides Schltr. (MO #1813946).

Micropsis DC.

Grains radially symmetrical and isopolar, oblate-spheroidal, 23.5-26 x 23.5-26μ; tricolporate; ora lalongate, rectangular to elliptical in outline (3-3.5μ maximum diameter), with lateral extensions, thickened margins, to inconspicuous; colpi narrow, thin margined, full length of polar axis, ± distinctly constricted in polar view; exine surface: spinulose, spinules less than 2μ, finely pointed, dense; caveae present.

Electron microscopy. No data available.

Species examined. M. heiteri Beauvd. (MO #927680).

Micropus L. Fig. 54, 57, 59.

Grains radially symmetrical and isopolar, oblate-spheroidal to prolate spheroidal, 20-26 x 20-28μ; tricolporate; ora mostly lolongate, rectangular to elliptical in outline (3-4μ maximum length), congruent with colpi, thickened margins, to ora lalongate, elliptical in outline (3μ maximum width), with less thick margins; colpi narrow, thin margined, deeply sunken, extending full length of polar axis; either constricting at equator or remaining open full length, constricting in polar view; exine surface: spinulose, spinules less than 2μ long, finely pointed, densely massed; caveae present.

Intra- and Interspecific variation. M. bombycinus has both types ora and colpi described above. M. californicus has lolongate ora only, with both colpi variations.

Electron microscopy. No data available.

Species examined. M. bombycinus Laj. (MSC #80817); M. californicus Fisch. et Mey. (MSC #196660, MO #1715308).

Psilocarphus Nutt. Fig. 56.

Grains radially symmetrical and isopolar, oblate-spheroidal to prolate spheroidal, 18-25 x 18-25μ; tricolporate, ora mostly lolongate, rectangular to elliptical in outline (3-4μ maximum length), thickened margins, congruent with colpi, to (rarely) a square form, also congruent with colpi; colpi narrow, thin margined, deeply sunken, extending full length of polar axis, either constricting at equator or remaining open full length, constricting in polar view; exine surface; spinulose, spinules less than 2μ long, in some cases almost appearing as knobby extensions of the exine, finely tipped or tips difficult to define because of minuteness, densely massed; caveae present.

Intra- and Interspecific variation. P. tenellus has both variations in ora and colpi described above. P. brevissimus and P. oregonus have lolongate ora, with both colpi types.

Electron microscopy. P. tenellus is similar to Fig. 6B.

Species examined. P. brevissimus Nutt. (MSC #80865); P. oregonus

Nutt. (MSC #196586); P. tenellus Nutt. (MSC #80871); P. tenellus Nutt. var. tenellus (MO #1160565).

Stylocline Nutt.

Grains are radially symmetrical and isopolar, oblate-spheroidal, 21-26 x 21-26μ; tricolporate; ora lolongate, rectangular to elliptical in outline (4-6μ maximum length), congruent with colpi, margins thickened; colpi wide, thin margined, deeply sunken, extending full length of polar axis, either constricting at equator or remaining open full length, constricting in polar view, exine surface: spinulose, spinules less than 2u in length, in some cases appearing as knobby extensions of the exine, finely tipped or tips difficult to define because of minuteness, densely massed; caveae present.

Electron microscopy (Fig. 295). S. filaginea is similar to Fig. 6D.

Species examined. S. filaginea Gray. (MSC #80879); S. gnaphalioides Nutt. (OKL #3170).

Symphyllocarpus Maxim. Fig. 84.

Grains radially symmetrical, isopolar, oblate-spheroidal, 20-24 x 20-24μ; tricolporate, ora difficult to define with certainty because mostly inconspicuous. In conspicuous cases, lolongate, rectangular in outline, (3-4μ maximum length), congruent with colpi; colpi wide, deeply sunken, thin margined, extending full length of polar axis, ± distinctly constrict-

ed in polar view; exine surface: spinulose, spinules 2μ or less in length, bluntly tipped, densely massed, to, rarely, 3μ in length, conical, finely rounded tips, more widely spaced; caveae present.

Electron microscopy. S. exilis is similar to Fig. 6A but internal foramina are not apparent.

Species examined. S. exilis Maxim. (NY

IV. GNAPHALIEAE

This subtribe consists of approximately 57 genera and 1400 species.

Series 1: Eugnaphalinae

Achyrocline Less.

Grains radially symmetrical and isopolar, prolate-spheroidal, 24-29 x 24-29μ; tricolporate; ora lalongate, rectangular to elliptical in outline (3-5μmaximum diameter), lateral extensions, ± pointed, thickened margins; colpi wide, deeply sunken, extending full length of polar axis, ± distinctly constricted in polar view; exine surface: spinose, spines 2.5-4μ in length, wide based, tapering gradually to finely rounded tips, dense; caveae present.

Electron microscopy. No data available.

Species examined. A. vargasiana DC. (MSC #188192).

Amphidoxa DC.

Grains radially symmetrical, isopolar, oblate-spheroidal, 21-25 x 22-25μ; tricolporate, ora lalongate, rectangular to elliptical in outline (3-4μ maximum diameter), lateral extensions ± pointed, thickened margins; colpi wide, deeply sunken, thin margined, full length of polar axis, tapering at equator, ± constricted in polar view; exine surface: spinose, spines 3 μ long, wide based, tapering to very fine tips, dense; caveae present.

Electron microscopy. No data available.

Species examined. A. gnaphalioides DC. (US #633369).

Anaphalis DC. Fig. 65; Fig. 88.

Grains radially symmetrical, isopolar, prolate-spheroidal, 22-30 x 22-30μ; tricolporate, ora circular to nearly square (3-4μ maximum diameter), congruent with colpi, margins thickened; colpi wide, running equidistant full length of polar axis, to narrow, constricting before reaching the equator, thin margined, deeply sunken; exine surface: spinulose, spinules 2μ or less in length, finely tipped, dense; caveae present.

Electron microscopy. A. margaritacea (OKL #265) and A. margaritacea var. occidentalis are similar to Fig. 6B.

Species examined. A. briscus (Ham.) Hand. Maz. (NY); A. margaritacea (L.) Benth. Hook. (OKL #46; OKL #265); A. margaritacea var. occidentalis Greene (TEX #199364).

Antennaria Gaertn. Fig. 93.

Grains radially symmetrical, isopolar, prolate-spheroidal, 27-34 x 26-33μ; tricolporate; ora square to mostly lalongate, rectangular to elliptical to irregular in outline (3-6μ maximum width), lateral extensions ± pointed or congruent with colpi, thickened margins; colpi wide, thin margined, extending equidistant the full length of the polar axis or tapering at equator, ± distinctly constricted in polar view, to narrow with above characteristics, to almost inconspicuous due to the size of the os; exine surface: spinulose, spinules 2.5μ in length, thin, tips finely rounded, dense; caveae present.

Interspecific and intraspecific variation. A. neglecta is the only species observed to have a square pore, although it also displays the lalongate ora. All species show variation in type of ora outline, and colpi width, although A. pulcherrina alone shows the very reduced colpus.

Electron microscopy (Fig. 306-307). A. microphylla, A. campestris and A. plantaginifolia are similar to Fig. 6D.

Species examined. A. campestris Rydb. (OKL #888); A. microphylla Rydb. (OKL); A. neglecta Greene (OKL #6396); A. pulcherrina (Hook.) Greene (OKL #4896); A. plantaginifolia (L.) Richards. (OKL #2366); A. umbrinella Rydb. (OKL #736).

Artemisiopsis S. Moore

Grains radially symmetrical, isopolar, oblate-spheroidal, 16-20 x 17.5-20μ; tricolporate, ora lalongate, irregular to elliptical in outline

(3-4μ maximum diameter), congruent with colpi or with lateral extensions ± pointed, margins thickened; colpi wide, thin margined, deeply sunken, extending full length of polar axis, ± distinctly constricted in polar view; exine surface; spinulose, spinules very reduced (ca. 1μ in length), appearing as knobby projections of the surface, dense; caveae present.

Electron microscopy. A. villosa is similar to Fig. 6A, with no internal foramina present.

Species examined. A. villosa S. Moore (MO #1775154).

Chevreulia Cass.

Grains radially symmetrical, isopolar, oblate-spheroidal, 21-26 x 21-26μ; tricolporate, ora lalongate, rectangular to elliptical in outline (2-3μ maximum diameter), congruent with colpi, margins thickened; colpi wide, thin margined, extending full length of the polar axis, ± distinctly constricted in polar view; exine surface: spinulose, spinules 2μ or less in length, thin, tips finely pointed, densely massed; caveae present.

Electron microscopy. No data available.

Species examined. C. acuminata Less. (MO #971770); C. stoloniferа Cass. (US #1131314).

Chiliocephalum Benth.

Grains radially symmetrical, isopolar, prolate-spheroidal, 21-27 x 21-26μ; tricolporate, ora square to circular in outline, margins not heavily thickened so difficult to determine, lateral extensions ± pointed to congruent with colpi; colpi narrow, thin margined, deeply sunken, extending full length of the polar axis, ± distinctly constricted in polar view; exine surface; spinose, spines 2.5-3.5μ in length, wide based, gradually tapering to finely rounded tips, densely massed; caveae present.

Electron microscopy. C. Schimperi is similar to Fig. 6B.

Species examined. C. Schimperi Benth. (US #945668).

Chionolaena DC. Fig. 83.

Grains radially symmetrical, isopolar, oblate-spheroidal to prolate-spheroidal, 24-32 x 24-34μ; tricolporate; ora square to lalongate, rectangular to elliptical in outline if lalongate (3-6μ maximum diameter) congruent with colpi or with lateral extensions, margins thickened; colpi narrow, thin margined, deeply sunken, extending the full length of the polar axis, tapering at the equator, ± distinctly constricted in polar view to wide, shallow, with other characteristics as above; exine surface: spinulose, spinules ca. 2μ in length, wide-based, gradually tapering to form finely rounded tips, to spinose, spines 3-3.5μ in length, thinner, more pointed, densely massed; caveae present.

Interspecific variation. C. lychnoporoides has the longer spine type.

Electron microscopy. C. isabellae is similar to Fig. 6B.

Species examined. C. isabellae Bak. (NY); C. lychnophoroides Sch. Bip. (NY).

Desmidium DC.

Grains radially symmetrical, isopolar, prolate-spheroida, 18-22 x 16-20μ; tricolporate; ora difficult to describe with certainty, not conspicuous in equatorial view for the most part, due either to poor acetolysis or specific position of grains on slide, when observable, lalongate with lateral extensions; colpi narrow, thin margined, extending full length polar axis, ± constricted in polar view; exine surface: spinulose, spines less than 2μ in length, finely pointed, densely massed; caveae present.

Electron microscopy. No data available.

Species examined. D. filagineum DC. (US #2155727).

Facelis Cass.

Grains radially symmetrical, isopolar, oblate-spheroidal, 24-33 x 26-28μ; tricolporate, ora lalongate and lolongate, rectangular to elliptical in outline (3-5μ maximum length or width), congruent with colpi, margins thickened; colpi narrow to wide, thin margined, extending full length of the polar axis, ± distinctly constricted in polar view, deeply sunken, to, rarely, more shallow, reduced; exine surface: spinulose, spinules less than 2μ in length, in some grains so reduced as to present a lobed

exine surface, to spinose, spines 2.5-3.5u in length, wide-based, bluntly tipped, densely massed; caveae present.

Intraspecific variation. F. retusa (NY) displays all the aperture varieties noted in the genus description, as well as the longer spines. F. retusa (OKL-2 collections) has, mostly, simple lolongate pores, and the very reduced spinules.

Electron microscopy (Fig. 304). F. retusa (NY) is similar to Fig. 6D, with a footlayer:endexine ratio of 1:2.

Species examined. F. retusa Sch. Bip. (NY, OKL, 2 collections).

Gnaphalium L. Fig. 94; 135, 140, 146, 155.

Grains radially symmetrical, isopolar, oblate-spheroidal to prolate-spheroidal, 18-32 x 19-33u; tricolporate; comprising a variety of types; colpi wide, thin-margined, deeply sunken, extending full length of the polar axis, ± distinctly constricted in polar view, to, rarely, more narrow with accompanying characteristics as described above; exine surface; spinose, spines 3-4u in length, narrow, finely tipped, to spinulose, spinules less than 3u in length, finely tipped, dense; caveae present.

Intra- and Interspecific variation. G. americanum: lalongate (3u maximum width) and lolongate ora (4u maximum length), rectangular in outline, thickened margins, congruent with colpi, spinulose. G. cheiranthifolium: circular to lalongate ora (4u maximum diameter), thicken-

ed margins, congruent with colpi, spinose. G. luteoalbum: square to lolongate ora (3-4μ maximum diameter or length) thickened margins, congruent with colpi, spinose. G. macounii: square to circular to lalongate ora (3-5μ maximum diameter), thickened margins, congruent with colpi, spinose, spines with wide bases, more bluntly tipped. G. polycephalum: lalongate ora, 3-4μ maximum width, irregularly rectangular to elliptical in outline, thickened margins, congruent with colpi or with lateral extensions ± pointed, spinose, spines with wide bases. G. obtusifolium: circular to square ora (2.5-4.5μ maximum diameter), thickened margins, congruent with colpi or with lateral extensions, spinose. G. palustre: square (3-4μ maximum diameter) to lolongate (4-6μ maximum diameter) to lolongate (4-6μ maximum length), rectangular in outline, thickened margins, congruent with colpi, spinulose, spinules less than 2μ in length. G. purpureum: lolongate ora (3-4μ maximum length) elliptical in outline, thickened margins, congruent with colpi, spinulose, spinules less than 2μ in length. G. stachydifolium: as in G. purpureum with spinules more densely massed. G. uliginosum: circular to irregularly outlined ora (3-3.5μ maximum diameter) congruent with colpi, thickened margins, spinulose.

Electron microscopy (Fig. 297). G. cheiranthifolium is similar to Fig. 6D.

Species examined. G. americanum Mill. (OKL #1634); G. cheiranthifolium Lam. (BLT #3857); G. luteoalbum Benth. (BLT #5512); G.

macounii Greene (OKL #14814); G. obtusifolium L. (OKL #5424); G. palustre Nutt. (OKL #581); G. polycephalum Mx. (OKL #3346); G. purpureum L. (OKL #7448); G. stachydifolium Lam. (BLT #3698); G. uliginosum L. (OKL #23029).

Lasiopogon Cass. Fig. 60, 63.

Grains radially symmetrical, isopolar, oblate-spheroidal, 20-24 x 20-24μ; tricolporate; ora circular to square, (2.5-4μ maximum diameter), congruent with colpi, margins thickened; colpi narrow, thin margined, deeply sunken, constricting before reaching the equator, or extending full length of the polar axis, ± distinctly constricted in polar view; exine surface: spinulose, spinules less than 2.5μ in length, finely tipped, very densely massed; caveae present.

Electron microscopy. No data available.

Species examined. L. muscoides (Desf.) DC. (NY, two collections); (MO #1740265).

Leontopodium R. Br. ex Cass.

Grains radially symmetrical, isopolar, oblate-spheroidal, 24-29 x 24-29μ; tricolporate; ora square, circular or lalongate, rectangular to elliptical in outline (2.5-4μ maximum diameter), congruent with colpi, margins thickened; colpi wide, thin margined, deeply sunken, extending the full length of the polar axis, ± distinctly constricted in polar view;

exine surface; spinulose, spinules less than 2.5μ long, wide based, finely tipped, to spinose, spines 3-4μ long, narrow, all types densely massed; caveae present.

Interspecific variation. L. alpinum is spinulose. L. andersonii is spinose, narrowly based, thin, tapering, finely tipped; L. artemisifolium is spinose, the spines narrowly based, more cylindrical, more bluntly tipped.

Electron microscopy. L. artemisifolium is similar to Fig. 6B.

Species examined. L. alpinum Cass. (OKL); L. andersonii C. B. Clarke (US #1210535); L. artemisifolium (Levl.) Bud. (US #2223947).

Loricaria Wedd. Fig. 66.

Grains radially symmetrical, isopolar, oblate-spheroidal to prolate-spheroidal, 22-28 x 23-27μ; tricolporate; ora circular to lalongate, rectangular to irregular in outline (2.5-6μ maximum diameter), congruent with colpi or with lateral extensions ± pointed, margins thickened; colpi wide, thin margined, deeply sunken, extending equidistant full length of the polar axis, ± distinctly constricted in polar view, at times os and colpus appearing as one; exine surface: spinulose, spinules ca. 1μ in length, reduced almost to knob-like extensions of the exine surface, dense; caveae present.

Electron microscopy. L. thuyoides (MO #1593351) is similar to Fig. 6B.

Species examined. L. thuyoides (Lam.) Sch. Bip. (MO #1651258; MO #1593351).

Luciliopsis Wedd. Fig. 100.

Grains radially symmetrical, isopolar, prolate-spheroidal, 21.5-26 x 21.5-26μ; tricolporate; ora circular, square to lalongate (rectangular in outline), 3-4μ maximum diameter, congruent with colpi, margins thickened; colpi narrow to wide, thin margined, extending full length of the polar axis, ± distinctly constricted in polar view; exine surface: spinulose, spinules 2μ or less, with wide bases and somewhat blunted tips, to very reduced, almost knob-like extensions; dense; caveae present.

Electron microscopy. No data available.

Species studied. L. sp. (US).

Oligandra Less.

Grains radially symmetrical, isopolar, oblate-spheroidal, 22-32 x 22-32μ; tricolporate.

Intraspecific variation. O. lycopodioides (US): 28-32 x 28-32μ, ora square (4μ maximum diameter) to lolongate (5.5μ maximum length), congruent with colpi or with ± pointed lateral extensions, margins thickened; colpi wide, thin margined, deeply sunken, extending equidistant full length of polar axis or tapering at equator, ± distinctly constricted in

polar view; exine surface: spinose, spines 4μ in length, wide based, tapering to a very finely tipped apex, dense. O. lycopodioides (MO) 22-24 x 22-25μ, ora square (3μ maximum diameter) to lalongate (4μ maximum diameter), otherwise as above; colpi as above; exine surface: spinulose, spinules mostly less than 3μ in length, narrow-based, finely tipped, dense.

Electron microscopy. No data available.

Species examined. O. lycopodioides Less. (MO #932719, US #2427653).

Phagnalon Cass. Fig. 147.

Grains radially symmetrical, isopolar, oblate-spheroidal, 25-34 x 25-34μ, tricolporate; ora circular or square (2-3.5μ maximum diameter) to lalongate, rectangular in outline (4μ maximum diameter), congruent with colpi or with ± pointed lateral extensions, margins thickened; colpi wide, thin margined, extending equidistant the full length of the polar axis or constricting somewhat at the equator, ± distinctly constricted in polar view; exine surface: spinose, spines 3-4μ in length, wide based, tapering gradually to finely rounded tips, dense; caveae present.

Electron microscopy (Fig. 326, 330, 301). P. saxatile and P. sordidum are similar to Fig. 6D. P. rupestre is similar to Fig. 6C, but shows vestiges of internal foramina.

Species examined. P. saxatile Cass. (MSC #191576); P. sordidum

DC. (MSC #80820); P. rupestre DC. (MO #1784579).

Psila Phil. Fig. 107.

Grains radially symmetrical, oblate-spheroidal, 18-24 x 18-25μ, tripcolporate; ora circular to square (2.5-3.5μ maximum width), to lalongate, rectangular in outline (3.5-4μ maximum width), congruent with colpi, margins thickened; colpi wide, thin margined, deeply sunken, extending equidistant the full length of the polar axis or tapering at equator, ± distinctly constricted in polar view; exine surface: spinulose, spinules 3μ in length to (mostly) less than 3μ, extremely narrow, thin, finely pointed tips, not dense; caveae present.

Electron microscopy. P. trinervis is similar to Figure 6B but has somewhat more elongate internal foramina.

Species examined. P. bolivensis (Wedd.) Cabr. (US #2370716); P. trinervis (Lem.) Cabr. (MO #1739402).

Raoulia Hook. f. Fig. 58; 78.

Grains radially symmetrical, isopolar, oblate-spheroidal to prolate-spheroidal, 21-26 x 21-26μ, tricolporate; ora square to circular to lalongate, rectangular to elliptical in outline, (2.5-4u maximum diameter), to lolongate (4μ maximum length), congruent with colpi or with lateral extensions ± pointed, heavily to very lightly thickened margins; colpi wide, deep, thin margined, extending equidistant the entire length of the polar

axis, or tapering at or before reaching the equator, ± distinctly constricted in polar view; exine surface: spinulose to subspinulose, spinules less than 2.5μ in length, frequently less than 1μ, appearing more as knobby projections from the exine surface, wide based, bluntly tipped, dense; caveae present.

Interspecific variation. The ora of R. monroi appear to have less heavily thickened margins, and are not easily distinguishable in the colpus.

Electron microscopy Fig. 310). R. monroi is similar to Fig. 6E but has more elongate basal columellae.

Species examined. R. australis Hook. (US #2394861); R. glabra Hook. (US #1994287); R. monroi Hook. f. (US #1553742); R. parkii Buch. (US #1994216).

Stuartina Sond. Fig. 62.

Grains radially symmetrical, isopolar, oblate-spheroidal, 18-22 x 19-23μ, tricolporate; ora square to circular to lalongate, rectangular to elliptical in outline, (2.5-4μ maximum diameter) to lolongate (2.5-4u maximum length), congruent with colpi, heavily to very lightly thickened margins; colpi wide (4μ) to narrow (2.5μ), deeply sunken, thin margined, extending equidistant the full length of the polar axis, ± distinctly constricted in polar view; exine surface: subspinulose, spinules ca. 1μ in length, appearing as finely tipped knobs in dense masses; caveae present.

Electron microscopy (Fig. 302). S. muelleri is similar to Fig. 6D, but has more elongate internal foramina.

Species examined. S. hamata W. R. Philipson (US #2072430); S. muelleri Sond. (US #2376055).

Stuchertiella Beauverd. Fig. 96.

Grains radially symmetrical, isopolar, oblate-spheroidal, 20-22 x 20-23μ, tricolporate; ora circular to square (2.5-3.5μ maximum diameter), congruent with colpi, thickened margins; colpi wide, thin margined, deeply sunken, extending equidistant the full length of the polar axis, ± distinctly constricted in polar view; exine surface: spinulose to subspinulose, spinules 2μ or less in length, appearing as finely tipped knobs in dense masses; caveae present.

Electron microscopy. S. capitata is similar to Fig. 6D.

Species examined. S. capitata (Wedd.) Beauvd. (US #1547974).

Series 2: Helichryseae

Acomis F. Muell. Fig. 137, 143, 154.

Grains radially symmetrical, isopolar, oblate-spheroidal, 26-32 x 28-32μ, tricolporate.

Interspecific variation. A. macra: ora circular to lalongate, elliptical in outline, (4-5μ maximum diameter), very large and conspicuous, congruent with colpi, thickened margins; colpi wide but very reduced in

length, not extending as far as the equator in equatorial view, shallow, in some grains appearing co-existent with ora, and not visible as a distinct character in polar view; exine surface: spinose, spines 3-4μ in length, wide based, tapering to a fine point, dense; caveae present. A. rutidosis: ora irregular in outline (3-4μ maximum diameter), lateral extensions ± pointed; colpi narrow, thin margined, deeply sunken, extending full length of the polar axis, tapering at equator, ± distinctly constricted in polar view; exine surface: spinose, spines 4.5μ in length, wide based, thin, tapering to a fine point, dense; caveae present.

Electron microscopy. A. macra is similar to Fig. 6E.

Species examined. A. macra F. Muell. (US #1671848); A. rutidosis F. Muell. (US #2243730).

Ammobium R. Br.

Grains radially symmetrical, isopolar, oblate-spheroidal, 23-24 x 22-26μ, tricolporate; ora square to lalongate, elliptical in outline (3-4μ maximum diameter), congruent with colpi or with lateral extensions ± pointed; colpi wide, extending full length of the polar axis, tapering to a point at the equator, ± distinctly constricted in polar view; exine surface: spinulose, spinules 2.5μ or less in length, wide based, finely rounded points, dense; caveae present.

Electron microscopy. A. olatum is similar to Fig. 6B.

Species examined. A. olatum R. Br. (MO).

Anaxeton Gaertn.

Grains radially symmetrical, isopolar, oblate-spheroidal, 21-26 x 21-26μ, tricolporate; ora square to lalongate, rectangular to elliptical in outline (2.5-4.μ in maximum diameter) congruent with colpi or with lateral extensions ± pointed, thickened margins; colpi narrow, deeply sunken, extending full length of the polar axis ± distinctly constricted in polar view, to wide, shallow, not extending as far as the equator in equatorial view, in some grains appearing co-existent with ora, and not visible as a distinct character in polar view; exine surface: spinules 3μ or less than 3μ in length, wide based, tapering gradually to a rounded tip, dense; caveae present.

Electron microscopy. A. aspenum is similar to Fig. 6B.

Species examined. A. aspenum DC. (MO #1603722; US #552322).

Cassinia R. Br. Fig. 71.

Grains radially symmetrical, isopolar, oblate-spheroidal to prolate-spheroidal, 22-26 x 22-26μ, tricolporate; ora square to lalongate to lolongate, rectangular to elliptical in outline, (2.5-4μ maximum width or length), congruent with colpi, rarely with lateral extensions ± pointed, margins thickened; colpi wide or narrow depending on os size, thin margined, deeply sunken, mostly extending the full length of the polar axis, ± distinctly constricted in polar view, to (rarely) reduced in length, shallow; exine surface: spinulose, spinules 2.4-3.5μ in length, wide

based, tapering smoothly to finely rounded tips, dense; caveae present.

Electron microscopy. No data available.

Species examined. C. fulvida Hook. (US #1994100); C. leptophylla R. Br. (US #1994598); C. retorta A. Cunn. (US #2159992).

Eriochlamys Sond. et F. Muell. Fig. 82.

Grains radially symmetrical, isopolar, oblate-spheroidal, 21-25 x 21-25μ, tricolporate; ora circular to square (3μ maximum diameter), congruent with colpi, margins not heavily thickened, often difficult to distinguish with certainty; colpi narrow, thin margined, deeply sunken, extending the full length of the polar axis, ± distinctly constricted in polar view; exine surface: spinulose, spinules 2.5μ maximum length, wide based, tapering to finely rounded tips, dense; caveae present.

Electron microscopy. No data available.

Species examined. E. behrii Sond. et F. Muell. (US #2159981).

Gilruthia Ewart Fig. 148-149.

Grains radially symmetrical, isopolar, prolate-spheroidal, 28-33 x 28-32μ, tricolporate; ora lalongate, rectangular to irregular in outline (3-4μ maximum diameter) congruent with colpi or with lateral extensions ± pointed, thickened margins; colpi wide, thin margined, deeply sunken, tapering at equator in equatorial view, ± distinctly constricted in polar view; exine surface: spinose, spines 4μ in length, wide based, tapering

gradually then extending further as a thin, finely tipped apex, dense; caveae present.

Electron microscopy (Fig. 321). G. osbornii is similar to Fig. 6E.

Species examined. G. osbornii Ewart et White (BLT #5425).

Helichrysum Mill. corr. Pers. Fig. 47-48; 102; 247-248.

Grains radially symmetrical, isopolar, oblate-spheroidal, tricolporate.

Interspecific variation. H. ambiguus, 32-34 x 32-36μ, ora cannot be delineated with any certainty, if present; colpi narrow, sunken, extending full length of polar axis, widening in the obvious os regions, distinct in polar view; exine surface: spinulose, spinules 2.5μ or less in length, wide based, tapering gradually to finely rounded tips, dense. H. bracteatum. 38-42 x 38-40μ, ora rectangular to irregularly circular (4-6μ maximum diameter), slight lateral extensions, thick margined; colpi wide, deep, greatly reduced in length, to wide, very shallow, almost a faint outline around the os, os and colpus appearing as one character; exine surface: spinose, spines 6.5u in length, narrow based, rising sharply to form long, thin, finely pointed tips, dense. H. davenportii. 32-36 x 32-28μ, ora rectangular (4-5.5μ maximum diameter) short lateral extensions, thickened margins; colpi greatly reduced in length, almost at one with the ora although somewhat more elongate; exine surface, in form like that of H. bracteatum, but shorter spines 5-5.5μ length; caveae present in all

forms.

Electron microscopy (Fig. 309, 311, 317-319). H. davenportii is similar to Fig. 6E.

Species studied. H. ambiguum Pers. (BLT #5583); H. bracteatum (Vent.) Andr. (BLT #5344A); H. davenportii F. Muell. (BLT #5441).

Helipteum DC. Fig. 41-43; 76; 171, 173.

Grains radially symmetrical, isopolar, oblate-spheroidal, 22-37 x 24-40μ, tricolporate; ora square to lalongate, rectangular to widely elliptical in form, in some species more thickened margins than in others congruent with colpi or with lateral extensions; colpi long, narrow, deeply sunken to wide, more shallow, very reduced in length; exine surface: subspinulose, spinules so reduced as to present an almost smooth surface, to spinose, spines 3-5μ in length, wide based, tapering quickly to a long, thin, finely tipped point, dense; caveae present.

Interspecific variation. H. battii represents the most deviation from the more typical pattern, having wide ora (4-6.5μ maximum diameter), almost exactly coincident with the colpi, sometimes a bit more extended in length, with very reduced spines. H. manglesii also displays an ora-colpi complex, the ora much more rounded and smaller (3-4μ) than in H. battii, and with a spine length of 4-5.5μ. H. australe, H. roseum and H. splendidum are similar in having ora 3-4μ maximum diameter, a colpus which is narrow, deeply sunken, extending full

length of the polar axis, and spines 4-5μ in length. H. spicatum has a more widened colpus, no definite os region in most grains, if ora are visible they are small (2.5-3μ maximum diameter) and square or circular; colpi are long, narrow, and deeply sunken; spines are somewhat reduced to mostly 2.5μ in length.

Electron microscopy (Fig. 313). H. manglesii and H. spicatum are similar to Fig. 6E.

Species examined. H. australe (Gray) Druce (BLT #5572); H. battii F.v.M. (BLT #5368); H. manglesii F.v.M. (BLT #5325); H. roseum Benth. (BLT #5259); H. spicatum (Steetz) Benth. (BLT #5356); H. splendidum Hemsl. (BLT #5360E).

Humea Sm. Fig. 37-38; 86-87.

Grains radially symmetrical, isopolar, oblate-spheroidal, 22-28 x 22-28μ, tricolporate.

Interspecific variation. H. cassiniana: ora square to lalongate, rectangular in outline, (3-4μ maximum diameter), congruent with colpi or with later extensions ± pointed, thickened margins; colpi wide, thin margined, deeply sunken, extending full length of the polar axis, tapering at equator, ± distinctly constricted in polar view; exine surface: spinulose, spinules 2.5-3μ in length, wide based, tapering to finely rounded tips, dense; caveae present. H. elegans: ora circular to square, (2.5-4μ maximum diameter), congruent with colpi, thickened margins;

colpi wide, thin margined, very reduced in length, about three times the size of the ora, tapering far before reaching the equator, not an observable characteristic in polar view; exine surface: subspinulose, projections presenting an almost smooth appearance.

Electron microscopy. No data available.

Species examined. H. cassiniacea F. Muell. (US); H. elegans Sm. (US #2073986).

Ixiolaena Benth. Fig. 90

Grains radially symmetrical, isopolar, oblate-spheroidal, 26-37 x 27-37μ, tricolporate; ora round to lalongate, rectangular to elliptical in outline (2.5-5μ maximum diameter), congruent with colpi, thickened margins; colpi wide, thin margined, deeply sunken, extending full length of polar axis, ± distinctly constricted in polar view; exine spinulose, spinules 2-3μ maximum length, tapering gradually, then extending further as a finely tipped apex, an inverted funnel form, dense; caveae present.

Electron microscopy. I. leptolepis is similar to Fig. 6E.

Species examined. I. leptolepis (DC.) Benth. (BLT #5209); I. tomentosa Sond. et F. Muell. ex Sond. (MSC #214608; MSC #214574).

Ixodia R. Br. Fig. 228.

Grains radially symmetrical, isopolar, oblate-spheroidal, 28-31 x

27-31μ, tricolporate; ora square to lalongate, elliptical to rectangular in outline (3-4μ maximum diameter), congruent with colpi or with lateral extensions ± pointed, thickened margins; colpi wide, thin margined, deeply sunken, extending the full length of the polar axis, ± distinctly constricted in polar view; exine surface: spinose, spines 3-4μ in length, wide based, tapering gradually to a finely rounded tip, not dense; caveae present.

Electron microscopy (Fig. 296). I. schilleoides is similar to Fig. 6D.

Species examined. I. schilleoides R. Br. (POS #1048).

Leontonyx Cass. Fig. 64.

Grains radially symmetrical, isopolar, oblate-spheroidal, 18-24 x 21-26μ, tricolporate; ora square to lalongate, elliptical to rectangular in outline (2.5-4μ maximum diameter), congruent with colpi or with lateral extensions ± pointed, thickened margins; colpi wide at ora, narrowing immediately, thin margined, deeply sunken, extending the full length of the polar axis, ± distinctly constricted in polar view; exine surface: spinulose, spinules very reduced, less than 1+u in length, with blunted tips, to longer, up to 3μ, and more pointed, dense; caveae present.

Interspecific variation. L. bicolor has the blunted spinules type; the other two species have the longer, more pointed form.

Electron microscopy. L. bicolor is similar to Fig. 6D.

Species examined. L. bicolor DC. (MO #1647587); L. glomeratus DC. (US #1029178); L. spathulatus Less. (MSC #1579585).

Leptorhynchus Less. Fig. 150.

Grains radially symmetrical, isopolar, oblate-spheroidal, 24-31 x 24-32μ, tricolporate; ora lalongate (rectangular in outline) to a few lolongate ora (2.5-4μ maximum diameter), congruent with colpi, margins thickened; colpi wide, deeply sunken, thin margined, extending the length of the polar axis ± distinctly constricted in polar view, to narrow, unexpanded, making interpretation of ora impossible in many instances; exine surface: spinose, spines 3-4μ in length, wide based, appearing as inverted funnelforms in some views, very finely rounded tips, dense; caveae present.

Electron microscopy (Fig. 322-323). L. ambiguus is similar to Fig. 6E but has a much thicker, imperforate tectum containing circular internal foramina.

Species examined. L. tetrachaetum (Schlechtal) J. M. Black (MSU #214596); L. waitzia Sond. (MSC #214588; BLT #5588).

Leucopholis Gardn. Fig. 85.

Grains radially symmetrical, isopolar, prolate-spheroidal, 24-27 x 24-27μ, tricolporate; ora square (2.4-5μ maximum diameter), mostly

congruent with colpi, rarely with lateral extensions, margins thickened but not as heavily as in many species; colpi wide, thin margined, deeply sunken, reduced in length, tapering to a point before reaching the equator in equatorial view, ± distinctly constricted in polar view; exine surface: spinulose, spinules less than 2.5μ in length, wide based, with a blunted tip, dense; caveae present.

Electron microscopy. L. capitata similar to Fig. 6D.

Species examined. L. capitata (Baker) Cufod. (NY).

Millotia Cass..

Grains radially symmetrical, isopolar, oblate-spheroidal to prolate-spheroidal, 23-26 x 24-28μ, tricolporate; ora square to lalongate, rectangular in outline (2.5-4μ maximum diameter), congruent with colpi, margins slightly thickened; colpi wide, deeply sunken, thin margined, extending the full length of the polar axis, ± distinctly constricted in polar view, to narrow, unexpanded, making interpretation of ora impossible in many grains; exine surface: spinose to spinulose, two varying patterns occurring in about equal numbers throughout the sample; spines 4u in length, with narrow tips, and fine points, to spinules 2.4μ in length, more bluntly tipped, dense; caveae present.

Electron microscopy (Fig. 300). M. myostidifolia is similar to Fig. 6D.

Species examined. M. myostidifolia (Benth.) Steetz (BLT #5482);

M. myostidifolia (Benth.) Steetz in Lehm.(MSC #187619).

Petalacte D. Don Fig. 110, 118.

Grains radially symmetrical, isopolar, oblate-spheroidal, 24-28 x 24-29μ, tricolporate; ora lalongate, elliptical in outline (4-5μ maximum diameter), congruent with colpi, or with lateral extensions ± pointed, thickened margins; colpi wide, thin margined, shallow, reduced in length, or extending full length of the polar axis, ± distinctly constricted in polar view; exine surface: spinulose, spinules 2.4-3μ in length, wide based, tapering to finely rounded tips, not dense; caveae present.

Electron microscopy (Fig. 294). P. coronata is similar to Fig. 6D, but has much larger internal foramina.

Species examined. P. coronata Don. (MO).

Petalactella N. E. Br.

Grains radially symmetrical, isopolar, oblate-spheroidal, 21-24 x 21-23μ, tricolporate; ora circular to lalongate, rectangular in outline, (2.5-3μ maximum diameter, congruent with colpi, thickened margins; colpi narrow, thin margined, tapering before reaching the equator in equatorial view, ± distinctly constricted in polar view; exine surface: spinulose, spinules 2.5μ long, wide based, finely pointed, forming an equilateral triangular pattern, dense; caveae present.

Electron microscopy. P. woodii is similar to Fig. 6D.

Species examined. Petalactella woodii N. E. Br. (MO).

Phacellothrix F. Muell.

Grains radially symmetrical, isopolar, oblate-spheroidal, 28-34 x 28-34μ, tricolporate, ora lalongate, elliptical in outline (4-5μ maximum diameter), congruent with colpi or with lateral extensions ± pointed, thickened margins; colpi wide, shallow, thin margined, reduced in length, not so readily visible as a distinct character in polar view; exine surface: spinose, spines 4-5μ in length, very wide bases, projecting from which are narrow, finely pointed tips, dense; caveae present.

Electron microscopy. No data available.

Species examined. P. cladochaeta F. Muell. (US #1943112).

Phaenocoma D. Don Fig. 115.

Grains radially symmetrical, isopolar, oblate-spheroidal, 24-29 x 25-32μ, tricolporate; ora lalongate, rectangular to elliptical in outline (4-5μ maximum diameter), congruent with colpi or with lateral extensions ± pointed, margins thickened; colpi wide, thin margined, deeply sunken, beginning to narrow at ora, tapering completely before reaching the equator in equatorial view, ± distinctly constricted in polar view; exine surface: spinulose, spinules 2.5-3μ in length, wide based, tapering to a blunted tip, not dense; caveae present.

Electron microscopy. No data available.

Species examined. P. prolifera D. Don (MO).

Pithocarpa Lindl. Fig. 136, 141.

Grains radially symmetrical, isopolar, oblate-spheroidal, 24-34 x 26-32μ, tricolporate; ora lalongate, elliptical to rectangular in outline (2.5-4μ maximum diameter), congruent with colpi or with lateral extensions ± pointed, thickened margins; colpi wide, thin margined, deeply sunken, tapering to a point at the equator in equatorial view, ± distinctly constricted in polar view; exine surface; spinose, spines 3-4μ in length, wide based, projecting from which are narrow, finely pointed tips, dense; caveae present.

Electron microscopy (Fig. 320). P. corymbulosa resembles Fig. 6E.

Species examined. P. corymbulosa Lindl. (US #916437; MO #1794625).

Podosperma Labill. = Podotheca Cass. Fig. 252-254.

Grains radially symmetrical, isopolar, prolate-spheroidal, 44-50 x 44-48μ, tricolporate; ora lolongate, rectangular in outline (5-6.5μ in length), mostly congruent with colpi, rarely with lateral extensions ± pointed, thickened margins; colpi wide, thin margined, deeply sunken, reduced in length, to very shallow, ± distinctly constricted in polar view; exine surface: spinose, spines 4-5.5μ in length, bases nearly as wide,

tapering, to narrow, rather long, finely pointed tips, dense; caveae present.

Electron microscopy. P. gnaphalioides is similar to Fig. 6B.

Species examined. P. gnaphalioides Grab. (BLT #5423).

Quinetia Cass.

Grains radially symmetrical, isopolar, oblate-spheroidal, 23-28 x 24-28μ, tricolporate; ora square to circular (3-4μ maximum diameter, congruent with colpi, thickened margins; colpi narrow, thin margined, deeply sunken, extending the full length of the polar axis, ± pointed in polar view, to more shallow, reduced in length, not so obvious a character in polar view; exine surface: spinulose, spinules 2-3μ in length, wide based, finely tipped, dense; caveae present.

Electron microscopy. No data available.

Species examined. Q. urvillei Cass. (BLT #5465).

Rutidosis DC. Fig. 80.

Grains radially symmetrical, isopolar, oblate-spheroidal, 20-30 x 20-31μ, tricolporate; caveae present.

Interspecific variation. R. helichrysoides: 28 x 29μ, ora lalongate, rectangular in outline (3-4μ maximum diameter), congruent with colpi, thickened margins; colpi wide, thin margined, deeply sunken, tapering at equator, ± distinctly constricted in polar view; exine surface: spinose,

spines 3-4u long, wide based, tapering gradually to finely rounded tips, dense. R. multiflorum: 21 x 22μ, ora square to circular (2.5-3u maximum diameter), congruent with colpi, slightly thickened margins; colpi narrow, thin margined, deeply sunken, reduced in length, tapering far before reaching equator, ± distinctly constricted in polar view; exine surface: spinulose, spinules mostly 2.5μ in length, sometimes reaching 3μ, wide based, tapering quickly to produce finely pointed tips, dense.

Electron microscopy. No data available.

Species examined. R. multiflora B. L. Robinson (BLT #5524); R. helichrysoides DC. (MSC #187659).

Schoenia Steetz Fig. 250.

Grains radially symmetrical, isopolar, oblate-spheroidal, 32-40 x 32-40μ, tricolporate; ora square (3-4μ maximum diameter) to circular (4.5-5μ maximum diameter), mostly congruent with colpi, more rarely with lateral extensions, ± pointed, thickened margins; colpi narrow to wide, thin margined, shallow, reduced in length, not as constricted in polar view; exine surface: spinose, spines 4.5-5μ in length, narrow based, rising sharply to form finely pointed tips, almost conical in form, dense; caveae present.

Electron microscopy (Fig. 312). S. cassiniana is similar to Fig. 6E.

Species examined. S. cassiniana (Gaud.) Stet. (US #916466, BLT

#5360A, 5360B, MO #1971375).

Stenocline DC. Fig. 119.

Grains radially symmetrical, isopolar, oblate-spheroidal, 23-32 x 25-32μ, tricolporate; ora circular to lalongate, rectangular to elliptical in outline (3-4μ maximum diameter), congruent with colpi or with lateral extensions ± pointed, margins thickened; colpi wide, thin margined, deeply sunken, extending equidistant full length of the polar axis, ± distinctly constricted in polar view, to tapering at equator in equatorial view; exine surface: spinulose, spinules mostly less than 2.5μ long, in form of equilateral triangle, not dense, to spinose, spines 3-4μ long, wide based, tapering gradually to form finely rounded tips, dense; caveae present.

Interspecific variation. S. chionaea has the spinulose exine; S. ericoides the spinose type.

Electron microscopy. S. chionaea is similar to Fig. 6D, but with more elongate internal foramina.

Species examined. S. chionaea DC. (US #2124132); S. ericoides DC. (US #808392).

Waitzia Wendl. Fig. 113.

Grains radially symmetrical, isopolar, oblate-spheroidal to prolate-spheroidal, 26-32 x 26-32μ; tricolporate.

Interspecific variation. W. acuminata: ora, a lalongate, slit-like

opening, (2-3μ maximum diameter), the opening appearing as a depression, with lateral extensions ± pointed, margins not thickened; colpi narrow, extending the full length of the polar axis, tapering at the equator, ± distinctly constricted in polar view; exine surface: spinulose, spinules 2-3μ long, wide based, tapering gradually, then terminating in a thin, fine point, not dense. W. citrina and W. suaveolans: ora impossible to delineate with any certainty; colpi not open, but constricted in equatorial view; exine surface: spinose, spines 3-4μ in length, wide based, tapering quickly terminating in a long, thin, fine point, dense; caveae present.

Electron microscopy. W. citrina and W. suaveolens are similar to Fig. 6D.

Species examined. W. acuminata Steetz in Lehm. (MSC #214620); W. citrina Steetz (BLT #5413); W. suaveolens (Benth.) Druce (BLT #5521).

V. ANGIANTHEAE

This subtribe consist of approximately 13 genera and 65 species.

Actinobole Endl.

Grains radially symmetrical, isopolar, oblate-spheroidal, 25-30 x 25-30μ, tricolporate; rarely tetracolporate; ora circular (2.5μ maximum diameter), congruent with colpi, to a slit-like lalongate type with lateral

extensions ± pointed, thickened margins; colpi narrow, thin margined, deeply sunken, extending the full length of the polar axis, tapering at the equator, ± distinctly constricted in polar view, to not open at all, but constricted in equatorial view; exine surface: spinose, spines 3-4μ long, wide based, tapering immediately and quickly, terminating in long, thin, fine points, dense; caveae present.

Electron microscopy. No data available.

Species examined. A. uliginosum (A. Gray) Eichler (MSC #214595).

Angianthus Wendl. Fig. 234.

Grains radially symmetrical, isopolar, oblate-spheroidal to prolate-spheroidal, 20-42 x 20-42μ, tricolporate; ora cannot be delinated with any certainty; the colpi are either constricted in equatorial view in every species examined, totally obscuring the ora, or, when open, the ora are inconspicuous due to no marginal thickening; exine surface: spinose, spinules ca. 2μ in length, wide based, finely tipped, dense, to spinose, spines 3μ in length, more narrow based, tapering immediately, terminating in a long, thin, fine point, not dense; caveae present.

Interspecific variation. A. brachypappus and A. strictus are spinulose; A. cunninghamii and A. tomentosus display the more intermediate form; A. sp. has the longest spines, and is also much larger than the other species studied, averaging at least 12μ larger in both polar and equatorial axes.

Electron microscopy. No data available.

Species examined. A. brachypappus F. Muel. (MSC #187644); A. cunninghamii (DC.) Benth. (MO #1786819); A. strictus (Steetz) Benth. (MSC #187645); A. tomentosus Wendl. (MSC #214564); A. sp. (BLT #5558).

Caesulia Roxb. Fig. 214.

Grains radially symmetrical, isopolar, oblate-spheroidal, 28-31 x 28-32μ, tricolporate; ora lalongate, widely elliptical in outline (4-6.5μ maximum diameter) with lateral extensions, frequently at one side only, margins thickened; colpi wide, shallow, becoming very narrow after the os region, or, more commonly, very reduced in length or extending from the os in an almost inconspicuous shallow form, frequently appearing as one with the os; exine surface: spinose, spines 4μ in length, very wide bases, tapering gradually to form rounded or blunted tips, not dense; caveae present.

Electron microscopy. C. axillaris is similar to Fig. 6B but with many circular internal foramina.

Species examined. C. axillaris Roxb. (MO #1625207).

Calocephalus R. Br.

Grains radially symmetrical, isopolar, oblate-spheroidal, 22-40 x 23-40μ, tricolporate; ora, when conspicuous, circular or square (2.5μ

maximum diameter), to lalongate, elliptical or rectangular in outline (3-4μ maximum diameter), congruent with colpi or with lateral extensions ± pointed, margins thickened, to no marginal thickening; colpi mostly constricted in equatorial view or wide, deeply sunken, thin margined, extending the full length of the polar axis, ± distinctly conspicuous in polar view; exine surface: spinulose, ca. 2μ in length, wide based, finely tipped, dense, to spinose 3-3.5μ in length, with narrow bases, sharply pointed tips, dense, to spinose 4-5.5μ in length, wide based, tapering immediately, terminating in long, thin, fine points, not dense; caveae present.

Interspecific variation. C. knappii and C. francisii are spinulose; C. brownii and C. skirrophora display the more intermediate form; C. drummondii has the longest spines, and is also much larger than the others, averaging at least 10μ larger in both polar and equatorial axes.

Electron microscopy. C. francisii and C. skirrophora are similar to Fig. 6B but with more internal foramina.

Species examined. C. brownii F. Muell. (MSC #194758); C. drummondii (Gray) Benth. (BLT #5559); C. francisii Benth. (BLT #5372); C. knappii (F. v. M.) Ewart and White; (BLT #5390); C. skirrophora (Sond.) Benth. (BLT #5420).

Cephalipterum A. Gray Fig. 156.

Grains radially symmetrical, isopolar, oblate-spheroidal to prolate-

spheroidal, 21-34 x 21-34μ, tricolporate; ora circular, square or lalongate, rectangular in outline (2.4-3μ maximum diameter), margins of this type not obviously thickened, the ora appearing as thinner segments of the colpi, to very large ora, lalongate, rectangular or elliptical in outline, (4-5.5μ maximum diameter), margins thickened, both types mostly congruent with colpi, more rarely with lateral extensions ± pointed; colpi narrow or wide, thin margined, deeply sunken, extending full length of the polar axis, ± distinctly constricted in polar view; exine surface: spinulose, spinules 2.5μ or less in length, wide based, with finely rounded tips, dense, to spinose, spines 3-4μ in length, wide based, tapering immediately terminating in a long, thin, fine point, dense; caveae present.

Intraspecific variation. Two collections (BLT #5350, US #2337560) display the smaller ora, the narrower colpi and the shorter spines, while two others (BLT #5417, BLT #5285) display the alternate conditions described above.

Electron microscopy. C. drummondii (BLT #5417) is similar to Fig. 6E.

Species examined. C. drummondii Gray (BLT #5417, #5285, #5350; US #2337560).

Chthonocephalus Steetz

Grains radially symmetrical, isopolar, prolate-spheroidal, 21-26 x 21-26μ, tricolporate; ora square or round, (2.5-3μ maximum diameter),

congruent with colpi, margins not obviously thickened, so not distinct in many grains; colpi narrow, thin margined, deeply sunken, extending full length of the polar axis, ± distinctly constricted in polar view; exine surface: spinulose, spinules 2.5μ or less in length, wide based with finely rounded tips, dense; caveae present.

Electron microscopy. C. pseudonox (BLT #5269) is similar to Fig. 6D, but has a foot layer: endexine ratio of 1:1, and many elongate internal foramina.

Species examined. C. pseudonox Steetz. (BLT #5269, US #1171044); C. sp. (BLT #5353).

Craspedia Forst. f.

Grains radially symmetrical, isopolar, oblate-spheroidal, 16-35 x 17-38μ, tricolporate; ora round to square (2.5-3μ maximum diameter), congruent with colpi, margins not obviously thickened, so not distinct in many grains, to very large, lalongate, rectangular to elliptical in outline, (3.5-5.5μ maximum diameter) congruent with colpi, margins thickened; colpi narrow to wide, thin margined, deeply sunken, extending the full length of the polar axis, ± distinctly constricted in polar view; exine surface: spinulose, spinules ca. 2μ in length, wide based, finely tipped, dense, to spinose, spines 3-4μ long, tapering gradually to finely tipped points, dense; caveae present.

Interspecific variation. C. chrysantha has the smaller ora, the

narrower colpi and the shorter spines, and averages at least 10μ smaller in both polar and equatorial axes.

Electron microscopy. C. uniflora is similar to Fig. 6B, but with many internal foramina

Species examined. C. chrysantha Benth. (MSC #214558); C. uniflora Forst. (BLT #5453, #5592).

Dimeresia A. Gray Fig. 238-239.

Grains radially symmetrical, isopolar, oblate-spheroidal, 30-37 x 32-40μ, tricolporate; ora square to lalongate, rectangular to elliptical in outline (4-5.5μ maximum diameter), congruent with colpi or with lateral extensions, margins thickened; colpi wide, thin margined, deeply sunken, tapering at equator, ± distinctly constricted in equator; exine surface: spinose, spines 5-6.5μ in length, wide based, tapering gradually to finely rounded tips, not dense; caveae present.

Electron microscopy (Fig. 285). D. howellii (US #2308056) is similar to Fig. 6B.

Species examined. D. howellii Gray (US #2308056, US #1921927).

Gnaphalodes A. Gray Fig. 199, 226.

Grains radially symmetrical, isopolar, oblate-spheroidal, 30-34 x 30-35μ, tricolporate; ora lalongate, rectangular to elliptical in outline (3-5μ maximum diameter), congruent with colpi or with lateral extens-

ions, margins thickened; colpi wide, thin margined, shallow, reduced in length, tapering before reaching the equator in equatorial view, ± distinctly constricted in polar view; exine surface: spinose, spines 3.5-4μ in length, wide based, tapering immediately, terminating in a long, narrow, finely pointed tip, not dense; caveae present.

Electron microscopy. G. condensatum is similar to Fig. 6B.

Species examined. G. condensatum Gray (BLT #5388).

Gnephosis Cass.

Grains radially symmetrical, isopolar, oblate-spheroidal, 19-32 x 19-32μ, tricolporate; ora square to round to slightly rectangular (2.5-3.5μ maximum diameter), margins not heavily thickened so difficult to delineate at times, congruent with colpi, or more commonly with lateral extensions, these extensions symmetrical, forming crescent-moon, lip or spindle-type patterns, which, at times, appear superimposed across the colpus rather than directly enclosed within it; colpi narrow, thin margined, deeply sunken, extending the full length of the polar axis, ± distinctly constricted in polar view; exine surface: spinulose (spinules ca. 2μ in length), wide based, fine tip a minute projection at the center of that base, dense, to spinose, spines 3-3.5μ in length, wide based, tapering to a finely rounded tip; caveae present.

Interspecific variation. G. cyathoppa and G. skirrophora have the spinulose pattern. The other two species are spinose.

Electron microscopy. G. gynotricha and G. skirrophora are similar to Fig. 6B.

Species studied. G. cyathoppa Benth. (US #1994725); G. eriocarpa Benth. (US 2158015); G. gynotricha Diels (BLT #5387); G. skirrophora (Sond et F. v. M.) Benth. (BLT #5577).

Myriocephalus Benth. Fig. 207-209, 212, 232.

Grains radially symmetrical, isopolar, oblate-spheroidal to prolate-spheroidal, 24-39 x 24-39μ, tricolporate; ora difficult to distinguish due to lack of marginal thickenings, when conspicuous, square to slightly rectangular or elliptical in outline (2.5-4μ maximum diameter), congruent with colpi or, more rarely, with lateral extensions ± pointed; colpi wide, deeply sunken, extending the full length of the polar axis to narrow, tapering at the equator, to very reduced; exine surface: spinose, spines 3.5-5μ in length, wide based, tapering immediately to form long, thin, finely pointed tips, not dense; caveae present.

Interspecific variation. M. gracilis has an irregular, superficial pore-type, and the most reduced colpus. A lip-type ora pattern is present in one of the M. stuartii collections (MSC #214560).

Electron microscopy (Fig. 289, 331). M. guerinae and M. stuartii are similar to Fig. 6B (Fig. 289), although Fig. 331, an oblique section through a spine area, depicts what might be incorrectly interpreted as a more complex pattern.

Species examined. M. gracilis (Gray) Benth. (BLT #5337); M. guerinae F. v. M. (BLT #5431); M. rhizocephalus (DC.) Benth. (MSC #214626); M. stuartii (F. v. M. et Sond. ex Sond.) Benth. (MSC #214615, MSC #214560).

Polycline Oliv. Fig. 217, 219.

Grains radially symmetrical, isopolar, oblate-spheroidal to prolate-spheroidal, 29-37 x 29-34μ, tricolporate; ora lalongate, rectangular to irregular in outline (3.5-6.5μ maximum diameter), mostly congruent with colpi, also with lateral extensions, margins thickened; colpi wide, thin margined, shallow, extending full length polar axis, ± distinctly constricted in polar view; exine surface: spinose, spines 3-4μ in length, wide based, tapering gradually to finely rounded points, not dense; caveae present.

Electron microscopy (Fig. 282, 286). P. proteiformis is similar to Fig. 6B.

Species examined. P. proteiformis Humbert (US #1528851); P. psyl-loides Oliv. (US #2127652).

VI. RELHANIEAE

This subtribe consists of approximately 15 genera and 217 species.

Disparago Gaertn. Fig. 70, 75, 79, 81; 230.

Grains radially symmetrical, polar, oblate-spheroidal to prolate-spheroidal, 22-35 x 22-35μ, tricolporate; caveae present.

Interspecific variation. D. anomala, D. ericoides, D. hoffmanniana: ora circular to lalongate, rectangular or elliptical in outline, (3.5μ maximum diameter), mostly congruent with colpi, also with lateral extensions ± pointed, margins thickened; colpi wide, thin margined, shallow, extending the full length of the polar axis, ± distinctly constricted in polar view; exine surface: spinulose, spinules 3μ or less in length, narrow based, finely rounded tips, dense; D. lasiocarpa: ora impossible to delineate with any certainty; colpi not open, but constricted in equatorial view, thus obscuring the ora; exine surface; spinose, spinules 3μ in length, wide based, spaced far apart, finely rounded tips.

Electron microscopy. D. lasiocarpa is similar to Fig. 6B.

Species examined. D. anomala Schltr. (US #1626674); D. ericoides Gaertn. (US #2062510); D. hoffmanniana Schltr. (US); D. lasiocarpa Cass. (MO #1649153).

Elytropappus Cass. Fig. 39-40.

Grains radially symmetrical, polar, oblate-spheroidal, 22-25 x 22-27μ, tricolporate; ora lalongate, rectangular, almost slit-like at times, in outline (2.5-4μ maximum diameter) congruent with colpi or rarely with lateral extensions ± pointed, margins somewhat thickened; colpi narrow, thin margined, deeply sunken, extending full length of polar axis,

tapering at equator in equatorial view, ± distinctly constricted in polar view; exine surface: subspinulose, spinules reduced to knobby projections of the exine, giving an almost lobed or smooth appearance to the surface; caveae present.

Electron microscopy (Fig. 324, 329). E. adpressus is similar to Fig. 6C, but has a more complex columellar pattern.

Species examined. E. adpressus Harv. (US #1627433); E. glandulosus Less. v. pallens (US #1170635).

Metalasia R. Br. Fig. 200, 215-216, 220.

Grains radially symmetrical, polar, oblate-spheroidal, to prolate-spheroidal, 28-34 x 28-34μ, tricolporate; caveae present.

Interspecific variation. M. cephalotea; ora lolongate when conspicuous, rectangular to elliptical in outline (3-4μ maximum length), congruent with colpi, thickened margins; colpi narrow, thin margined, deeply sunken, extending the full length of the polar axis, tapering at equator, not an obvious character in polar view; exine surface: spinulose, spinules 3 μ in length, wide based, spaced far apart, finely rounded tips, almost blunted; M. ericoides: ora lalongate, mostly wide, rectangular or elliptical in outline, congruent with colpi, or a thinner, slit-like rectangle, with lateral extensions ± pointed, forming crescent-moon or lip-like patterns (3-5μ maximum diameter); colpi mostly wide, thin margined, shallow, extending equidistant the full length of the polar axis, or taper-

ing at the equator in equatorial view, ± distinctly constricted in polar view; exine surface: spinose, spines 4.0μ in length, narrow-based, thin, almost conical in form, finely rounded tips, not dense; M. macrocephala, M. muricata: ora as in M. ericoides; colpi as in M. ericoides; exine surface: spinose, spines 4-4.5μ in length, wide-based, tapering very gradually to a finely rounded, almost blunted point, not dense.

Electron microscopy. No data available.

Species examined. M. cephalotea (Thunb.) Less. (MO #1641803); M. ericoides Hutch. (US #1529070); M. macrocephala Schltr. (US #552246); M. muricata R. Br. (MO #1606699; US #1528993).

Nestlera Spreng. Fig. 89, 95; 104-106.

Grains radially symmetrical, polar, oblate-spheroidal, 28-39 x 28-39μ, tricolporate, ora lalongate, elliptical in outline (4-7μ maximum diameter), congruent with colpi or with faint lateral extensions, thickened margins; colpi wide, thin-margined, deeply sunken, extending equidistant the full length of polar axis, ± distinctly constricted in polar view; exine surface: spinulose, spinules 2-3μ in length, present in dense masses, finely tipped; caveae present.

Electron microscopy. N. humilis is similar to Fig. 6B.

Species examined. N. conferta DC. (US #1529006); N. humilis Less. (MO #4679).

Pterothrix DC.

Grains radially symmetrical, isopolar, oblate-spheroidal, to prolate-spheroidal, 28-39 x 28-36μ, tricolporate; ora lalongate, rectangular to widely elliptical in outline (3-4μ maximum diameter), congruent with colpi or with lateral extensions ± pointed, margins thickened; colpi wide, thin margined, deeply sunken in some instances, quite shallow in others, tapering in width immediately after os region, or so reduced that colpus and os seem as one; exine surface: spinulose, spinules less than 3u in length, masses of finely rounded tips; caveae present.

Electron microscopy (Fig. 293). P. flaccida is similar to Fig. 6D but shows a foot layer: endexine ratio of about 1:8.

Species examined. P. flaccida Schltr. (MO); (US #553038).

Relhania L'Herit. Fig. 67; 185, 218.

Grains radially symmetrical, isopolar, oblate-spheroidal, 24-27 x 23-29μ, tricolporate; ora square (3μ maximum diameter) to lalongate, rectangular to elliptical in outline (4-5μ maximum diameter), congruent with colpi or with faint lateral extensions, margins thickened; colpi wide, thin margined, deeply sunken, expanding full length of polar axis, tapering at equator in equatorial view, ± distinctly constricted in polar view; exine surface: spinulose, spinules less than 2μ in length, narrow based, thin, finely pointed, dense, to spinose, spines 3μ in length, wide based, tapering to long, narrow, finely rounded points, not dense; caveae pres-

ent.

Interspecific variation. R. genistaefolia is spinulose; R. quinquinervis displays a spinose pattern.

Electron microscopy. Both species are similar to Fig. 6D but show minute internal foramina.

Species examined. R. genistaefolia L'Herit. (US #1029328; MO #1641165); R. quinquinervis Thunb. (US #1378774).

Stoebe L. Fig. 50, 61; 194.

Grains radially symmetrical, isopolar, oblate-spheroidal, 19-29 x 20-30μ, tricolporate, ora square or circular to rectangular (3.5-4.5μ maximum diameter), margins thickened, congruent with colpi or with lateral extensions; colpi wide, thin margined, deeply sunken, extending full length of the polar axis, ± distinctly constricted in polar view; exine surface: subspinulose, spinules reduced to knobby projections of the exine, giving an almost lobed appearance to the surface, to spinose, spines 4u in length, wide based, tapering gradually to a rather blunt tip, not dense; caveae present.

Interspecific variation. S. spiralis has the subspinulose pattern; the other two species are spinose.

Electron microscopy (Fig. 298). Both species are similar to Fig. 6C, but have thinner columellae in the distal portion of the exine, and smaller internal foramina.

Species examined. S. capitata Berg. (MO #1647810); S. sphaerocephala Schltr. (US #551783); S. spiralis Less. (US #1579550).

Syncephalum DC.

Grains radially symmetrical, isopolar, oblate-spheroidal, 22-24 x 22-24μ; ora lalongate, rectangular to widely elliptical in outline (2.5-5μ maximum diameter), congruent with colpi or with faint lateral extensions, margins thickened; colpi wide, thin margined, deeply sunken, extending full length of the polar axis, ± distinctly constricted in polar view, to very reduced, appearing almost as one with pore; exine surface: spinulose, spinules 2.5μ or less, wide based, tapering to bluntly rounded tips, dense; caveae present.

Electron microscopy (Fig. 299, 308). S. candidum is similar to Fig. 6D.

Species examined. S. candidum Humbert (US #1271903); S. stereoclinoides Humbert (US #2155169).

Zoutpansbergia Hutch. Fig. 131-133.

Grains radially symmetrical, isopolar, prolate-spheroidal, 35-44 x 34-40μ; ora square (3.5-4.5μ maximum diameter) to inconspicuous, margins not heavily thickened; so difficult to distinguish at times, congruent with colpi or with lateral extensions ± pointed; colpi wide, thin margined, deeply sunken, extending full length of the polar axis, very distinctly

constricted in polar view; exine surface: spinulose, spinules 3u in length, wide based, spaced far apart, finely rounded tips, almost blunted; caveae present.

Electron microscopy. Z. caerulea is similar to Fig. 6A but columellae appear somewhat longer.

Species examined. Z. caerulea Hutch. (MO #1667546).

VII. ATHRIXIEAE

This subtribe consists of approximately seven genera and 59 species.

Antithrixia DC. Fig. 111, 116.

Grains radially symmetrical, isopolar, prolate-spheroidal, 27-32 x 26-31μ; ora lalongate, rectangular to widely elliptical in outline (3.5-5μ maximum diameter), with lateral extensions ± pointed, margins thickened, to inconspicuous; colpi long, narrow, sunken, extending the full length of the polar axis, tapering at equator in equatorial view, ± distinctly constricted in polar view; colpi frequently constricted, obscuring pores in at least half the grains; exine surface: spinulose, spinules less than 2.5μ in length, wide based, spaced far apart, bluntly rounded tips, to spinose, spines 3.5-4μ in length, wide based, bluntly tipped, not dense; caveae present.

Interspecific variation. A. abyssinica has the spinulose pattern; A. angustifolia is spinose.

Electron microscopy (Fig. 325, 328). Both species are similar to Fig. 6C.

Species examined. A. abyssinica (Sch. Bip.) B. et H. K. (MO #1620740); A. angustifolia Oliv. et Hiern. (US #945672).

Arrowsmithia DC.

Grains radially symmetrical, isopolar, oblate, spheroidal, 30-34 x 30-35μ; ora impossible to delineate with certainty, faint outlines suggesting a very wide lalongate form with wide colpi; exine surface: spinose, spines 3.5-4μ in length, masses of spines in two patterns: narrow, conical, to wide, triangular, both terminating in finely rounded, almost blunted tips; caveae present.

Electron microscopy. A. stypheloides is similar to Fig. 6D.

Species examined. A. stypheloides DC. (MO #1736047).

Athrixia Ker-Gawl. Fig. 142, 151; 189, 210.

Grains radially symmetrical, isopolar, oblate-spheroidal, 24-33 x 22-35μ; caveae present.

Intra and interspecific variation. A. athrixioides: ora lalongate, rectangular in outline (2.5-3.5μ maximum diameter), when conspicuous, margins not thickened to slightly thickened to very thick; when not thickened at all, appearing simply as faint depressions within the colpus, congruent with it in all observable cases; colpi wide to narrow, thin mar-

gined, deeply sunken, reduced in length, tapering before reaching the equator in equatorial view, ± distinctly constricted in polar view; exine surface: spinose, spines 3.5-4μ in length, wide based, tapering quickly to form long, thin, finely rounded tips, dense; A. australis: ora square to rectangular, (ca. 3μ in diameter), lateral extensions ± pointed, margins thickened; colpi narrow, deeply sunken, extending the full length of the polar axis, tapering at equator in equatorial view, ± distinctly constricted in polar view; exine surface: spinose, spines 4-5μ long, wide based, tapering gradually to form rounded tips, not dense; A. oblonga: ora as in A. australis, but with lalongate detail sometimes very irregular; colpi as in A. australis; exine surface: as in A. australis.

Electron microscopy (Fig. 303, 314, 316). A. athrixioides is similar to Fig. 6E; A. oblonga is similar to Fig. 6D.

Species examined. A. athrixioides (Sond. et F. Muell.) Druce (MSC #214553) (BLT #5575); A. australis Steetz (US #915683); A. oblonga S. Moore (MO #1652069).

Heterolepis Cass. Fig. 255-256.

Grains radially symmetrical, isopolar, oblate-spheroidal to prolate-spheroidal, 42-56 x 44-56μ; ora square (4.5-6.5μ maximum diameter), congruent with colpi or with obvious lateral extensions ± pointed, thickened margins; colpi wide or narrow, if wide at ora tapering immediately, much before equator in equatorial view, thin margined, deeply sunken,

± distinctly constricted in polar view; exine surface: spinose, spines 5-5.5μ long, very widely based, tapering gradually to a blunted tip, not dense; caveae present.

Electron microscopy. H. aliena is similar to Fig. 6A.

Species examined. H. aliena (L.f.) Druce (US #2063056; MO #1602206).

Leyssera Batsch Fig. 51, 68; 127, 130.

Grains radially symmetrical, isopolar, oblate-spheroidal to prolate-spheroidal, 25-37 x 25-37μ; ora inconspicuous to square (2.5-4μ maximum diameter) to lalongate, rectangular to widely elliptical in outline, (4-6μ maximum diameter), congruent with colpi, thickened margins; colpi constricted in equatorial view, obscuring pores, to narrow, deeply sunken, extending full length of polar axis, to wide, deep, extending equidistant the full length of polar axis, or more shallow, reduced in length, ± distinctly constricted in polar view; exine surface: spinulose, spinules less than 2.5μ in length, wide based, rather bluntly tipped, evenly spaced, not dense, to more spinose, spines 3.0μ or more in length, wide based, finely tipped, dense; caveae present.

Interspecific variation: L. capillifolia has inconspicuous to square ora, the narrow or constricted colpi, and the shorter spines. The other two species have the alternate characteristics as described above.

Electron microscopy. L. gnaphalioides is similar to Fig. 6B.

Species examined. L. capillifolia DC. (US #550374); L. gnaphalioides (DC.) Thunb. (MO #1640907); L. tenella DC. (US #553204).

Macowania Oliv. Fig. 167, 172.

Grains radially symmetrical, isopolar, oblate-spheroidal to prolate-spheroidal, 28-34 x 28-34μ; ora circular to lalongate (3-5u maximum diameter or length), congruent with colpi, thickened margins; colpi narrow to wide, thin margined, extending the full length of the polar axis, tapering at equator in equatorial view, ± distinctly congruent in polar view; exine surface: spinose, spines 3.5-4μ long, wide based, tapering smoothly to finely rounded tips, dense; caveae present.

Electron microscopy. M. revoluta is similar to Fig. 6B.

Species examined. M. revoluta Oliv. (MO #1704936; US#807710).

Podolepis Labill. Fig. 138, 144; 201; 246.

Grains radially symmetrical, isopolar, oblate-spheroidal, 24-42 x 24-42μ; ora circular, heavily thickened margins with obvious lateral extensions ± pointed, to lalongate, widely elliptical in outline (2.5-8μ maximum diameter), margins thickened, congruent with colpi; colpi wide, thin margined, deeply sunken, extending full length of the polar axis ± distinctly constricted in polar view, to very reduced in length, appearing as part of a pore-colpus complex in many grains; exine surface: spinose, spines 4μ in length, variable density, wide based, tapering gradually to a

rather blunt tip, to 5μ in length, dense.

Interspecific variation. P. rugata averages 12-14μ longer than the other two species in both polar and equatorial axes, has the longer (5u) spine length, and an os diameter range of 5-8μ; the other two species have the shorter (4μ) spine type (dense in P. cupulata; not dense in P. capillaris) and a narrower (2.5-4.5μ) os range.

Electron microscopy. P. capillaris is similar to Fig. 6B but has very large internal foramina.

Species examined. P. capillaris (Steetz.) Diels (MO #1796965); P. cupulata Maiden et Betche (US #1940455); P. rugata Labill. (MSC # 214580).

VIII. INULINEAE

This subtribe consists of approximately 27 genera and 357 species.

Adenocaulon Hook. Fig. 29-31.

Grains radially symmetrical, isopolar, prolate-spheroidal, 27-36 x 26-32μ; ora rectangular or elliptical in outline or a simple depression at and crossing the midcolpal region, not distinctly thickened, the colpus even constricting at that area in some grains; colpus very narrow, thin margined, deeply sunken, extending the full length of the grain, distinctly constricted in polar view; exine surface: subspinulose, so reduced that the exine appears almost smooth, except for infrequent "knob-like"

projections; caveae not present.

Electron microscopy (Fig. 270). A. bicolor is similar to Fig. C but has thinner upper columellae and a slightly imperforate tectum.

Species examined. A. bicolor Hook. (TEX #199365; MSC #159361; OKL #576).

Allagopappus Cass.

Grains radially symmetrical, isopolar, oblate-spheroidal, 27-31 x 26-31μ; ora lalongate, rectangular in outline (5-6.5μ maximum diameter), with lateral extensions ± pointed, margins thickened; colpin wide, thin margined, very shallow, somewhat reduced, ± distinctly constricted in polar view; exine surface: spinose, spines ca. 3-4μ in length, narrow based, tapering gently to finely rounded tips, almost an equilaterally triangular form, dense; caveae present.

Electron microscopy (Fig. 277). A. dichotomus is similar to Fig. 6A.

Species examined. A. dichotomus Cass. (MO).

Amblyocarpum Fisch. et Mey. Fig. 205.

Grains radially symmetrical, isopolar, oblate-spheroidal, 22-26 x 24-30μ; ora lalongate, narrowly rectangular in outline (5-6.5μ maximum diameter), lateral extensions symmetrical, forming a common, elongated

"lip" pattern, thickened margins; colpi narrow, thin margined, deeply sunken, extending the full length of the polar axis, tapering at equator, ± distinctly constricted in polar view; exine surface: spinose, spines 4μ in length, wide based, tapering gradually to rounded or blunted tips, not dense; caveae present.

Electron microscopy (Fig. 279). A. inuloides is similar to Fig. 6A.

Species examined. A. inuloides F. v. M. (US #2189196).

Calostephane Benth.

Grains radially symmetrical, isopolar, prolate-spheroidal, 32-40 x 30-36μ; ora mostly square (4μ maximum diameter), with lateral extensions often symmetrical, forming an elongated "lip" pattern, thickened margins; colpi narrow, thin margined, sunken, extending the full length of the polar axis, or very reduced in length, more shallow; exine surface: spinose, spines 4μ in length, wide based, tapering gradually to rounded or blunted tips, dense; caveae present.

Electron microscopy (Fig. 275). C. divaricata is similar to Fig. 6A.

Species examined. C. divaricata Benth. (MO #1603178).

Carpesium L. Fig. 157, 162; 235-236.

Grains radially symmetrical, isopolar, oblate-spheroidal to prolate-spheroidal, 29-36 x 30-35μ; exine surface: spinose, spines 4-5μ in length, wide based, tapering gradually to rounded or blunted tips, variable dens-

ity; caveae present.

Interspecific variation. C. abrotanoides: ora narrow, slit-like without lateral extensions or extended only on one side, or "lip"-like in form (4-8μ maximum diameter), thickened margins; colpi almost completely reduced, visible in faint outline, very shallow, thin margined; spines dense. C. cernuum: ora rectangular or irregular in form (3-6μ maximum diameter), lateral extensions on one side only, thickened margins; colpi as above, or at times more deeply sunken, narrow, extending the full length of the polar axis, spines not dense.

Electron microscopy. No data available.

Species examined. C. abrotanoides L. (US #2064977); C. cernuum L. (US #1757423).

Codonocephalum Fenzl. Fig. 163, 178.

Grains radially symmetrical, isopolar, oblate-spheroidal, 33-40 x 36-40μ ora very large, lalongate, rectangular to widely elliptical in outline (5-8μ maximum diameter), with lateral extensions at one or both sides, thickened margins; colpi wide, much reduced in length and depth, recognizable only in faint outline, or as a very shallow depression, not seen as a distinct character in polar view; exine surface: spinose, spines ca. 3μ in length, narrow based, tapering to a finely rounded tip, equilaterally triangular in form, dense; caveae present.

Electron microscopy. C. peacockianum is similar to Fig. 6A.

Species examined. C. peacockianum Aitch. et Hemsl. (MO)

Grantia Boiss. Fig. 224-225, 227.

Grains radially symmetrical, isopolar, oblate-spheroidal, 32-40 x 31-37μ; ora lalongate, a flattened ellipse in outline, (4-8μ maximum diameter), lateral extensions symmetrical, margins thickened, colpi very thickened; colpi very wide in region of pore, narrowing immediately, and very reduced in length, thin margined, shallow, not an immediately distinct character in polar view; exine surface: spinulose, spinules 2.5-3.5μ in length, wide based, tapering gradually, then narrowing quickly to a long, finely rounded tip, not dense; caveae present.

Electron microscopy (Fig. 284, 288). G. aurliuz is similar to Fig. 6B.

Species examined. G. aurliuz Boiss. (MO #1619483).

Inula L. Fig. 160-161, 165, 168, 176-177; 184, 193.

Grains radially symmetrical, isopolar, oblate-spheroidal, 22-37 x 24-40μ; ora lalongate to irregular, forming a "lip" pattern, flattened to widened rectangular to flattened elliptical in outline (4-8μ maximum diameter), congruent with colpi or, mostly, with symmetrical lateral extensions, margins thickened; colpi narrow, thin margined, extending full length of the polar axis, tapering at the equator in equatorial view, or, mostly, much reduced in length and depth, recognizable only in faint

outline, or as a very shallow depression, not seen as a distinct character in polar view; exine surface: spinose, spines 3-4μ in length, wide based, tapering gradually to an almost blunted tip, dense, to narrow based, tapering quickly, almost conical in form, to a finely rounded tip, dense; caveae present.

Interspecific variation. I. graveolens alone has spines in a conical form. The narrow, deeply sunken colpus was observable only in I. britannica and I. germanica, and in these species the wider, more shallow and reduced form is also presented.

Electron microscopy. I. helenium is similar to Fig. 6A.

Species examined. I. bifrons L. (MSC #186344); I. britannica L. (MSC #191995); I. candida (L.) Cass. (MSC #191562); I. conyza DC. (MSC #84781); I. germanica L. (MSC #191999); I. graveolens (L.) Desf. (OKL #509; MSC #84820); I. helenium L. (OKL #509; MSC #84820); I. salicina L. (MSC #84794).

Iphiona Cass. Fig. 174-175.

Grains radially symmetrical, isopolar, oblate-spheroidal, 32-35 x 32-36μ; ora lalongate, rectangular in outline (4-8μ maximum diameter), mostly congruent with colpi, also with lateral extensions, margins thickened; colpi narrow, thin margined, deeply sunken, extending full length of polar axis, tapering at equator in equatorial view, to reduced in length and depth, recognizable as a very shallow, finely outlined depression,

not seen as a distinct character in polar view; exine surface: spinose, spines 4μ in length, very wide based, tapering very gradually to finely rounded tips, dense; caveae present.

Electron microscopy. I. scalra is similar to Fig. 6A.

Species examined. I. scalra DC. (MO #1619483).

Jasonia Cass.

Grains radially symmetrical, isopolar, oblate-spheroidal, 28-35 x 30-35μ; ora lalongate, rectangular in outline (4-5μ maximum diameter), congruent with colpi, margins thickened; colpi wide, thin margined, extending full length of the polar axis, but much reduced in depth, very shallow, appearing only as a slight depression, not a distinct character in polar view; exine surface: spinose, spines 5-5.5μ in length, narrow based, very long, narrow and tapering to a thin, fine point, dense; cavea present.

Electron microscopy. J. sicula is similar to Fig. 6A.

Species examined. J. sicula DC. (MO #1796089).

Pegolettia Cass. Fig. 223

Grains radially symmetrical, isopolar, oblate-spheroidal, 27-37 x 28-38μ; ora lalongate, broadly elliptical in outline (5-8μ maximum diameter); lateral extensions, margins thickened; colpi wide, but very reduced in length and depth, very shallow, appearing only as a slight depres-

sion, not as a distinct character in polar view; exine surface: spinose, spines 3.5-4.5μ in length, wide based, tapering gradually to a finely rounded tip, not dense; caveae present.

Electron microscopy. P. senegalensis is similar to Fig. 6D.

Species examined. P. senegalensis Cass. (MO #1761463).

Perralderia Cass. Fig. 170.

Grains radially symmetrical, isopolar, oblate-spheroidal, 29-32 x 29-32μ; ora lalongate, mostly rectangular to irregularly circular in outline (3-8μ maximum diameter), with lateral extensions, forming a wide "lip" pattern in some instances, margins thickened; colpi wide, very shallow, distinguishable only in faint outline, not a distinct character in polar view, to, rarely, narrow, long, deep; exine surface: spinose, spines 3-4μ maximum diameter, narrow based, tapering gradually to finely rounded tips, very dense; caveae present.

Electron microscopy. Both collections are similar to Fig. 6A.

Species examined. P. coronopifolia Cass. (MO #1715328; US #550371).

Printzia Cass. Fig. 231, 233.

Grains radially symmetrical, isopolar, oblate-spheroidal, 28-40 x 32-38μ; ora rectangular to circular to irregular in outline (4-6μ maximum diameter), congruent with colpi or with lateral extensions, margins

thickened; colpi narrow, thin margined, deeply sunken, extending full length of the polar axis, distinctly visible in polar view, to wide, reduced in length and width, visible as a shallow depression only; exine surface: spinulose, spinules mostly ca. 2.5μ in length, dense, to spinose, 3.5-4μ in length, both wide based, tapering gradually to finely rounded tips, not dense; caveae present.

Interspecific variation. P. densifolia is spinulose; P. pyrifolia is spinose.

Electron microscopy. P. densifolia is similar to Fig. 6D.

Species examined. P. densifolia Wood et Evans (MO); P. pyrifolia Less. (US #1175735).

Pulicaria Gaertn. Fig. 251.

Grains radially symmetrical, isopolar, oblate-spheroidal; caveae present.

Interspecific variation. P. dysenterica 23-25 x 24-26μ; ora wide, rectangular to almost circular in outline (4-5μ maximum diameter), mostly congruent with colpi, also with lateral extensions, margins thickened; colpi wide, very reduced in length and depth, visible as a shallow depression; exine surface: spinose, spines 4.5μ in length, narrow based, thin, almost conical, with rounded tips, dense. P. sicula. 31-37 x 31-38μ; ora square to lalongate, rectangular in outline, (4-8μ maximum diameter), congruent with colpi, mostly with symmetrical lateral exten-

sions, margins thickened; colpi narrow, thin margined, deeply sunken, extending the full length of polar axis, ± distinctly constricted in polar view, to wide, reduced in length and width, visible only as a shallow depression; exine surface: spinose, spines 5μ in length, wide based, tapering gradually to finely rounded tips, dense.

Electron microscopy. P. dysenterica is similar to Fig. 6A.

Species examined. P. dysenterica L. (OKL #3160); P. sicula Moris (MSC #84784).

Varthemia DC. Fig. 180-182.

Grains radially symmetrical, isopolar, prolate-spheroidal, 35-45 x 35-39μ; ora circular to lalongate, rectangular to irregular in outline, (4-7μ maximum diameter), congruent with colpi or with lateral extensions, thickened margins; colpi narrow, thin margined, deeply sunken, running full length of polar axis, to wide, reduced in length and width, appearing only as a shallow depression, both distinctly constricted in polar view; exine surface: spinose, spines 3.5-4μ in length, wide based, tapering gradually to finely rounded tips, dense; caveae present.

Electron microscopy. V. iphionoides is similar to Fig. 6A.

Species examined. V. iphionoides Boiss. (MO).

IX. BUPHTHALMEAE

This subtribe consists of approximately 20 genera and 144 species.

Anisopappus Hook. et Arn. Fig. 117, 122, 124-126.

Grains radially symmetrical, isopolar, prolate-spheroidal, 28-36 x 26-32μ; ora lalongate, rectangular to widely elliptical in outline (5-8μ maximum diameter), congruent with colpi or, mostly, with symmetrical lateral extensions, margins thickened; colpi wide, thin margined, shallow, extending the full length of the polar axis, tapering at the equator in equatorial view, to very shallow, rarely, observable only in faint outline, colpus and pore almost appearing as one, ± distinctly constricted in polar view; exine surface: spinulose, spinules 2.5-3μ in length, wide based, tapering to finely rounded tips, not dense; caveae present.

Electron microscopy. A. kirkii is similar to Fig. 6B.

Species examined. A. kirkii (Oliv.) Brenan (MSC #1796156); A. smutsii Hutch. (US #2377178).

Anvillea DC. Fig. 152, 159, 169.

Grains radially symmetrical, isopolar, oblate-spheroidal, 26-37 x 28-36μ; ora lalongate, rectangular to widely elliptical or circular in outline (4-8μ maximum diameter), congruent with colpi or, mostly, with symmetrical lateral extensions; colpi wide, thin margined, quite shallow, extending the full length of the polar axis, tapering at the equator in equatorial view, to very shallow, observable only in faint outline, in some instances colpus and pore almost appearing as one, ± distinctly constricted in polar view; exine surface: spinulos, spinules 2.5-3μ in

length, wide based, tapering to finely rounded tips; dense; caveae present.

Electron microscopy. A. garcini is similar to Fig. 6A.

Species examined. A. australis Clevall. (US #550547); A. garcini (Burm.) DC. (MO #3214; NY); A. radiata Cass. (US #1666913).

Buphthalmum L. Fig. 153.

Grains radially symmetrical, isopolar, obalte-spheroidal to prolate-spheroidal, 28-32 x 28-32μ; ora lalongate, slit-like or more openly rectangular in form (2.5-5μ maximum diameter) lateral extensions on one margin only or, mostly, symmetrical, thickened to obscure margins; colpi narrow if ora are slit-like, or wide, if ora are more openly rectangular, thin margined, sunken, tapering before reaching equator in equatorial view, ± distinctly conspicuous in polar view; exine surface: spinose, spines ca. 4μ in length, wide based, tapering gradually to rounded tips, dense; caveae present.

Electron microscopy. B. salicifolium is similar to Fig. 6A.

Species examined. B. salicifolium L. (TEX #150553; OKL #12213; MSC #84762).

Callilepis DC. Fig. 123, 128-129.

Grains radially symmetrical, isopolar, oblate-spheroidal, 35-39 x 32-39μ; ora square to lalongate, rectangular to slightly irregular in form

(2.5-6μ maximum diameter), symmetrical lateral extensions producing, in cases, a "lip" pattern, margins thickened; colpi wide, thin margined, sunken, tapering at equator, ± distinctly constricted in polar view; exine surface: spinulose, spinules 2.5μ in length, wide based, widely separated, bluntly tipped, not dense; caveae present.

Electron microscopy (Fig. 291). C. laureola is similar to Fig. 6D but shows traces of minute internal foramina, and a foot layer: endexine ratio of about 1:6.

Species examined. C. laureola DC. (NY); C. leptophylla Harv. (US #1378772).

Chrysophthalmum Sch. Bip. Fig. 188, 222.

Grains radially symmetrical, isopolar, prolate-spheroidal, 30-35 x 28-33u; oralongate, rectangular to slightly irregular in outline (4-8μ maximum diameter), symmetrical lateral extensions producing, in most grains, a "lip" pattern; margins thickened; colpi wide, thin margined, sunken, tapering at equator, ± distinctly conspicuous in polar view; exine surface: spinose, spines 3-4μ in length, wide based, tapering gradually to rounded tips, not dense; caveae present.

Electron microscopy (Fig. 290). C. sternutatorium is similar to Fig. 6D.

Species examined. C. sternutatorium Sch. Bip. (US #482335).

Geigeria Less. Fig. 206; 249.

Grains radially symmetrical, isopolar, oblate-spheroidal to prolate-spheroidal; 28-41 x 28-41μ; caveae present.

Interspecific variation. G. aspera and G. brevifolia: oblate-spheroidal; ora lalongate, rectangular to widely elliptical in form (4-6.5μ maximum diameter), symmetrical lateral extensions forming a "lip" pattern in some grains, margins thickened; colpi wide, thin margined, narrow and deep in some grains, or very shallow and reduced in length if the pore is especially large, colpus and pore almost appearing as one; exine surface: spinose, spines 4.5-6μ in length, wide based, tapering gradually at first, then very swiftly to form long, thin, finely pointed tips, dense; G. vigintisquamea: prolate-spheroidal; ora cannot be delineated with any certainty; colpi are constricted in equatorial view; exine surface: spinose, spines 3-4μ in length, wide based, tapering gradually to finely rounded tips, spaced far apart, not dense.

Electron microscopy (Fig. 287). G. vigintisquamea is similar to Fig. 6B but has larger internal foramina.

Species examined. G. aspera Harv. (US #2377215); G. brevifolia Harv. (US #2062918; MO #1610675); G. vigintisquamea O. Hoffm. (MO #1762928).

Gymnarrhena Desf. Fig. 26-28.

Grains radially symmetrical and isopolar, oblate-spheroidal, 28-34 x 30-36μ; tricolporate; ora difficult to delimit with certainty due to the

poor acetolysis of the grains as well as the position of most of the grains on the slide. However, a wide variety of types seems present, ranging from lalongate (3-4μ maximum diameter), with lateral extensions, to lolongate (3-4μ maximum length), congruent with colpi, all with thickened margins; colpi wide, deeply sunken, thin margined, ± distinctly constricted in polar view; exine surface: spinulose, spinules very tiny (less than 2μ long), pointed and widely spaced; no caveae present.

Electron microscopy (Fig. 268). G. micrantha is similar to Fig. 5C, but has a more complex upper columellar pattern.

Species examined. G. micrantha Desf. (NY); (MO).

Odontospermum Neck. ex Sch. Bip. Fig. 213.

Grains radially symmetrical, isopolar, oblate-spheroidal, 28-32 x 28-32μ; ora lalongate, rectangular to widely elliptical in outline (4-6.5μ maximum diameter), congruent with colpi or with symmetrical lateral extensions; margins thickened; colpi wide, shallow, tapering immediately after the pore region, very reduced in length, ± distinctly conspicuous in polar view; exine surface: spinose, spines ca. 3μ in length, wide based, tapering gradually to finely rounded tips, not dense; caveae present.

Electron microscopy (Fig. 276). O. maritimum is similar to Fig. 6A, but the foot layer: endexine ratio is about 1:5 or 1:6.

Species studied. O. maritimum Sch. Bip. (MO #1733914).

Ondetia Benth. Fig. 164.

Grains radially symmetrical, isopolar, oblate-spheroidal, 30-33 x 30-34μ; ora lalongate, rectangular to widely elliptical in outline (5.5-8μ maximum diameter), symmetrical lateral extensions, thickened margins; colpi wide, shallow, visible in superficial outline, extending the full length, almost co-existent with the ora in some grains, ± distinctly conspicuous in polar view; exine surface: spinose, spines 4-5μ in length, wide based, tapering gradually to finely rounded tips, dense; appears non-caveate with light microscopy, but there is no EM work to substantiate this observation.

Electron microscopy: No data available.

Species examined. O. linearis Benth. (MO #1647302).

Osmites L. Fig. 32-34.

Grains radially symmetrical, isopolar, oblate-spheroidal, 32-37 x 32-38μ; ora square to circular (3-4.5μ maximum diameter), congruent with colpi, margins thickened; colpi narrow, thin margined, deeply sunken, extending the full length of the polar axis, ± distinctly conspicuous in polar view; exine surface: spinose, spines ca. 4μ in length, narrow based, tapering gradually to finely rounded tips, not dense; caveae not present.

Electron microscopy (Fig. 266). O. parvifolia is similar to Fig. 6B.

Species examined. O. angustifolia (DC.) (US #1991285); O. parvifolia DC. (MO #1624969).

Osmitopsis Cass. Fig. 35-36.

Grains radially symmetrical, isopolar, oblate-spheroidal, 34-43 x 36-46μ; ora varied, irregular to slit-like in outline (4-5.5μ maximum diameter), frequently not well defined, thin margined, congruent with colpi or with lateral extensions, in all cases very flattened, i.e., from pole to pole, in dimension; colpi deeply sunken to shallow, narrow to wide, in all cases extending the full length of the polar axis, very conspicuous in polar view; exine surface: spinose, spines 5-5.5μ in length, wide based, tapering gradually to finely rounded tips, not dense; caveae not present.

Electron microscopy (Fig. 267, 269). O. asteriscoides (both collections) is similar to Fig. 5B.

Species examined. O. asteriscoides (L.) Cass. (US #1179808; (MO).

Pallenis (Cass.) Cass.

Grains radially symmetrical, isopolar, oblate-spheroidal, 22-28 x 24-30μ; ora square to lalongate, rectangular to widely elliptical in outline (3-5.5μ maximum diameter), congruent with colpi or with symmetrical lateral extensions, margins thickened; colpi long, narrow, deep in case of square ora, more widened, somewhat reduced in length and depth in the lalongate forms, tapering at the equator in both instances, ± distinctly constricted in polar view; exine surface: spinose, spines 3-4μ

in length, wide based, tapering to bluntly rounded tips, dense; caveae present.

Electron microscopy. No data available.

Species examined. P. spinosa (L.) Cass. (MSC #187600); P. spinosa Cass. (OKL #1162).

Philyrophyllum O. Hoffm. corr. Schinz. Fig. 112.

Grains radially symmetrical, isopolar, prolate-spheroidal, 24-29 x 21-26μ; ora cannot be delineated with any certainty, since the colpi are constricted in equatorial view, providing no information about size, etc., of any apertures, except that the colpi extend the full length of the polar axis, tapering at the equator in equatorial view and distinctly constricted in polar view; exine surface: subspinulose, spines ca. 1.5μ in length; not dense; caveae present.

Electron microscopy. P. schinzii is similar to Fig. 6A.

Species examined. P. schinzii O. Hoffm. (MO #1794220).

Rhanterium Desf.

Slides too poor for light determinations.

Electron microscopy (Fig. 274). R. adpressum is similar to Fig. 6A.

Species examined. R. adpressum Cass et Dur. (MO #1098551; US #1674002).

Table 1. Genera and species studied, with averaged specific characteristics.

Species	P (μ)	E (μ)	Spine length (μ)	Pore width (μ)	Identifying number if more than one collection of the same species was studied
TARCHONANTHEAE					
Brachylaena					
discolor	27	25	**	***	
elliptica	30	26	**	***	
hutchinsii	29	27	**	***	EA 4
hutchinsii	30	29	**	***	US 1373483
nereifolia	32	30	**	***	
rhodesiana	26	26	**	***	
rotundata	29	25	**	2.8	
transvallensis	27	26	**	***	
uniflora	27	25	**	***	
Tarchonanthus					
angustissimus	29	28	**	***	
camphoratus	25	23	**	3.1	MO 1646623
camphoratus	27	25	**	3.1	US 9047
camphoratus	28	25	**	4.0	US 2247
camphoratus	30	26	**	3.2	US 2247291
minor	29	26	**	***	
PLUCHEINEAE					
Blumea					
ambigua	24	24	3.0	***	
laciniata	31	32	4.5	5.6	
mollis	27	28	3.7	4.0	

Symbols used

*: fewer than 10 grains measured

**: less than 1μ in length

***: not well defined; difficult to measure with accuracy

Table 1 (cont'd)

Denekia					
copensis	24	25	3.2	3.1	
Epaltes					
cunninghamii	19	20	2.6	4.3	
mexicana	24	26	3.0	3.1	
Laggera					
alata	30	32	4.0	6.3	
brevipes	26	28	3.6	4.5	
Nanothamnus					
sericeus	35	37	6.1	6.8	
Pluchea					
camphorata	30	31	3.6	4.3	
foetida	28	29	4.4	5.1	
odorata*	27	27	3.3	4.5	
Pterigeron					
liatroides	32	33	5.4	3.3*	
Pterocaulon					
interruptum	22	23	2.9	***	
sphacelatum	23	24	2.8	***	MSC 187662
sphacelatum	23	24	2.6	***	MSC 214577
undulatum	32	31	5.2	3.2	
virgatum	27	27	4.4	3.9	
Rhodogeron					
coronopifolius	36	38	5.5	5.6	
Sachsia					
polycephala	33	35	4.2	4.8	
Sphaeranthus					
africanus	25	26	4.2	6.5	
Stenachenium					
campestre	32	35	3.1	9.9	
riedelii	48	47	5.0	5.3	
Tessaria					
integrifolia	28	30	4.3	5.2	
Thespidium					
basiflorum	25	27	2.4	5.7	
Triplocephalum					
holtsii	26	27	4.0	4.6	
FILAGINEAE					
Athroisma					
laciniata	28	29	3.8	4.4	
Blepharispermum					
zanquebaricum	24	21	1+	***	

Table 1 (cont'd)

Cylindrocline						
commersoni	29	31	3.1	4.5		
Evax						
candida	23	23	1+	3.0*		
multicaulis	24	23	**	3.3	OKL	295
multicaulis	20	22	1+	***	MSC	80262
multicaulis	no measurements made				TEX	150585
prolifera	25	24	1+	***	OKL	4309
prolifera	22	21	1+	***	MSC	80628
rotundata	24	22	**	***		
Filago						
arizonica*	28	29	1+	***		
arvensis	22	23	1+	2.4		
californica*	25	23	1+	***		
germanica*	24	24	1+	3.2*		
logopus	24	24	1+	3.5*		
montana	22	23	2+	2.4*		
[1] Gymnarrhena						
micrantha	30	32	1+	***	MO	1592062
micrantha*	29	30	1+	***	NY	
Ifloga						
fontanesii	no measurements made					
seriphioides	20	21	1+	2.9		
Micropsis						
heiteri	24	25	1+	3.2*		
Micropus						
bombycinus	22	23	1+	2.7		
californicus	25	25	1+	2.9	MO	1715308
californicus	25	24	1+	2.4*	MSC	196660
Psilocarphus						
brevissimus	22	22	1+	2.4		
oregonus	23	24	**	2.2		
tenellus	23	22	**	2.4*	MSC	80871
tenellus	18	19	**	2.8	MO	1160565
Stylocline						
filaginea*	23	23	1+	5.1+	OKL	3170
filaginea	23	24	1+	2.2*	MSC	80879
gnaphalioides	24	24	1+	4.7		
Symphyllocarpus						
exilis	22	22	2.0	***		

GNAPHALIEAE - Series 1

Achyrocline

Table 1 (cont'd)

Achyrocline						
vargasiana	26	26	2.9	***		
Amphidoxa						
gnaphalioides	24	24	3.2	3.2		
Anaphalis						
briscus*	22	22	1+	3.2		
margaritica	28	27	2.0	3.2*		
Antennaria						
campestris	no measurements made					
microphylla	30	28	2.8	3.2*		
neglecta	29	28	2.4	4.0		
pulcherrina	31	30	2.6	4.7		
plantaginifolia	no measurements made					
umbrinella	35	32	2.4	3.8		
Artemisiopsis						
villosa	19	19	1+	3.1		
Chevreulia						
acuminata	23	24	1+	2.8*		
stolonifera	23	24	1+	***		
Chiliocephalum						
shimperi	24	23	2.4	***		
Chionolaena						
isabellae	26	26	2.4	3.6		
lychnophoroides*	30	27	3.2	3.6		
Desmidium						
filagineum	20	18	1+	***		
Facelis						
retusa	28	28	1+	3.7*	OKL	
retusa	26	27	2.6	3.9	NY	
retusa*	26	26	1+	4.8	OKL	
Gnaphalium						
americanum	23	23	2.4	3.2		
cheiranthifolium	29	29	3.5	3.3		
luteoalbum	23	24	3.1	3.0		
macounii	27	27	3.1	3.5		
obtusifolium	28	29	3.1	3.7		
palustre	25	27	1+	3.5		
polycephalum	28	29	3.3	3.2		
purpureum	22	24	1+	3.2		
stachydifolium	22	24	1+	4.0		
uliginosum	22	22	2.6	3.0		
Lasiopogon						
muscoides	21	22	1+	2.9	NY	
muscoides	21	21	1+	2.9	MO	1740265

Table 1 (cont'd)

Lasiopogon						
muscoides	21	21	1+	3.1	NY	
Leontopodium						
alpinum	25	25	2.0	4.0		
andersonii	27	28	3.0	3.5		
artemisifolium	26	28	3.0	3.5		
Loricaria						
thuyoides	24	25	**	4.0	MO	16512588
thuyoides	27	25	**	4.7	MO	1593351
Luciliopsis sp.	24	23	1+	3.4		
Oligandra						
lycopodioides	23	24	2.6	3.5	MO	932719
lycopodioides*	30	30	4.0*	4.3	US	2427653
Ondetia						
linearis	no measurements taken					
Phagnalon						
rupestre	30	30	3.8	3.5		
sordidum	25	26	3.1	3.2		
Psila						
bolivensis	21	22	2.6	3.0		
trinervis	24	24	2.5	3.0		
Raoulia						
australis	22	22	**	3.5		
glabra	25	25	2.4	3.5		
monroi	22	22	2.3	3.1		
parkii	23	24	2.0	3.0		
Stuartina						
muelleri	19	20	1+	3.2		
hamata	18	19	1+	2.1*		
Stuchertiella						
capitata	21	21	1+	2.9		
GNAPHALIEAE - Series 2						
Acomis						
macra	28	29	4.0	4.3		
rutidosis	30	31	4.5	3.2		
Ammobium						
olatum	24	24	2.2	3.6		
Amaxeton						
aspenum	22	22	2.6	3.1	MO	1603722
aspenum	25	25	3.2	3.3	US	552322
Cassinia						
fulvida	25	24	2.4	3.2		

Table 1 (cont'd)

Cassinia						
leptophylla	25	25	3.0	3.3		
retorta	22	22	2.7	3.2*		
Eriochlamys						
behrii	23	23	2.4	***		
Gilruthia						
osbornii	30	29	4.0	3.5		
Helichrysum						
ambiguus	33	34	2.0	***		
bracteatum	40	40	6.4	4.5		
davenportii	35	35	5.0	4.2		
Helipterum						
australe	32	33	4.0	3.4		
battii	33	34	**	5.0		
manglesii	35	35	4.5	3.4		
roseum	30	30	3.9	3.4		
spicatum	25	26	2.6	2.6		
splendidum	29	29	4.0	3.9		
Humea						
cassiniana	26	26	2.7	3.3		
elegans	23	23	**	3.2		
Ixiolaena						
tomentosa	32	33	2.8	3.7	MSC	214574
tomentosa	30	30	2.7	2.8	MSC	214608
Ixodia						
schilleoides	29	29	3.5	3.4		
Leontonyx						
bicolor	23	23	1+	3.4		
glomeratus	21	22	1+	2.6		
spathulatus	23	24	2.9	2.0		
Leptorhynchus						
tetrachaetum	26	27	3.3	3.0		
waitzia*	33	33	3.8	4.0	BLT	5588
waitzia	29	30	3.4	3.4	MSC	214588
Leucopholis						
capitata	26	25	2.0	3.0		
Millotia						
myostidifolia	32	30	4.1	3.7	BLT	5482
myostidifolia	25	26	3.4	3.0	MSC	187619
tenuifolia*	38	37	4.2	***		
Petalacte						
coronata	26	27	2.5	4.3		
Petalactella						
woodii	21	22	2.4	2.8		

Table 1 (cont'd)

Phacellothrix						
cladochaeta*	31	29	4.2*	4.2*		
Phaenocoma						
prolifera	27	28	2.8	4.4		
Pithocarpa						
corymbulosa	31	31	3.4	2.6	US	916437
corymbulosa	27	28	3.5	3.4	MO	1794625
Podosperma						
gnaphalioides	47	46	4.9	5.1		
Quinetia						
urvillei	26	26	2.9	3.3		
Rutidosis						
helichrysoides*	29	29	3.4	3.0		
multiflorum	22	22	2.5	2.5*		
Schoenia						
cassiniana	32	32	4.6	4.9	BLT	5360(A)
cassiniana	37	37	5.3	6.1	BLT	5360(B)
cassiniana	36	36	4.6	3.9	US	916466
cassiniana	36	36	5.3	3.7	MO	1971375
Stenocline						
chionaea	25	26	2.4	3.8		
ericoides	27	28	3.2	3.6		
Waitzia						
acuminata*	29	29	2.4	2.4		
citrina	28	28	3.2	***		
suaveolens*	32	29	3.8	***		
ANGIANTHEAE						
Actinobole						
uliginosum	28	28	3.7	***		
Angianthus						
brachypappus	22	23	2.0	***		
cunninghamii	27	26	3.2	***		
strictus	27	27	3.2	***		
tomentosus	21	21	2.5	***		
sp.	38	38	4.4	***		
Caesulia						
auxillaris	30	30	4.0	5.7		
Calocephalus						
brownii	24	25	3.0	***		
drummondii	38	38	4.6	***		
francisii	no measurements made					

Table 1 (cont'd)

Calocephalus						
knappii	27	27	2.0	***		
skeirrophora	32	32	3.3	4.0*		
Cephalipterum						
drummondii	28	28	3.5	4.5	BLT	5417
drummondii	31	30	3.2	3.8*	BLT	5285
drummondii	24	24	1+	2.5	BLT	5350
drummondii	22	22	1+	2.5	US	2337560
Chthonocephalus						
pseudonox	24	24	2.5	***		
pseudonox	24	23	2.0	***	US	1171044
Craspedia						
chrysantha	18	19	1+	2.5		
uniflora	26	27	3.1	3.2	BLT	5592
uniflora	31	32	3.2	4.2	BLT	5453
Dimeresia						
Howellii	33	34	5.6	4.6	US	1921927
Howellii	34	35	5.6	5.1	US	2308056
Gnaphalodes						
condensatum	32	32	3.4	3.0		
Gnephosis						
cyathoppa	20	20	1+	***		
eriocarpa	24	24	2.2	2.9*		
gynotricha	29	29	2.5	***		
skirrophora	25	25	1+	***		
Myriocephalus						
gracilis	32	31	4.0	***		
guerinae	36	35	4.4	4.0		
rhizocephalus	26	26	3.2	***		
stuartii	30	30	4.5	3.9*	MSC	214615
stuartii	34	31	3.9	2.5	MSC	214560
Polycline						
proteiformis	33	32	3.6	3.5*		
psylloides	30	32	3.4	4.4		
RELHANIEAE						
Disparago						
anomala	24	25	2.7	3.4		
ericoides	25	25	2.4	4.4		
Hoffmanniana	25	26	3.0	3.8		
lasiocarpa	33	32	3.2	***		
Elytropappus						
adpressus	24	24	**	3.0		

Table 1 (cont'd)

Elytropappus						
glandulos	25	25	**	3.5		
Metalasia						
cephalotea	32	30	3.3	3.7*		
ericoides	29	29	4.0	3.5		
macrocephala	32	31	4.0	3.9		
muricata	32	31	3.9	4.8	MO	1606699
muricata	32	32	3.8	4.2	US	1528993
Nestlera						
conferta	29	30	2.4	4.4		
humilis	36	37	2.9	7.1		
Pterothrix						
flaccida	29	29	2.0	4.2	US	552038
flaccida	35	32	2.8	3.8	MO	
Relhania						
genistaefolia	25	27	1+	4.3	MO	1641165
genistaefolia	26	26	1+	3.6	US	1029328
quinquinervis	29	29	3.2	4.0		
Stoebe						
capitata	27	29	3.6	3.8		
spiralis	20	22	**	3.8		
sphaerocephala	24	25	3.4	3.6		
Syncephalum						
candidum*	22	23	2.0	2.0		
stereoclinoides	23	23	2.0	3.9		
Zoutpansbergia						
caerulea	40	37	2.5	3.8		
ATHRIXIEAE						
Antithrixia						
abyssinica	29	28	2.4	4.2*		
angustifolia	29	27	3.0	***		
Arrowsmithia						
stypheloides*	33	32	3.3	***		
Athrixia						
athrixioides	28	30	3.5	3.1	BLT	5575
athrixioides	24	25	2.9	***	MSC	214553
australis	32	33	4.2	3.2		
oblonga	27	27	3.2	4.0		
Heterolepis						
aliena	47	48	5.0	5.4	MO	1602206
aliena	53	52	5.3	5.6*	US	2063056
Leyssera						

Table 1 (cont'd)

Leyssera						
capillifolia	34	33	2.2	2.8		
gnaphalioides	30	30	3.1	4.3		
tenella	27	27	1+	5.0		
Macowania						
revoluta	32	32	3.9	3.8*	MO	1704936
revoluta	29	31	3.4	4.2	US	807710
Podolepis						
capillaris	24	26	3.2	3.4		
cupulata	27	27	3.2	3.6		
rugata	39	40	4.8	5.3		
INULINEAE						
Allagopappus						
dichotomus	28	28	3.2	6.1		
Amblyocarpum						
inuloides	25	26	4.0	6.1		
Calostephane						
divaricata	35	33	4.0	4.6		
Carpesium						
abrotanoides	33	32	4.0	5.4		
cernuum	31	32	4.8	4.6		
Codonocephalum						
peacockianum	36	38	3.2	7.5		
Grantia						
aurliuz	34	33	3.1	5.2*		
Inula						
bifrons	28	28	3.3	5.0		
brittanica	30	31	4.1	4.9		
candida	24	25	3.8	4.4		
conyza	33	33	4.0	6.4		
germanica	30	30	3.4	4.6		
graveolens	34	35	4.2	4.4*	MSC	214597
graveolens	34	34	4.0	4.4	MSC	214568
helenium	33	34	4.0	5.3	MSC	84820
helenium	32	35	4.0	4.7	OKL	509
salicina	30	31	4.0	4.5		
Iphiona						
scalra	33	34	4.0	5.0		
Jasonia						
sicula	31	32	5.2	4.5		
Pegolettia						
senegalensis	34	34	3.9	6.4		

Table 1 (cont'd)

Perralderia						
coronopifolia	31	31	3.4	5.4	MO	1715328
coronopifolia	no measurements made				US	550371
Printzia						
densifolia	33	33	2.6	4.6		
pyrifolia	34	35	3.4	4.3		
Pulicaria						
dysenterica*	24	26	4.2	4.0		
sicula	34	34	4.8	5.1		
Varthemia						
iphionoides	39	37	4.0	5.0		
BUPHTHALMEAE						
[2]Adenocaulon						
bicolor	29	29	**	***	MSC	159361
bicolor	34	31	**	***	OKL	576
bicolor	no measurements made				TEX	199365
Anisopappus						
kirkii	31	30	2.8	5.7		
smutsii	31	30	2.4	6.6		
Anvillea						
australis	30	31	3.2	6.6		
garcini	31	32	3.1	5.8	MO	3214
garcini	35	34	3.4	6.2	NY	
radiata	28	29	3.1	5.1		
Buphthalmum						
salicifolium	29	29	4.0	3.1	MSC	84762
salicifolium	31	31	3.8	4.4	OKL	12213
salicifolium	no measurements made				TEX	150553
Callilepis						
laureola	37	38	2.6	4.0*		
leptophylla	36	36	2.4	4.6		
Chrysophthalmum						
sternutatorium	32	30	3.6	6.3*		
Geigeria						
aspera	35	36	5.4	5.1		
brevifolia*	36	36	5.6	6.0	US	2062918
brevifolia	37	38	5.6	6.3	MO	1610675
vigintisquamea	32	30	3.4	***		
Odontospermum						
maritemum	30	30	3.3	5.0		
Ondetia						

Table 1 (cont'd)

Ondetia linearis	32	32	4.0	6.5		
Osmites angustifolia	35	35	3.2	3.2*		
Osmites parvifolia	34	36	4.4	3.0		
Osmitopsis asteriscoides	38	41	5.1	4.5*	MO	
Osmitopsis asteriscoides*	36	36	4.8	3.0	US	1179808
Pallenis spinosa	24	25	3.1	3.8	OKL	1172
Pallenis spinosa	27	27	3.5	4.4	MSC	187600
Philyrophyllum schinzii	26	24	2.0	***		
Rhanterium adpressum	no measurements made				MO	1098551

[1] Gymnarrhena should be placed with the Buphthalmeae (Bentham and Hooker, 1873).

[2] Adenocaulon should be placed with the Inuleae (Hoffman, 1897).

ILLUSTRATIONS

The following descriptions, through Fig. 259, are of light micrographs of pollen whole mounts.

Fig. 7. Brachylaena discolor: Polar optical section; tricolporate. Fig. 8. B. elliptica: Polar surface. Fig. 9. B. elliptica: Polar surface; tetracolporate, colpi somewhat rounded at tips. Fig. 10. B. hutchinsii: Polar surface; tetracolporate; smooth exine surface. Fig. 11. B. nereifolia: Polar surface; colpi thick-margined, constricted. Fig. 12. B. nereifolia: Equatorial view; colpi shortened. Fig. 13. B. elliptica: Polar surface; tetracolporate. Fig. 14. B. rhodesiana: Oblique section; "knobby" spines. Fig. 15. B. discolor: Equatorial surface; lalongate, thin-margined os. Fig. 16. B. hutchinsii: Equatorial view; tetracolporate, pores inconspicuous. Fig. 17. Tarchonanthus camphoratus: Equatorial view; colpi and os thin-margined. Fig. 18. Brachylaena hutchinsii: Equatorial view; colpi thick-margined. Fig. 19. T. angustissimus: Equatorial view; colpi narrow; lalongate os. Fig. 20. T. camphoratus: Equatorial view; lolongate os. Fig. 21. T. angustissimus: Polar view; optical midsection. Fig. 22. T. camphoratus: Equatorial view; lolongate os. Fig. 23. T. camphoratus: Equatorial surface; lalongate os. Fig. 24. T. camphoratus: Equatorial view; colpi equidistant the full length of polar axis; lateral extensions in os region. Fig. 25. T. camphoratus: Polar optical section; smooth exine surface.

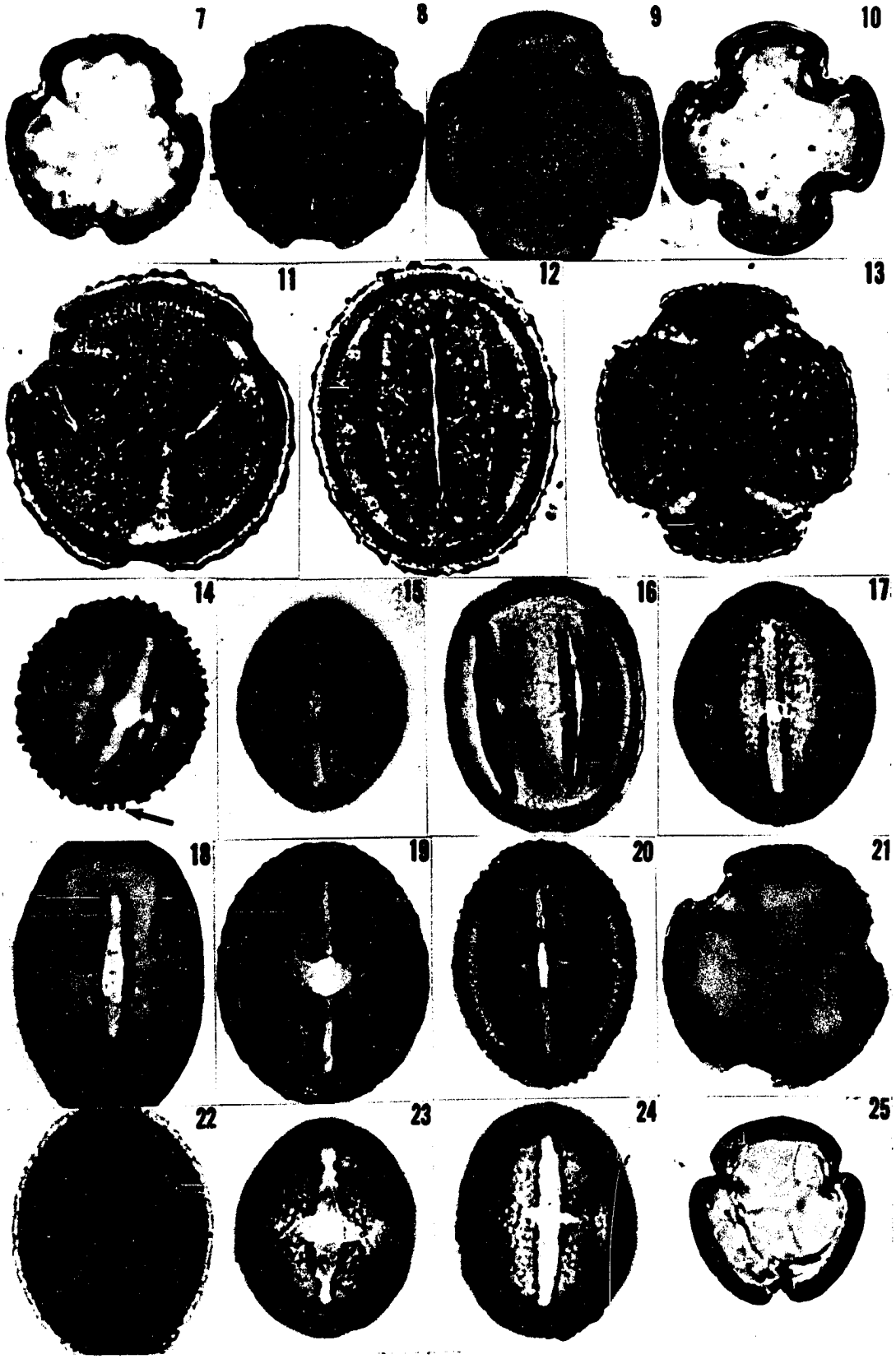
7
8
9
10
11
12
13
14
15
16
17
18
19
20
21
22
23
24
25

Fig 26. Gymnarrhena micrantha: Oblique section. Fig. 27. G. micrantha: Polar surface; short spinules. Fig. 28. G. micrantha: Equatorial view; pore margins thickened; colpus shortened. Fig. 29. Adenocaulon bicolor: Equatorial view; colpi equidistant the length of polar axis; os not clearly defined. Fig. 30. A. bicolor: Polar midsection. Fig. 31. A. bicolor: Equatorial view; colpus closed at pore area. Fig. 32. Osmites parvifolia: Oblique equatorial view; note thick exine. Fig. 33. O. parvifolia: Polar surface, spinose. Fig. 34. O. parvifolia: Oblique section; irregularly defined pore. Fig. 35. Osmitopsis asteriscoides: Polar midsection; non-caveate. Fig. 36. O. asteriscoides: Equatorial view.

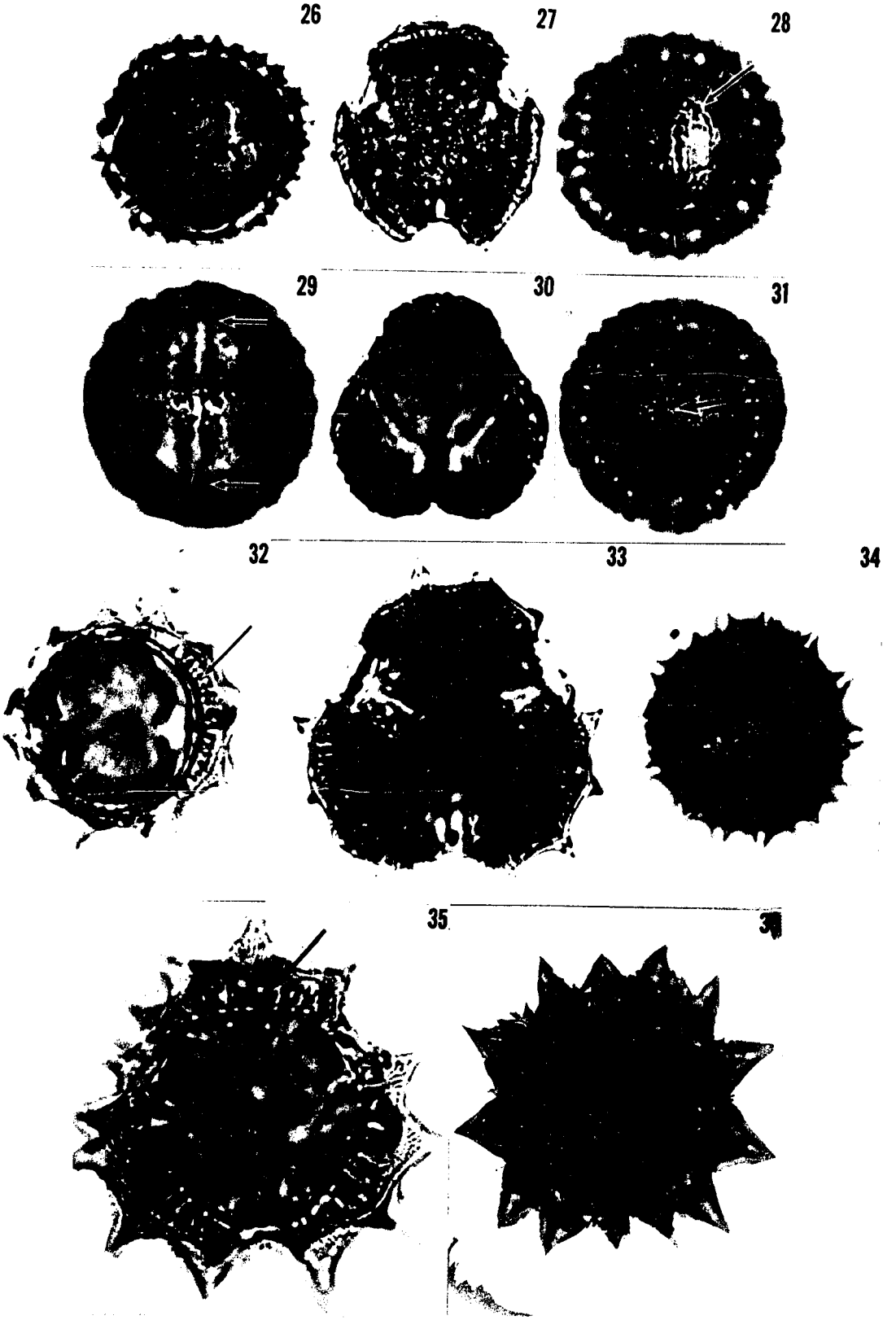
26
27
28
29
30
31
32
33
34
35
36

Fig. 37. Humea elegans: Equatorial surface; pore margins thickened; colpus reduced. Fig. 38. H. elegans: Polar midsection; nearly smooth exine surface. Fig. 39. Elytropappus adpressus: Polar midsection; nearly smooth exine surface, cavus present. Fig. 40. E. adpressus: Equatorial surface; narrow, thin-margined colpus; pore inconspicuous. Fig. 41. Helipterum battii: Equatorial surface; "pore-colpus complex," thick-margined. Fig. 42. H. battii: Polar midsection; nearly smooth exine surface. Fig. 43. H. battii: Equatorial surface; lalongate pore; very reduced colpus. Fig. 44. Nanothamnus sericeus: Polar midsection; spines not dense, wide-based. Fig. 45. N. sericeus: Equatorial midsection; note spine detail. Fig. 46. N. sericeus: Equatorial surface; very large, lalongate, thick-margined os; colpus thin-margined; superficial. Fig. 47. Helichrysum bracteatum: Equatorial surface; lalongate os; colpus superficial. Fig. 48. H. bracteatum: Polar midsection; spines dense, narrow based, solid tipped.

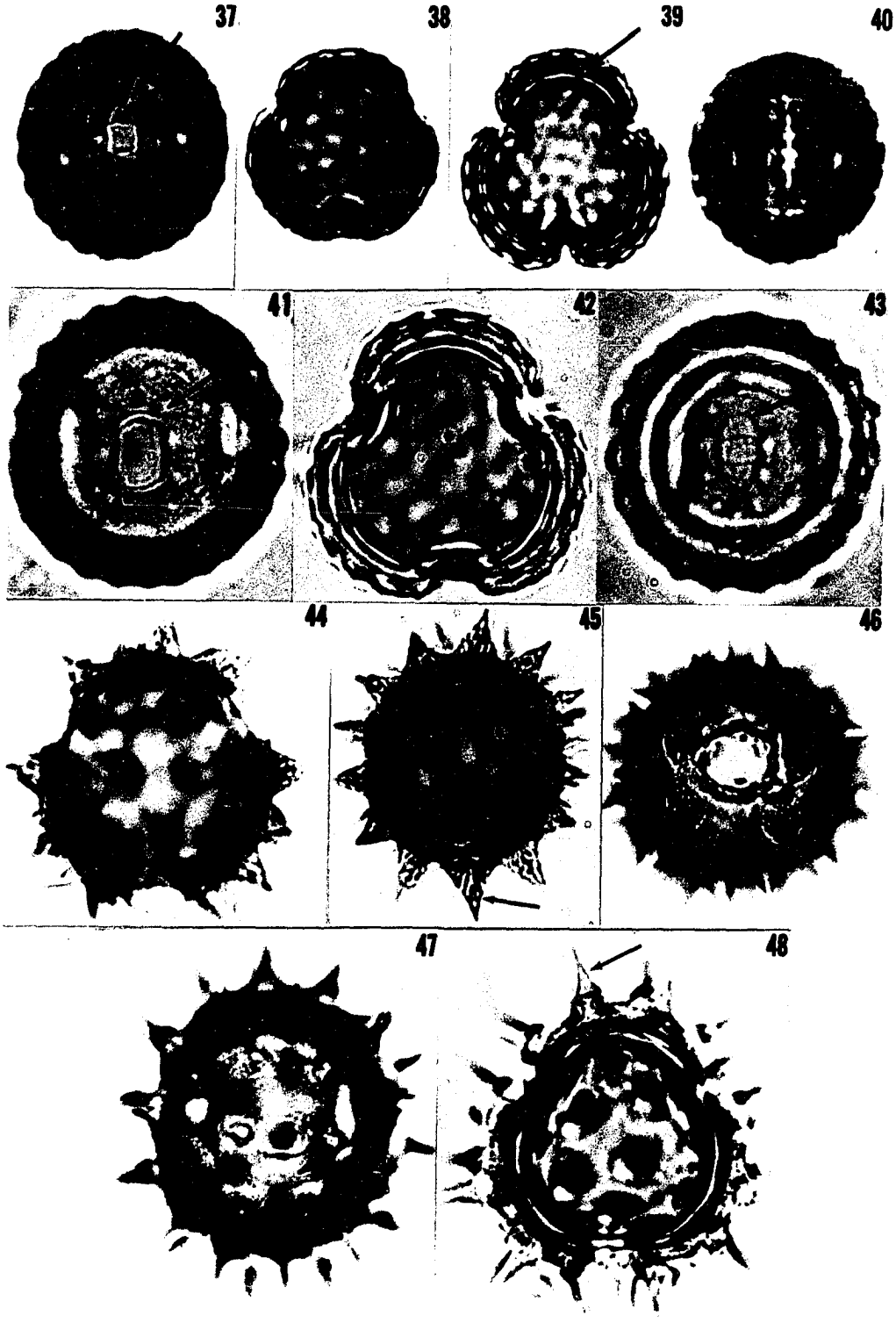
37
38
39
40
41
42
43
44
45
46
47
48

Fig. 49. Ghephosis cyathoppa: Oblique polar midsection; spines dense. Fig. 50. Stoebe spiralis: Polar midsection; spines dense. Fig. 51. Leyssera tenella: Polar surface; spines dense. Fig. 52. Filago arizonica: Polar midsection; spines dense. Fig. 53. Evax candida: Equatorial surface; narrow colpus; lolongate os. Fig. 54. Micropus californicus: Equatorial surface; narrow colpus; lolongate, thin-margined os. Fig. 55. Evax rotundata: Equatorial surface; narrow colpus, extending equidistant the full length of polar axis. Fig. 56. Psilocarphus oregonus: Equatorial midsection. Fig. 57. Micropus bombycinus: Equatorial surface; lolongate, os; narrow colpus, tapering at os. Fig. 58. Raoulia australis: Equatorial surface; lolongate, thin-margined os; narrow colpus. Fig. 59. Micropus bombycinus: Equatorial surface; spherical, thin-margined os. Fig. 60. Lasiopogon muscoides: Equatorial surface; irregularly shaped os. Fig. 61. Stoebe spiralis: Equatorial surface; lalongate os; thin-margined, shallow colpus. Fig. 62. Stuartina muelleri: Oblique equatorial surface; lolongate os. Fig. 63. Lasiopogon muscoides: Oblique equatorial surface. Fig. 64. Leontonyx bicolor: Equatorial surface; square, thick-margined os; reduced colpus. Fig. 65. Anaphalis briscus: Oblique equatorial surface. Fig. 66. Loricaria thuyoides: Equatorial surface; lolongate os with lateral extension; wide colpus. Fig. 67. Relhania genistaefolia: Equatorial surface. Fig. 68. Leyssera tenella: Equatorial surface; thick-margined os; wide, thin-margined colpus.

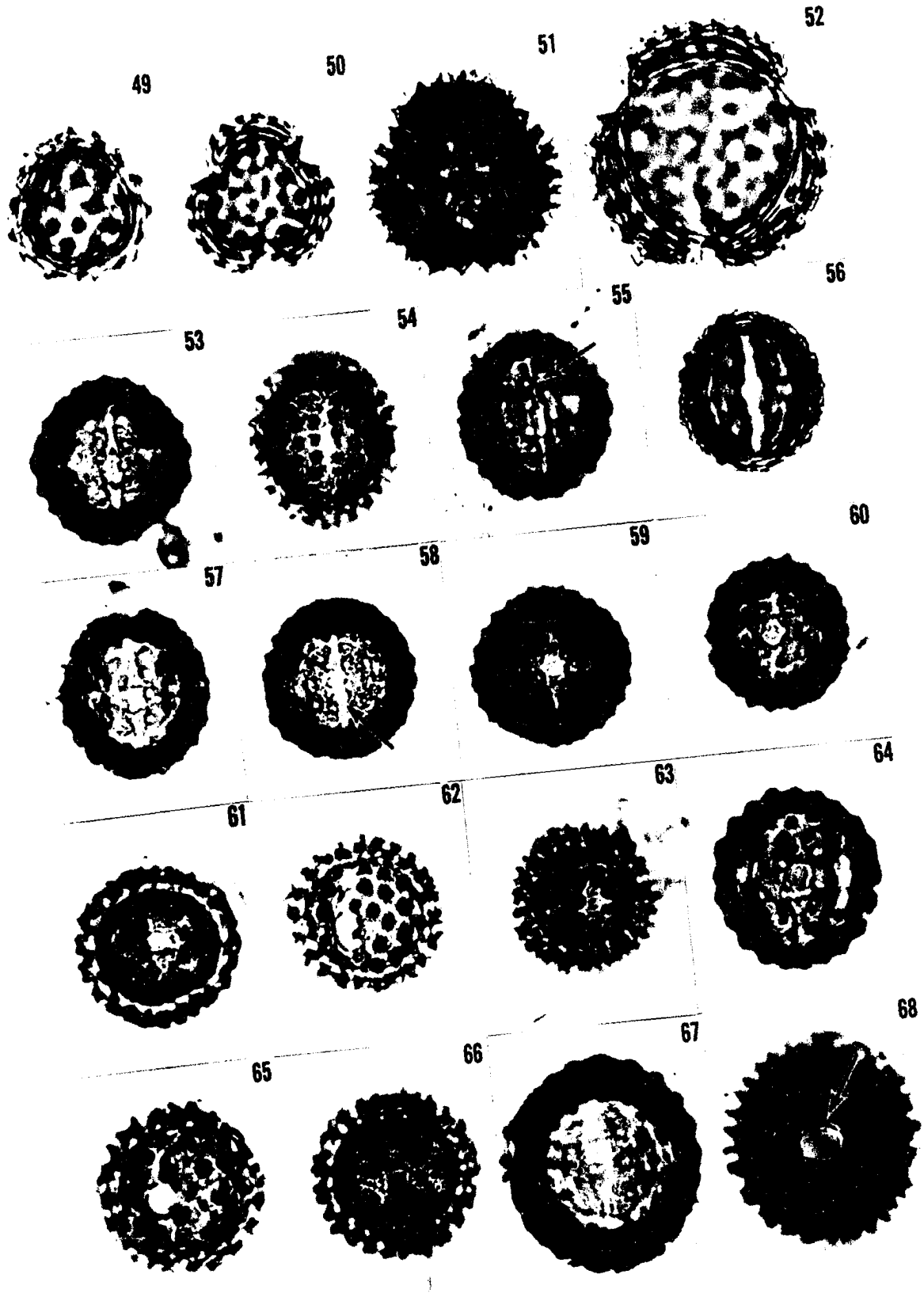
49
50
51
52
53
54
55
56
57
58
59
60
61
62
63
64
65
66
67
68

Fig. 69. Syncephalum candidum: Polar section; reduced spines. Fig. 70. Disparago hoffmaniana: Polar section; spines wide-based; dense. Fig. 71. Cassinia leptophylla: Polar section; spines wide-based. Fig. 72. Blumea ambigua: Polar midsection; spines narrow-based; pointed. Fig. 73. Syncephalum stereoclinoides: Equatorial surface; square os; wide, thick-margined colpus. Fig. 74. S. stereoclinoides: Equatorial surface; thick-margined os; narrow colpus. Fig. 75. Disparago ericoides: Equatorial surface; lolongate os; wide, thin-margined, sunken colpus. Fig. 76. Helipterum spicatum: Polar section; tetracolporate form. Fig. 77. Thespidium basiflorum: Equatorial surface; enlarged, thick-margined os; wide, thin-margined colpus. Fig. 78. Raulia glabra: Oblique equatorial surface; lalongate os. Fig. 79. Disparago anomala: Equatorial surface; circular os. Fig. 80. Rutidosis multiflorum: Equatorial surface; narrow, thin-margined colpus. Fig. 81. Disparago hoffmaniana: Equatorial surface; thick-margined, circular os. Fig. 82. Eriochlamys behrii: Equatorial surface; inconspicuous os; irregularly shaped colpus. Fig. 83. Chionolaena isabellae: Equatorial surface; inconspicuous os; narrow colpus. Fig. 84. Symphyllocarpus exilis: Equatorial midsection. Fig. 85. Leucopholis capitata: Equatorial surface; square os. Fig. 86. Humea cassiniana: Equatorial surface; os with lateral extensions. Fig. 87. H. cassiniana: Equatorial surface; slit-like os; colpus tapering at os. Fig. 88. Anaphalis margaritica: Equatorial surface; inconspicuous os; reduced colpus.

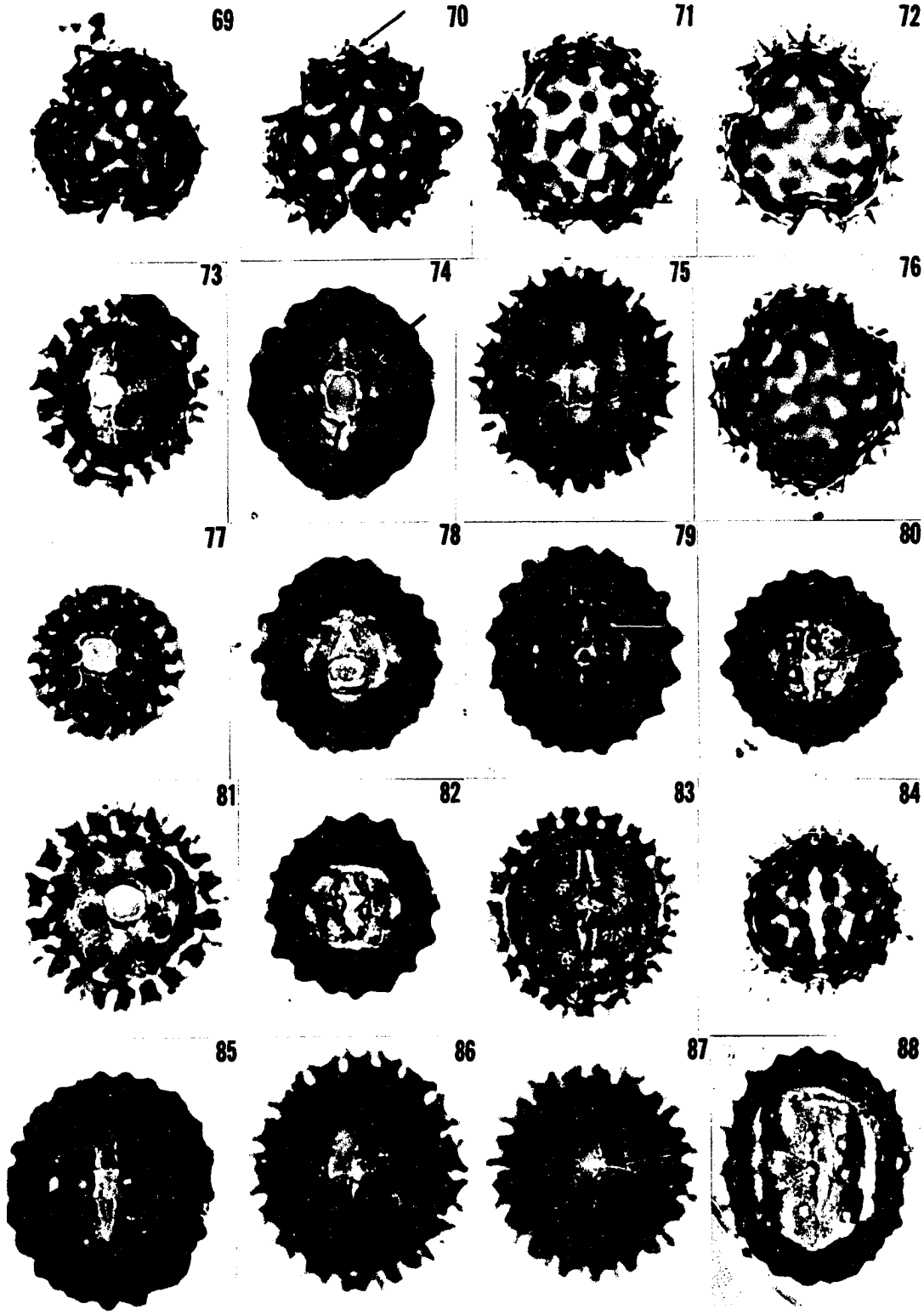
69
70
71
72
73
74
75
76
77
78
79
80
81
82
83
84
85
86
87
88

Fig. 89. Nestlera conferta: Equatorial surface; thick-margined, circular os. Fig. 90. Ixiolaena tomentosa: Polar midsection; dense spinos. Fig. 91. Leucopholis capitata: Polar midsection. Fig. 92. Printzia densifolia: Equatorial surface; os with symmetrical lateral extensions. Fig. 93. Antennaria pulcherrina: Equatorial surface; thin-margined, irregularly shaped os. Fig. 94. Gnaphalium americanum: Equatorial surface; thick-margined os. Fig. 95. Nestlera conferta: Equatorial surface; colpus deeply sunken. Fig. 96. Stuchertiella capitata: Equatorial surface; thick-margined os; colpus tapering at os region. Fig. 97. Pterothrix flaccida: Equatorial surface, wide os; narrow colpus. Fig. 98. P. flaccida: Polar surface, spines triangular in shape. Fig. 99. P. flaccida: Slightly oblique equatorial surface. Fig. 100. Luciliopsis sp.: Equatorial surface, wide os; narrow colpus. Fig. 101. Printzia densifolia: Polar midsection. Fig. 102. Helichrysum ambiguus: Equatorial surface; os inconspicuous; colpus reduced. Fig. 103. Printzia densifolia: Equatorial surface; os irregularly shaped; colpus thin-margined. Fig. 104. Nestlera humilis: Polar section; densely massed triangular spines. Fig. 105. N. humilis: Equatorial surface; thick-margined lalongate os; colpus reduced. Fig. 106. N. humilis: Polar surface.

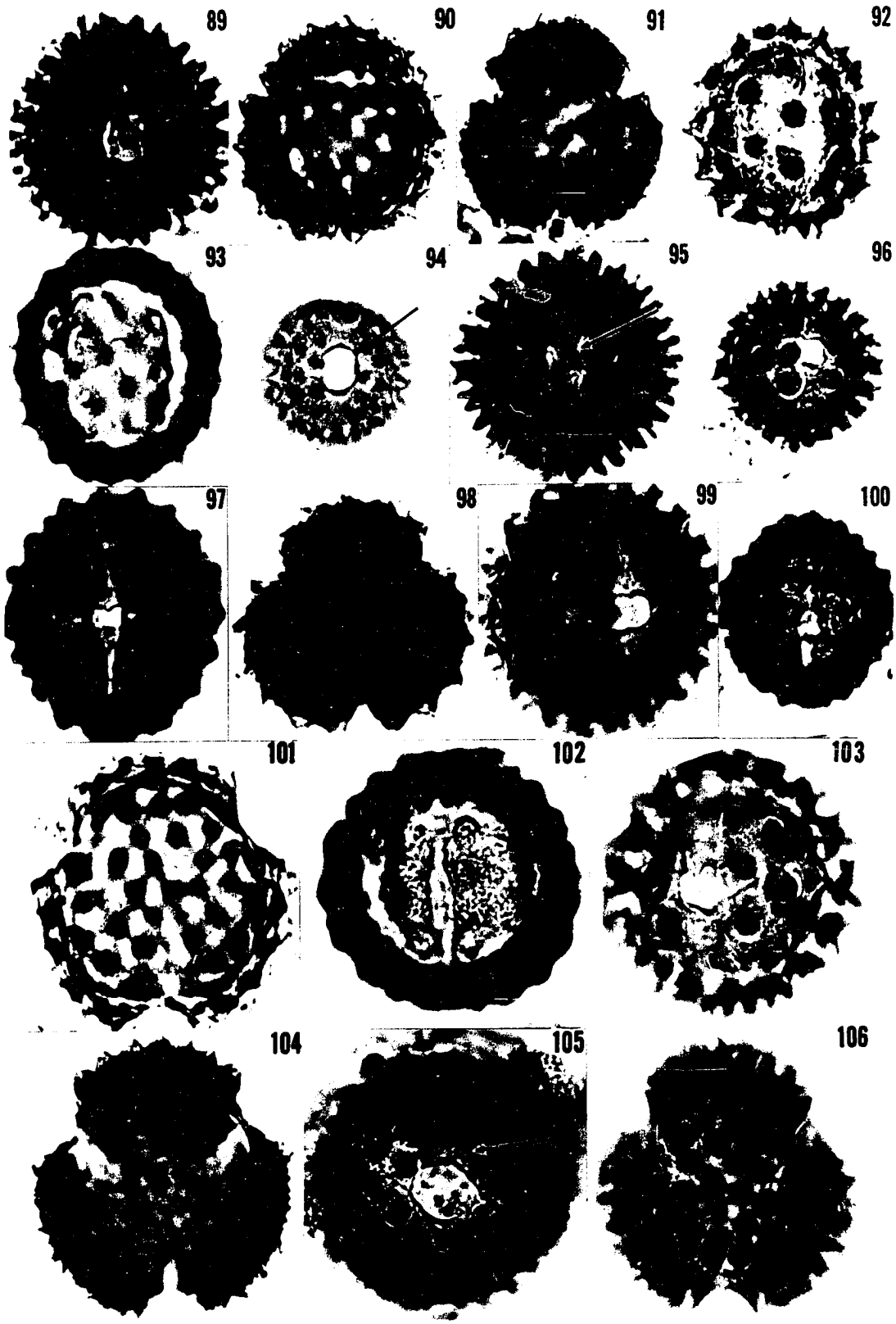
89
90
91
92
93
94
95
96
97
98
99
100
101
102
103
104
105
106

Fig. 107. Psila trinervis: Polar view; spines widely spaced. Fig. 108. Epaltes cunninghamii: Polar midsection; narrow spines. Fig. 109. Pterocaulon sphacelatum: Polar view; triangular spines. Fig. 110. Petalacte coronata: Polar view. Fig. 111. Antithrixia abyssinica: Polar midsection; spines short, widely spaced. Fig. 112. Philyrophyllum schinzii: Polar surface; colpi very long. Fig. 113. Waitzia acuminata: Equatorial surface; thin-margined os; long, narrow colpus. Fig. 114. Pterocaulon interruptum: Equatorial surface; colpus connected by a "bridge" at os region; spines short, bluntly tipped. Fig. 115. Phaenocoma prolifera: Polar view; spines wide-based. Fig. 116. Antithrixia abyssinica: Equatorial surface; inconspicuous os; reduced colpus. Fig. 117. Anisopappus smutsii: Equatorial surface; thick-margined os; colpus superficial. Fig. 118. Petalacte coronata: Equatorial surface; os with lateral extensions; narrow, constricted colpus. Fig. 119. Stenocline chionaea: Equatorial surface; thick-margined os; wide colpus. Fig. 120. Antithrixia abyssinica: Equatorial surface; thick-margined, rectangular os. Fig. 121. Philyrophyllum schinzii: Equatorial surface; inconspicuous os. Fig. 122. Anisopappus smutsii: Oblique equatorial surface; thick-margined os; superficial colpus. Fig. 123. Callilepis laureola: Equatorial surface; slit-like os; deeply sunken colpus. Fig. 124. Anisopappus kirkii: Equatorial surface; os with lateral extensions; colpus reduced. Fig. 125. A. kirkii: As above, with long, wide colpus.

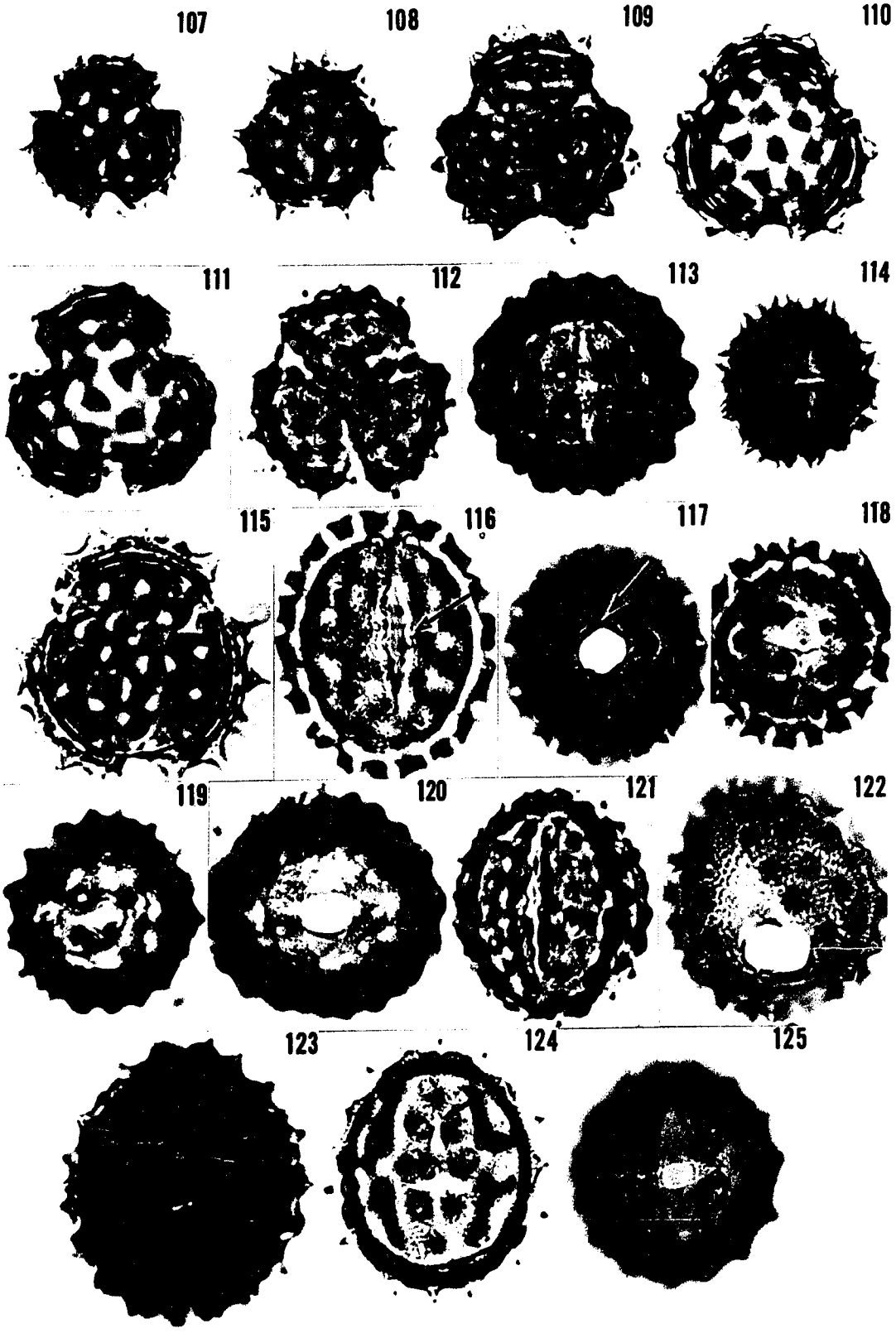
107
108
109
110
111
112
113
114
115
116
117
118
119
120
121
122
123
124
125

Fig. 126. Anisopappus kirkii: Polar surface; spines short, spaced widely. Fig. 127. Leyssera capillifolia: Equatorial surface; os inconspicuous; narrow colpus. Fig. 128. Callilepis laureola: Equatorial surface; "lip-like" pore pattern. Fig. 129. Callilepis leptophylla: Polar mid-section. Fig. 130. Leyssera capillifolia: Polar surface; spines on inverted funnel-form. Fig. 131. Zoutpansbergia caerulea: Equatorial surface; thin-margined os. Fig. 132. Z. caerulea: Polar surface. Fig. 133. Z. caerulea: Equatorial surface; inconspicuous os; wide, deeply sunken colpus.

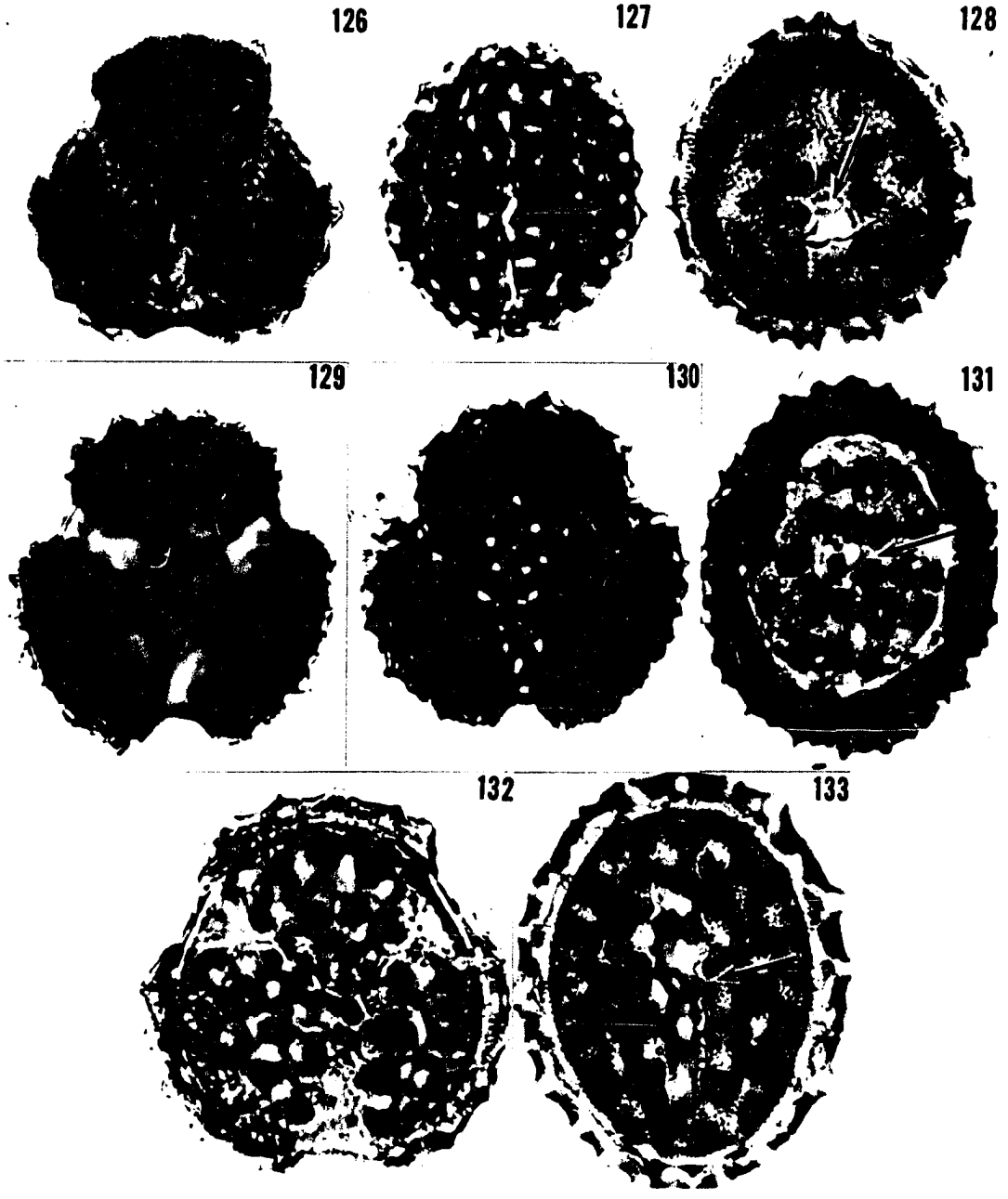
126
127
128
129
130
131
132
133

Fig. 134. Denekia copensis: Polar view; densely massed, finely tipped spines. Fig. 135. Gnaphalium luteoalbum: Polar midsection. Fig. 136. Pithocarpa corymbulosa: Polar view. Fig. 137. Acomis rutidosis: Polar view; long, finely tipped spines. Fig. 138. Podolepis cupulata: Polar view. Fig. 139. Pterocaulon virgatum: Polar view; grain distorted; spines long, bluntly tipped. Fig. 140. Gnaphalium obtusifolium: Polar midsection; spines narrow, finely tipped. Fig. 141. Pithocarpa corymbulosa: Equatorial surface; narrow, or, closed colpus. Fig. 142. Athrixia athrixioides: Equatorial surface; thin-margined lalongate os. Fig. 143. Acomis macra: Polar view; triangular spines. Fig. 144. Podolepis cupulata: Equatorial surface; thick-margined os. Fig. 145. Denekia copensis: Equatorial surface; thin-margined, irregular os, with lateral extensions. Fig. 146. Gnaphalium cheiranthifolium: Equatorial surface; thick-margined, rectangular os. Fig. 147. Phagnalon rupestre: Equatorial surface; thin-margined os and colpus. Fig. 148. Gilruthia osbornii: Equatorial surface; thin-margined os; colpus somewhat reduced. Fig. 149. G. osbornii: Equatorial surface; thin-margined, lalongate os. Fig. 150. Leptorhynchus waitzia: Polar view; wide-based, finely pointed spines. Fig. 151. Athrixia athrixioides: Polar view; wide-based, gradually tapering spines. Fig. 152. Anvillea Garcini: Polar view; wide-based, blunted spines.

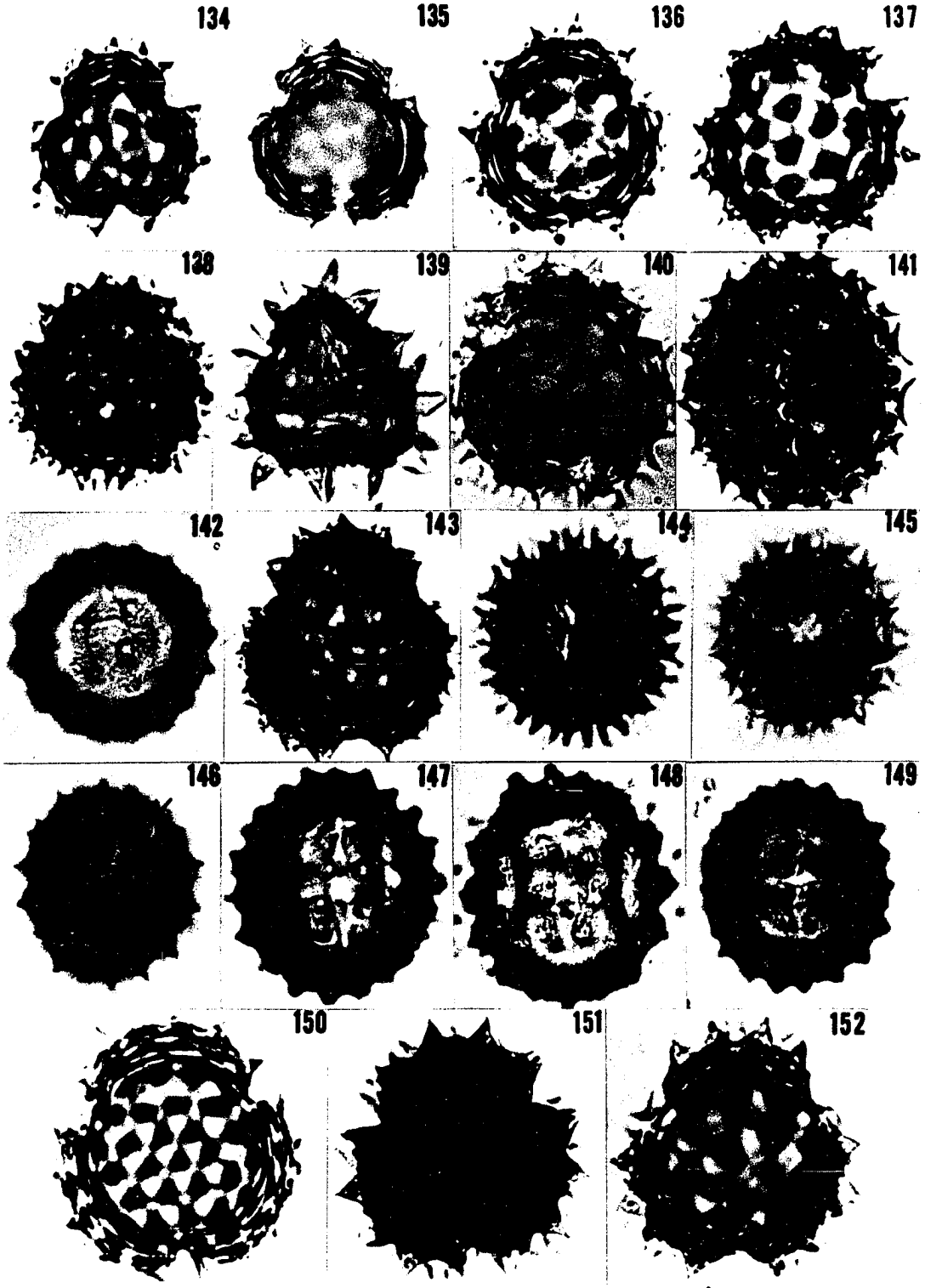
134
135
136
137
138
139
140
141
142
143
144
145
146
147
148
149
150
151
152

Fig. 153. Bupthalmum salicifolium: Equatorial surface; thin-margined os and colpus. Fig. 154. Acomis macra: Equatorial surface; thick-margined, round os; colpus very superficial, if present. Fig. 155. Gnaphalium obtusifolium: Equatorial surface; thin-margined os with lateral extensions. Fig. 157. Cephalipterum drummondii: Equatorial surface; thick-margined os; colpus indistinct. Fig. 157. Carpesium abrotanoides: Equatorial surface; "lip-patterned" os; reduced colpus. Fig. 158. Cylindocline commersoni: Equatorial surface; rectangular os; colpus indistinct. Fig. 159. Anvillea garcini: Equatorial surface; os with lateral extensions; thin-margined colpus. Fig. 160. Inula britannica: Equatorial face; "lip-patterned" pore; long, thin-margined colpus. Fig. 161. Inula salicina: Equatorial surface; thick-margined, rectangular os; thin-margined, reduced colpus. Fig. 162. Carpesium abrotanoides: Equatorial surface; os wide; colpus indistinct. Fig. 163. Codonocephalum peacockianum: Equatorial surface; extraordinarily wide os. Fig. 164. Ondetia linearis: Equatorial view; "lip-patterned" os. Fig. 165. Inula helenium: Polar view; wide, bluntly tipped spines. Fig. 166. Stenachenium campestre: Fig. 167. Macowania revoluta: Equatorial surface; lolongate os. Fig. 168. Inula conyza: Slightly oblique equatorial surface, wide os; colpus tapering at os region. Fig. 169. Anvillea garcini: Slightly oblique equatorial surface; wide os; colpus tapering at os region. Fig. 170. Perralderia coronopifolia: Equatorial surface; thick-margined os.

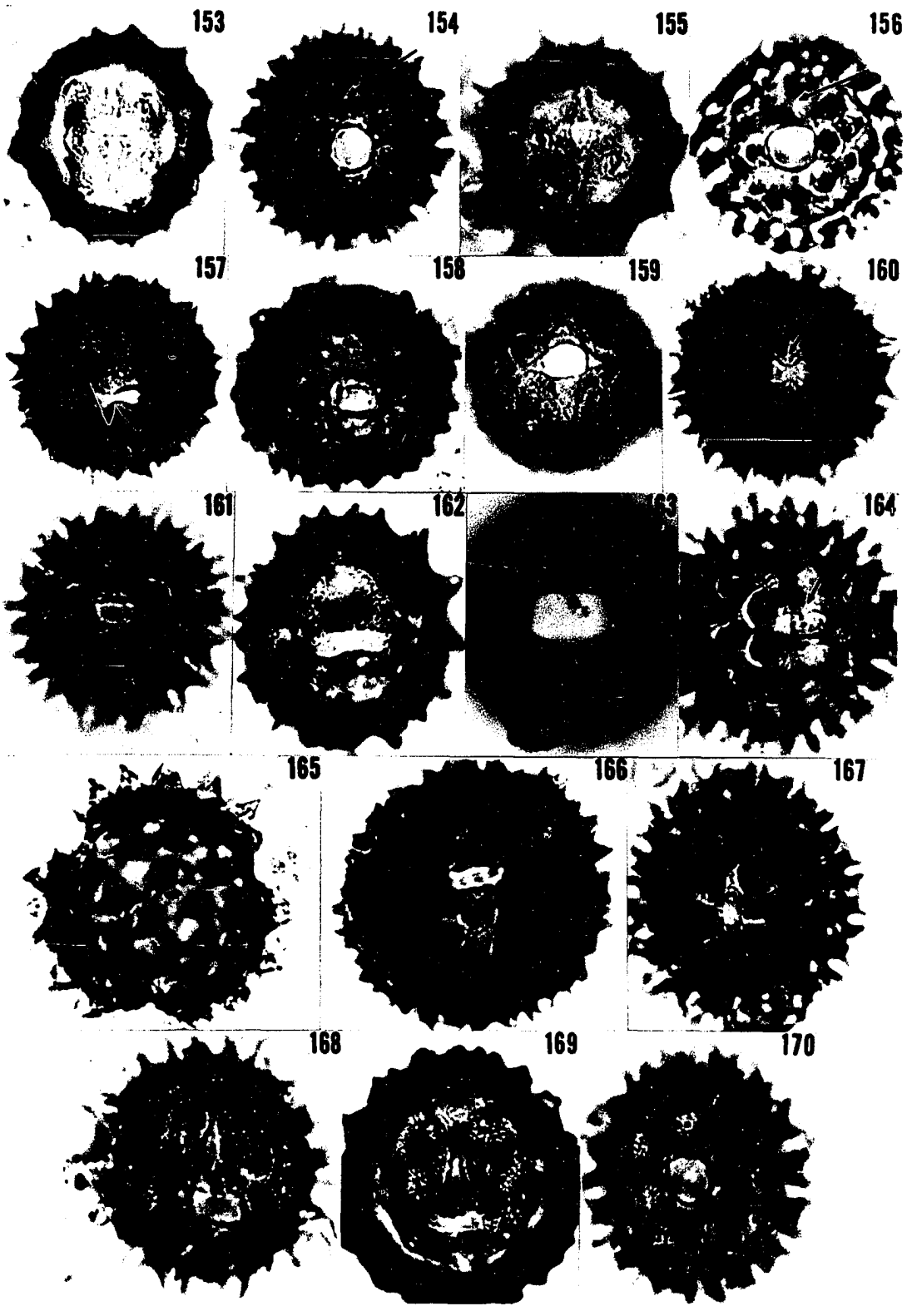
153
154
155
156
157
158
159
160
161
162
164
165
166
167
168
169
170

Fig. 171. Helipterum manglesii: Polar view; long, finely tipped spines. Fig. 172. Macowania revoluta: Polar surface. Fig. 173. Helipterum australe: Polar view. Fig. 174. Iphiona scalra: Polar surface; triangular, blunted spines. Fig. 175. I. scalra: Equatorial surface; thick-margined os; thin-margined colpus. Fig. 176. Inula graveolens: Oblique equatorial surface; conical spines. Fig. 177. I. graveolens: Polar view; spines equilateral in form, densely massed. Fig. 178. Codonocephalum peacockianum: Polar view; spines short, with blunted tips. Fig. 179. Stenachenium campestre: Polar midsection. Fig. 180. Varthemia iphionoides: Polar surface; tightly packed spines. Fig. 181. V. iphionoides: Equatorial surface; lolongate os; narrow colpus. Fig. 182. V. iphionoides: Equatorial surface; lalongate os; reduced colpus.

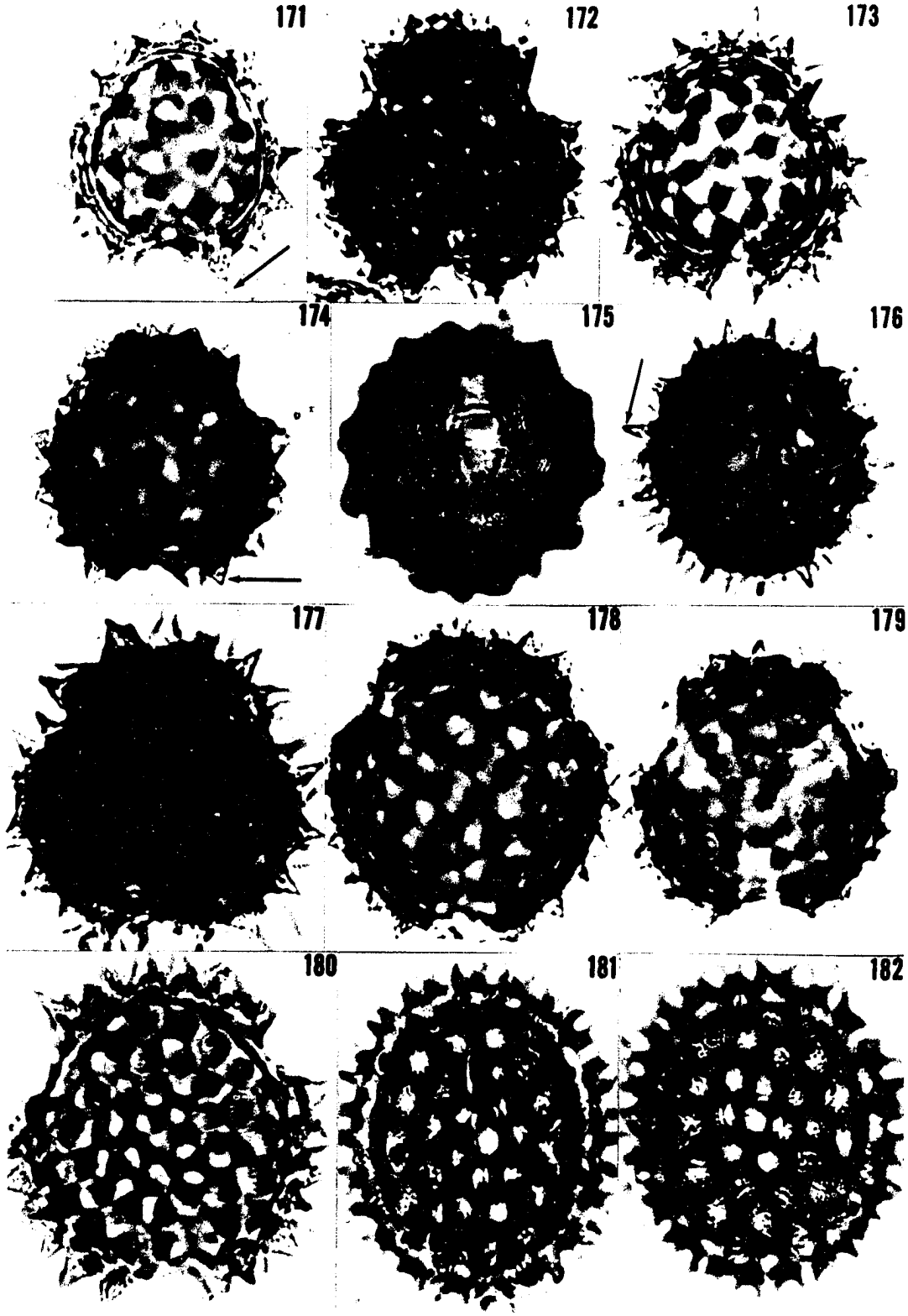
171
172
173
174
175
176
177
178
179
180
181
182

Fig. 183. Sphaeranthus africanus: Polar midsection; gradually tapering, finely pointed spines. Fig. 184. Inula candida: Polar view, spines wide-based with blunted tips. Fig. 185. Relhania quinquinervis: Polar view; spine tips finely extended. Fig. 186. Sachsia polycephala: Polar mid-section; spines widely spaced. Fig. 187. Pluchea camphorata: Polar midsection; gradually tapering spines. Fig. 188. Chrysophthalmum sternutatorium: Polar view; wide-based, triangular spines. Fig. 189. Athrixia australe: Polar view. Fig. 190. Triplocephalum holtsii: Equatorial surface; thin-margined os with lateral extensions. Fig. 191. Blumea mollis: Polar view; widely spaced spines. Fig. 192. Sphaeranthus africanus: Equatorial surface; thin-margined os and colpus. Fig. 193. Inula candida: Equatorial surface; reduced colpus. Fig. 194. Stoebe sphaerocephala: Equatorial surface; thick-margined os. Fig. 195. Tessaria integrifolia: Oblique equatorial surface; irregularly shaped os. Fig. 196. T. integrifolia: Equatorial surface; colpus indistinct. Fig. 197. Odontospermum maritemum: Equatorial surface; thin-margined colpus. Fig. 198. Laggera alata: Equatorial surface; superficial colpus. Fig. 199. Gnaphalodes condensatum: Oblique equatorial surface. Fig. 200. Metalasia cephalotea: Equatorial surface; thin-margined colpus. Fig. 201. Podolepis capillaris: Equatorial surface; colpus reduced. Fig. 202. Blumea mollis: Equatorial surface; thick-margined os.

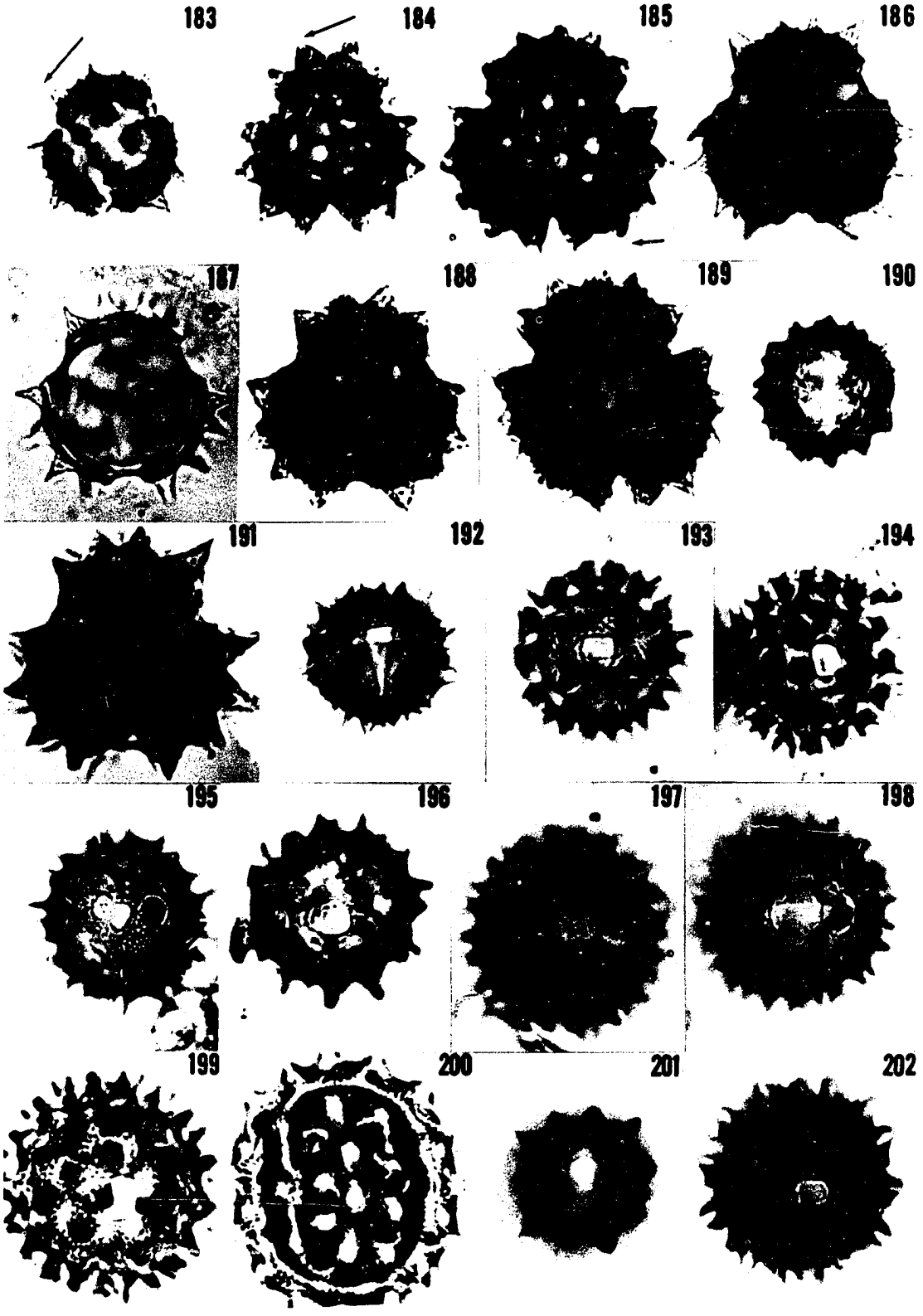
183
184
185
186
187
188
189
190
191
192
193
194
195
196
197
198
199
200
201
202

Fig. 203. Tessaria integrifolia: Oblique view; spines conical. Fig. 204. Laggera alata: Equatorial surface; colpus very reduced. Fig. 205. Amblyocarpum inuloides: Equatorial surface; "lip-patterned" os; narrow colpus. Fig. 206. Geigeria vigintisquamea: Oblique equatorial view; narrow colpus. Fig. 207. Myriocephalus stuartii: Oblique view; slit-like os; reduced colpus. Fig. 208. M. stuartii: Equatorial surface; reduced colpus. Fig. 209. M. gracilis: Equatorial surface; reduced; irregular colpus. Fig. 210. Athrixia oblonga: Equatorial surface; deeply sunken colpus. Fig. 211. Pluchea odorata: Oblique equatorial midsection; conical spines. Fig. 212. Myriocephalus stuartii: Polar view; widely spaced spines. Fig. 213: Odontospermum maritemum: Oblique view; thick-margined os; narrow colpus. Fig. 214. Caesulia axillaris: Equatorial surface; reduced colpus. Fig. 215. Metalasia macrocephala: Polar view; wide-based spines. Fig. 216. M. cephalotea: Polar view; spine tips solid. Fig. 217. Polycline proteiformis: Equatorial surface; "lip-patterned" os; narrow colpus. Fig. 218. Relhania quinquinervis: Equatorial surface; long, thin-margined colpus. Fig. 219. Polycline proteiformis: Equatorial surface; wide colpus. Fig. 220. Metalasia macrocephala: Equatorial surface; "lip-patterned" os. Fig. 221. Pluchea odorata: Equatorial surface; os with one main lateral extension; narrow colpus. Fig. 222. Chrysolphthalmum sternutatorium: Equatorial surface; "lip-patterned" os; colpus indistinct.

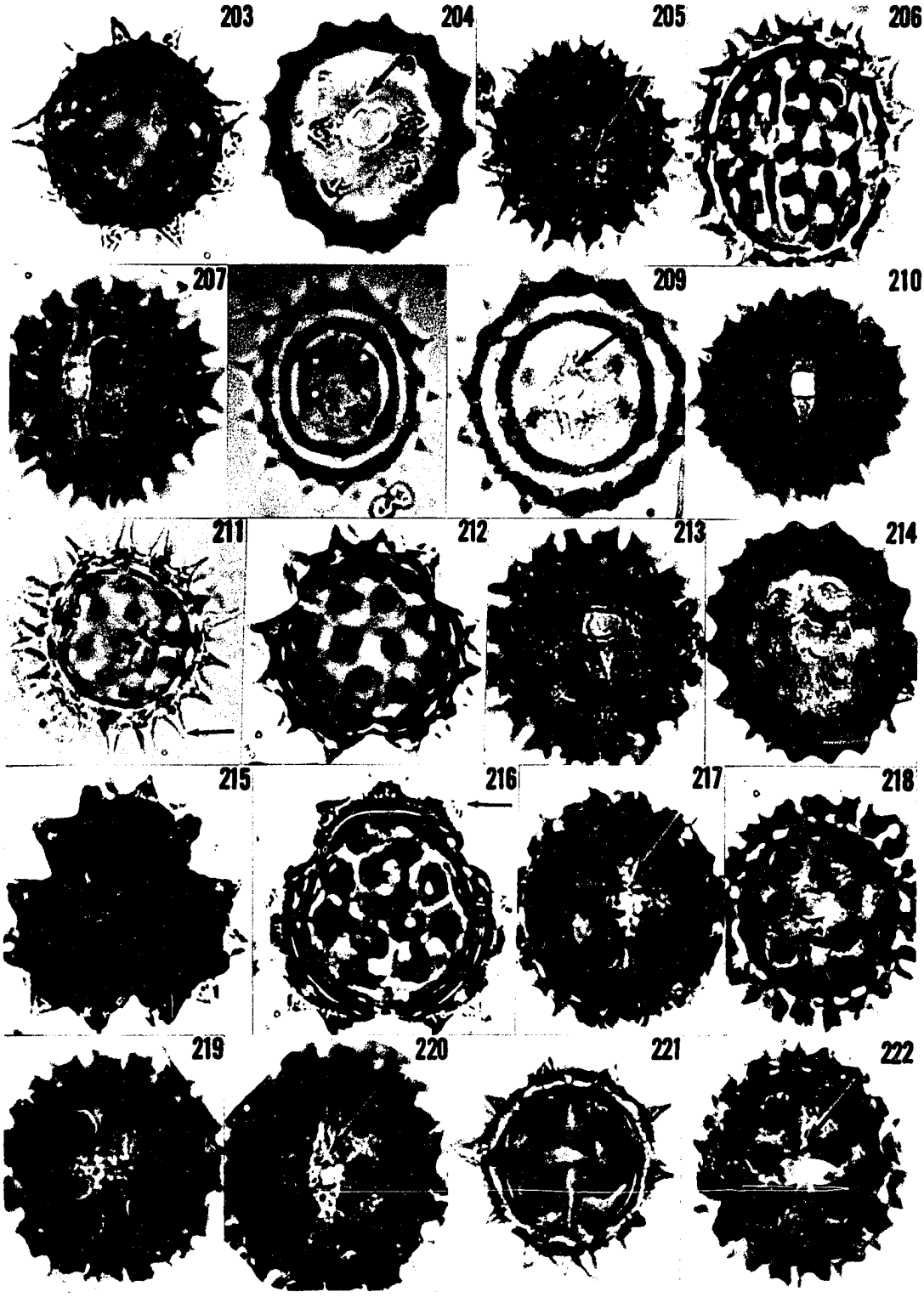
203
204
205
206
207
209
210
211
212
213
214
215
216
217
218
219
220
221
222

Fig. 223. Pegolettia senegalensis: Polar view; wide-based, bluntly tipped spines. Fig. 224. Grantia aurliuz: Polar midsection, wide-based, finely pointed spines. Fig. 225. Grantia aurliuz: Equatorial surface; os with one lateral extension; reduced colpus. Fig. 226. Gnaphalodes condensatum: Oblique equatorial view; wide-based spines with solid tips. Fig. 227. Grantia aurliuz: Equatorial surface; os with lateral extensions; reduced colpus. Fig. 228. Ixodia scheilloides: Oblique equatorial view. Fig. 229. Sachsia polycephala: Polar midsection. Fig. 230. Disparago lasiocarpa: Polar surface; blunted spine tips. Fig. 231. Printzia pyrifolia: Oblique equatorial view; wide-based spines with blunted tips. Fig. 232. Myriocephalis gracilis: Polar view; wide cavus. Fig. 233. Printzia pyrifolia: Oblique equatorial view; thick-margined os; superficial colpus. Fig. 234. Angianthus sp.: Polar view; widely spaced, finely tipped spines.

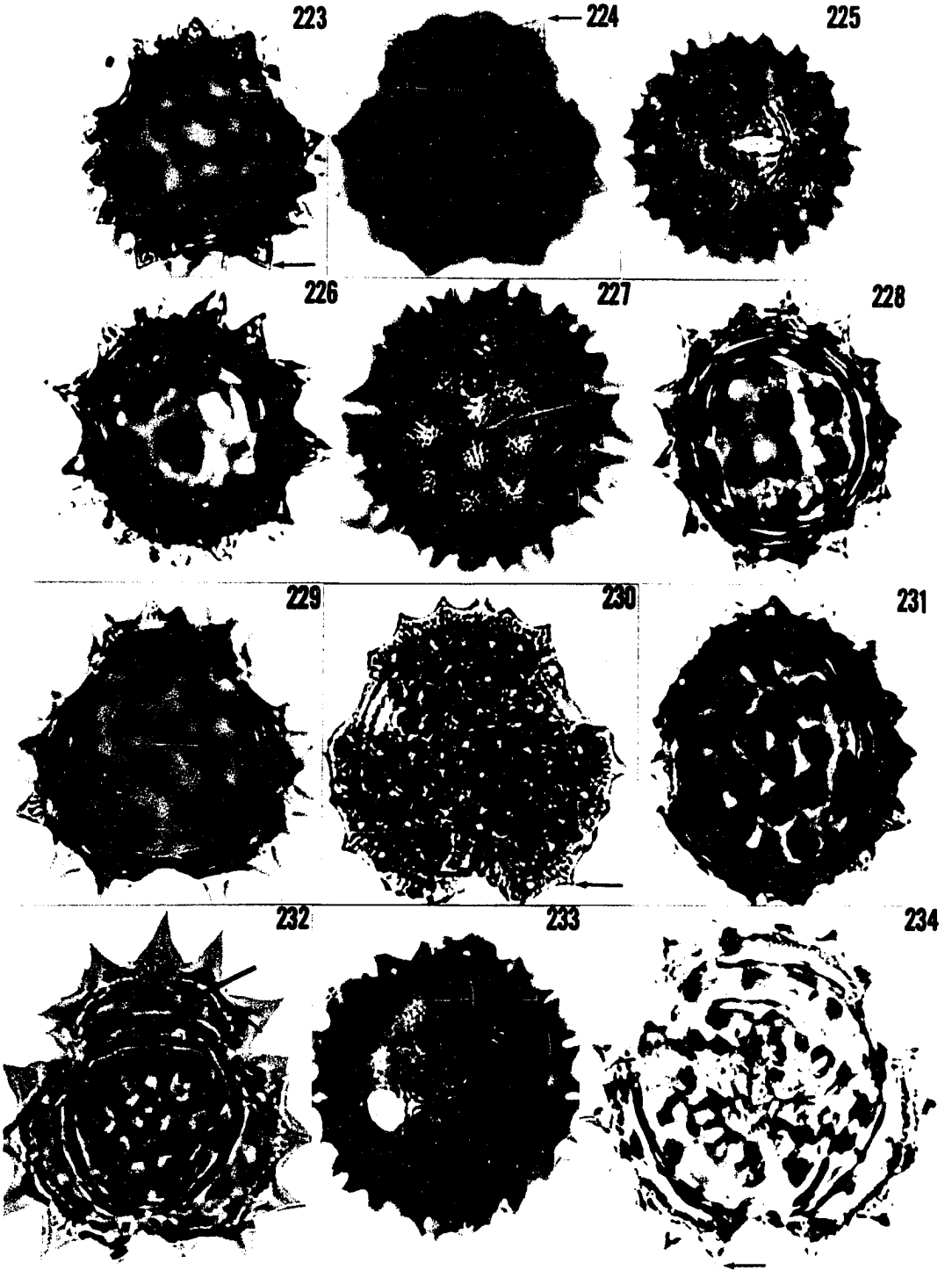
223
224
225
226
227
228
229
230
231
232
233
234

Fig. 235. Carpesium cernuum: Polar midsection; rounded spine tips. Fig. 236. C. cernuum: Oblique equatorial view; thick-margined os; shallow colpus. Fig. 237. Pterigeron liatroides: Equatorial surface; long, tapering colpus. Fig. 238 Dimeresia howellii: Equatorial surface; rectangular os; narrow colpus. Fig. 239. D. howellii: Polar view; wide-based, long, solid tipped spines. Fig. 240. Rhodogeron coronopifolia: Polar view; wide-based, long, bluntly tipped spines. Fig. 241. R. coronopifolia: Oblique view. Fig. 242. Pterocaulon undulatum: Polar view; narrow-based, long spines. Fig. 243. Jasonia sicula: Equatorial surface; thick-margined os; thin-margined colpus. Fig. 244. J. sicula: Equatorial surface; indistinct colpus. Fig. 245. J. sicula: Equatorial midsection; conical spines. Fig. 246. Podolepis rugata: Oblique polar view; long spines with solid tips. Fig. 247. Helichrysum davenportii: Polar view; long, very finely tipped spines. Fig. 248. H. davenportii: Equatorial surface; indistinct colpus.

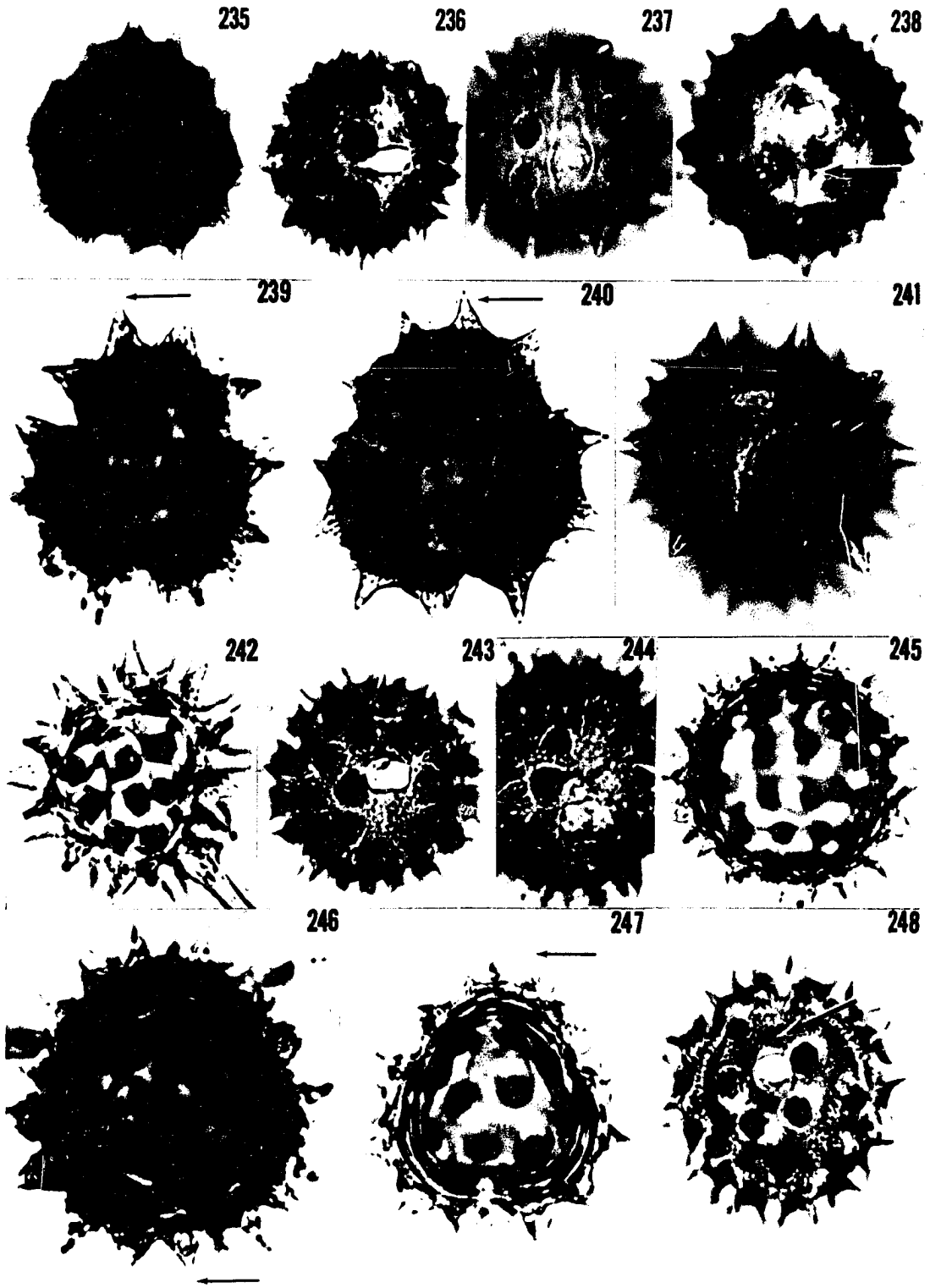
235
236
237
238
239
240
241
242
243
244
245
246
247
248

Fig. 249. Geigeria aspera: Equatorial surface; shallow colpus. Fig. 250. Schoenia cassiniana: Equatorial surface; thick-margined os; colpus indistinct. Fig. 251. Pulicaria sicula: Oblique equatorial surface; wide os; narrow, thin-margined colpus. Fig. 252. Podosperma gnaphalioides: Equatorial surface; thick-margined os; colpus indistinct. Fig. 253. P. gnaphalioides: Polar midsection. Fig. 254. P. gnaphalioides: Equatorial surface; thick-margined lolongate os, reduced colpus. Fig. 255. Heterolepis aliena: Equatorial surface; os with symmetrical lateral extensions; thin-margined, reduced colpus. Fig. 256. H. aliena: Oblique polar midsection; wide-based, bluntly tipped spines. Fig. 257. Stenachenium riedelii: Polar view; widely spaced spines. Fig. 258. S. riedelii: Oblique equatorial view; "lip"-patterned os; narrow colpus. Fig. 259. S. riedelii: Equatorial surface; thickened os; reduced colpus.

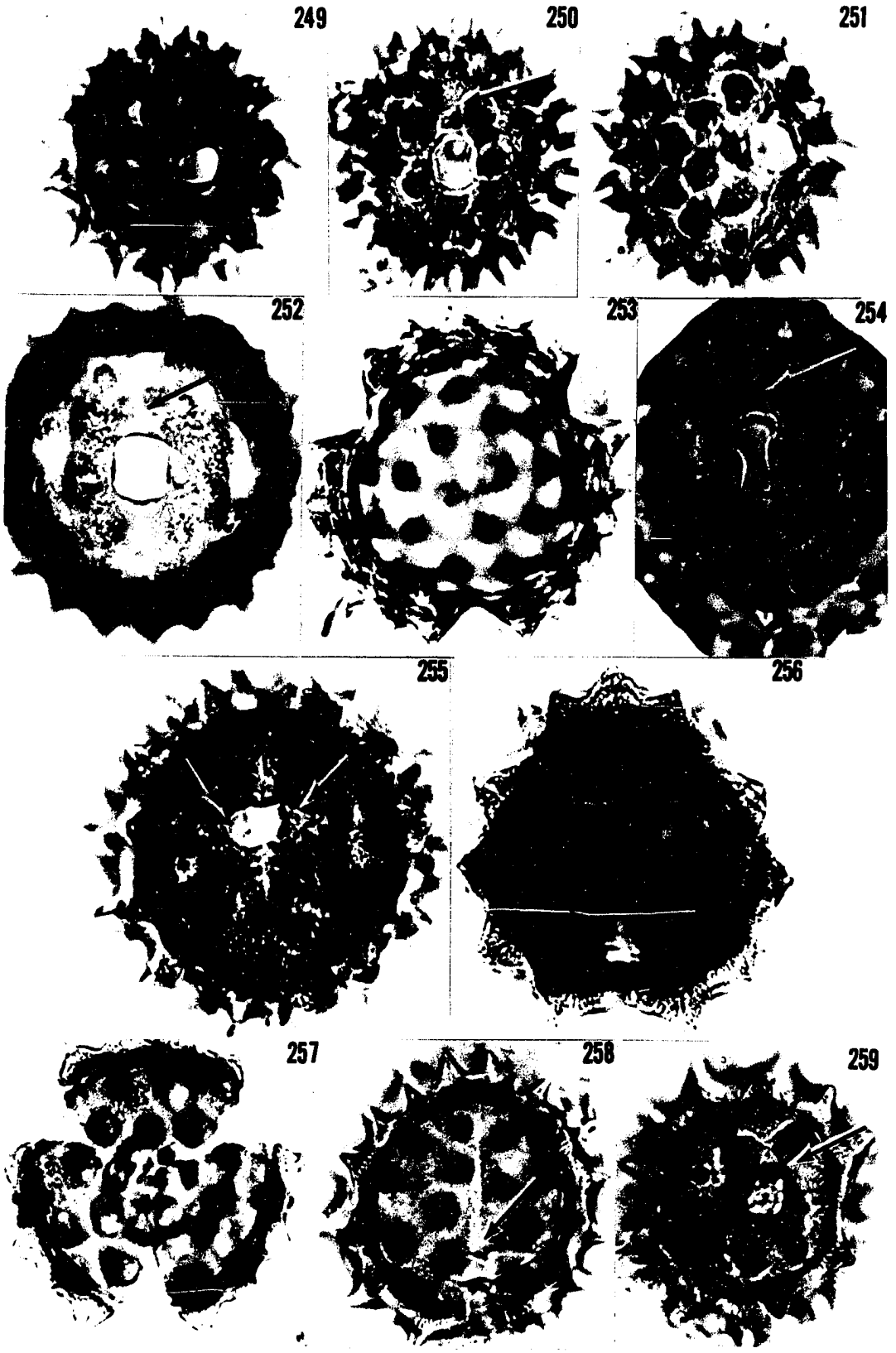
249
250
251
252
253
254
255
256
257
258
259

Key to Symbols Used in Electron Micrographs

1.	cav.	cavus
2.	c.	columella
3.	cb.	columellar bases
4.	cc.	conjunct columellae
5.	dc.	digitate columellae
6.	en.	endexine
7.	f.	foramina
8.	cf.	circular foramina
9.	ef.	elongate foramina
10.	fl.	foot layer
11.	ft.	foraminal traces
12.	it.	internal tectum
13.	pt.	perforate tectum
14.	se.	sub-basal extensions
15.	t.	tectum

The following descriptions, through Fig. 331, are of electron micrographs of pollen thin sections.

Fig. 260. Brachylaena elliptica. Tangential section. x6,300. Note lack of internal foramina.

Fig. 261. B. hutchinsii. Section through aperture. x5,760. Note thickened endexine in apertural region.

Fig. 262. B. hutchinsii. Section through mesocolpial area. x33,600. Note thickened, imperforate tectum, internal tecta and columellae. Foot layer and endexine (somewhat disrupted) are similarly proportioned.

Fig. 263. Tarchonanthus camphoratus. Mesocolpial section. x39,200. Note thin, perforate tectum, finely structured internal tecta, and thin columellae. Ektexine and endexine are sharply differentiated.

Fig. 264. Brachylaena nereifolia. Mesocolpial section. x22,750. Note perforate tectum; foot layer: endexine ratio approximates 2:1 in some areas. Black dots are osmium tetroxide (OsO_4) precipitate.

Fig. 265. Tarchonanthus camphoratus. Mesocolpial section. x18,900. Note in this, as in all preceding figures, that the foot layer is tightly appressed to the endexine, with consequent absence of caveae.

Staining procedures. All Figures except Fig. 263 are of pollen walls prestained with 1-2% OsO_4 followed by 0.5% uranyl acetate (UA). The pollen wall shown in Fig. 263 was not stained prior to embedding. All pollen was post-stained with UA and lead citrate (PbCit.).

260

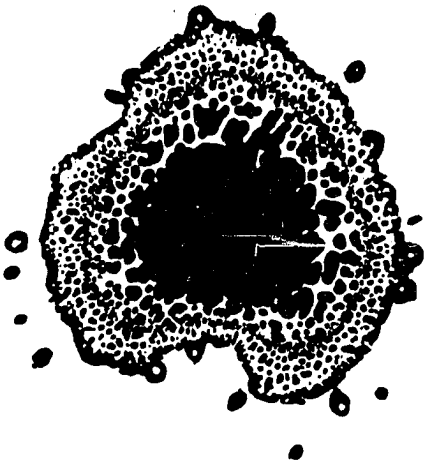

261



262



263

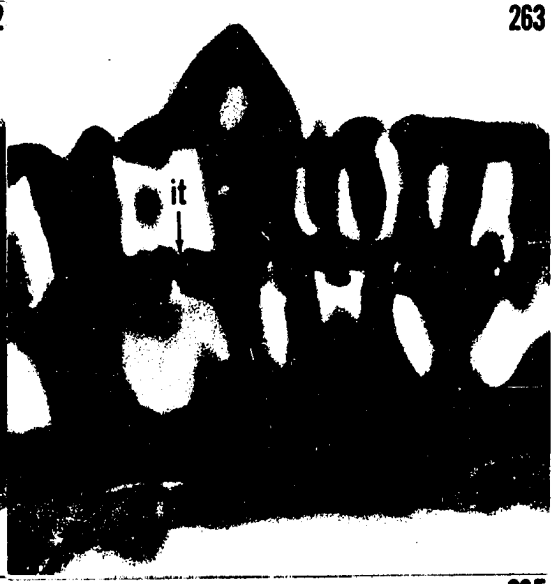

264



265

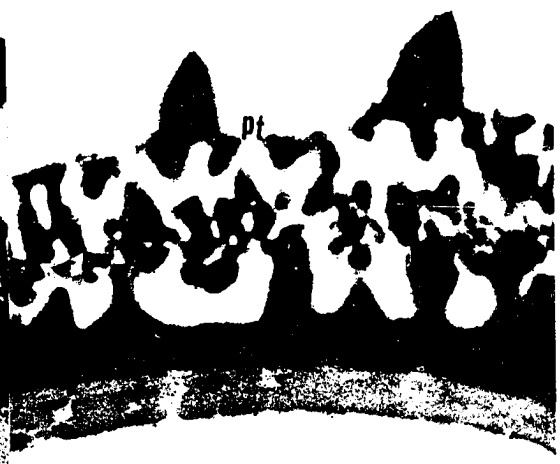

Fig. 266. Osmites parvifolia. Mesocolpial section including spines. x20,800. Note long basal columellae, layer or layers of internal tecta, and perforate tectum.

Fig. 267. Osmitopsis asteriscoides. Mesocolpial section including spine. x9,280. Similar to above, with some of the larger columellae digitate. Foot layer: endexine ratio approximates 1:1.

Fig. 268. Gymnarrhena micrantha. Mesocolpial section. x11,400. Note complexly ramified and fused levels of internal tecta and columellae. Also note thickened foot layer as compared to endexine.

Fig. 269. Osmitopsis asteriscoides. Mesocolpial section between spines. x9,280. As in Fig. 267, with less disrupted endexine.

Fig. 270. Adenocaulon bicolor. Mesocolpial section showing spinules. x12,160. Note extremely fine internal tecta components, above which rises a second distinct layer of thin columellae. Also note thickened foot layer.

Staining procedures. Only the pollen wall shown in Fig. 268 was prestained with 1-2% OsO_4 and UA. It was post-stained with UA and PbCit. All other figures represent pollen post-stained with OsO_4, UA and PbCit.


266
267
pt
268
it
269
en
270
it
fl
en

Fig. 271. Cylindrocline commersoni. Mesocolpial section through spinule. x16,200. Note slightly perforate tectum, single columellar units; foot layer: endexine stain differentiation not striking, but ratio appears 1:2; endexine disrupted, foramina not present; black dots are OsO_4 precipitate. Note variation in size of cavus immediately beneath spinule.

Fig. 272. Cylindrocline commersoni. Mesocolpial section. x33,600. Note that the OsO_4 precipitate appears appressed to the surface of the columellae, not within foot layer: endexine differentiation is seen as a nondisrupted layer versus a disrupted layer.

Fig. 273. Blumea mollis. Mesocolpial section. x27,200. Note perforate tectum; lack of internal foramina; highly disrupted endexine.

Fig. 274. Rhanterium adpressum. Mesocolpial section. x16,200. Note OsO_4 precipitate and severely disrupted endexine.

Fig. 275. Catostephane divaricata. Mesocolpial section. x22,100. Note presence of sparse foraminal traces; foot layer and endexine are differentiated chiefly by composition. Note sub-basal extension uniting with foot layer at far right.

Fig. 276. Odontospermum maritemum. Mesocolpial section. x25,500. Note thick, somewhat perforate tectum, a white precipitate throughout the columellae and tectum, and a very thin foot layer in relation to the endexine.

Fig. 277. Allagopappus dichotomus. Mesocolpial section. x29,750.

Fig. 278. Tessaria integrifolia. Mesocolpial section. x43,100. This magnification shows three columellae in great detail, the precipitate more obviously appearing appressed to the columellae rather than filling holes within them. Foot layer: endexine ration approximates 1:4.

Fig. 279. Amblyocarpum inuloides. Mesocolpial oblique section including spines. Note spine variation due to the angular section. Black dots are OsO_4 precipitate.

Fig. 280. Laggera alata. Mesocolpial section. x44,100. Note traces of internal foramina and traces of sub-basal extensions uniting with the foot layer. Foot layer and endexine are not distinguishable.

Staining procedures. Figs. 275-277, 280 are of pollen that was not prestained. All figures are of pollen prestained in 1-2% OsO_4 followed by 0.5% UA. All pollen except that shown in Fig. 276 were post-stained with UA followed by PbCit. Fig. 276 is of pollen post-stained with OsO_4, UA and PbCit.


271
cav
272
t
c
en
273
pt
274
cav
275
ft
en
276
t
c
en
277
278
279
280
ft
en

Fig. 281. Athroisma laciniata. Mesocolpial section including spine. x21,600. Note internal foramina filled with OsO_4 precipitate; foot layer: endexine ratio approximates 1:2.

Fig. 282. Polycline proteiformis. Mesocolpial section. x11,400. Note thin, perforate tectum; internal foramina filled with OsO_4 precipitate; both foot layer and endexine are highly disrupted.

Fig. 283. Blepharispermum zanquebarium. Mescolpial section including spinule. x 19,500. As above, with tiny columella-like structures adhering to the foot layer.

Fig. 284. Grantia aurliuz. Mesocolpial section. x27,200. Foramina obvious, though very minute; little differentiation between foot layer and endexine.

Fig. 285. Dimeresia howellii. Mesocolpial section. x27,200. Note thickened, imperforate tectum; foramina are obvious, since only partially filled with precipitate; foot layer:endexine ratio approximates 1:5.

Fig. 286. Polycline proteiformis. Mesocolpial oblique section including spine. x 5,800. As in Fig. 282, except that the complete columella unit cannot be seen; note that the columellae are more complexly ramified in the spine region.

Fig. 287. Geigeria vigintisquamea. Mesocolpial section. x35,840. Foramina are both circular and very elongate throughout columellae and tectum. Note the sub-basal extension connecting with the foot layer;

footlayer and endexine are not well differentiated.

Fig. 288. Grantia aurliuz. Mesocolpial section. x27,200. As in Fig. 284, with more easily distinguishable foot layer: endexine pattern.

Fig. 289. Myriocephalus stuartii. Mesocolpial section. x12,160. Note columellae-foot layer connection, thick foot layer and correspondingly thick endexine, which is totally disrupted beneath this point of connection. Another view of this same species is shown in Fig. 331.

Staining procedures. Figures 284, 287, 288 are of pollen that was not prestained. All others are of pollen prestained with 2% OsO_4, UA and PbCit.

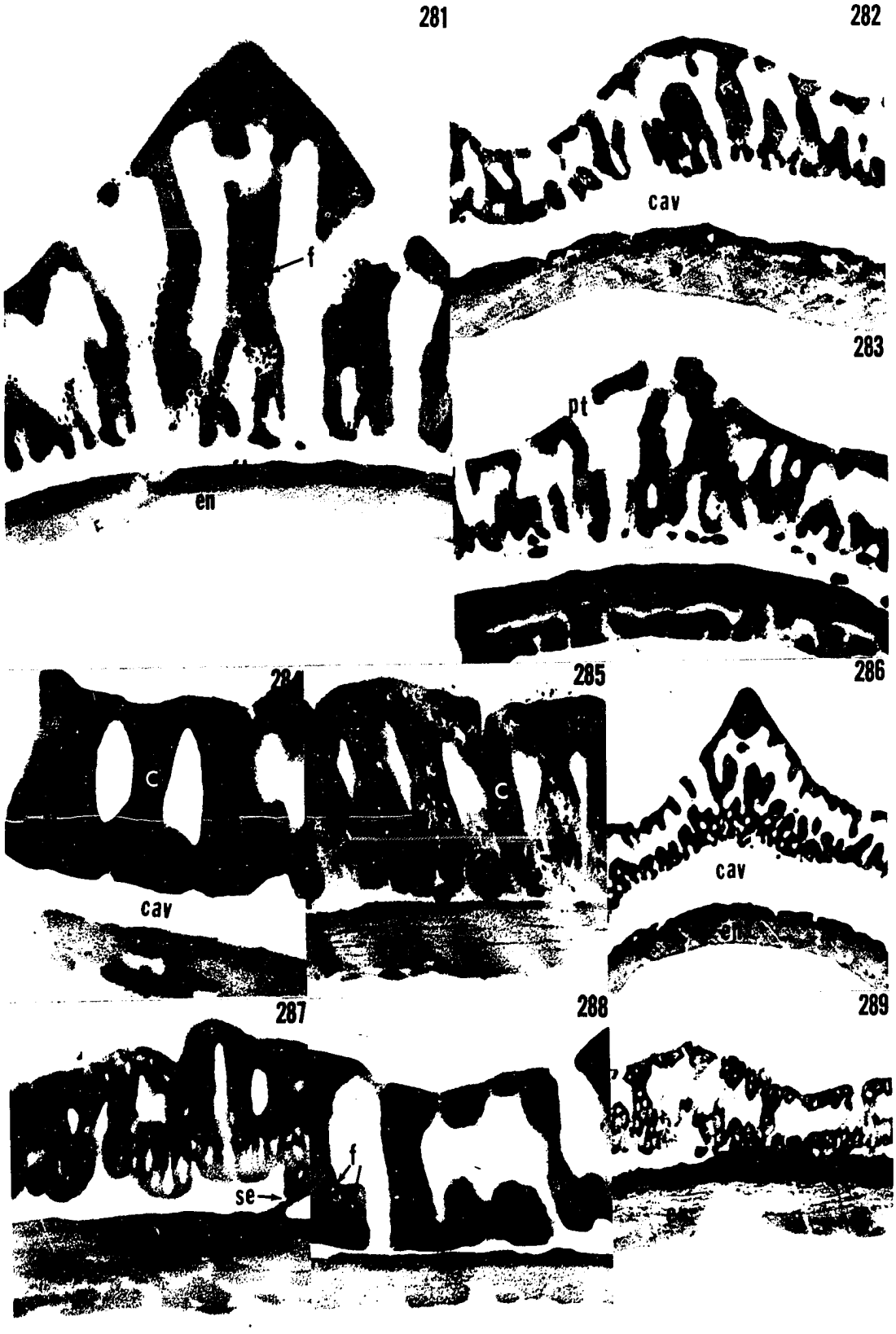
281
282
f
cav
283
en
pt
285
286
284
c
c
cav
cav
287
288
289
se
f

Fig. 290. Chrysophthalmum sternutatorium. Mesocolpial section including spine. x16,900. Basal columellae thin, loosely fused; irregularly shaped foramina sparsely scattered throughout; endexine very disrupted.

Fig. 291. Callilepis laureola. Mesocolpial section. x14,040. Perforate tectum; ramified basal columellae, not basally fused (arrows) in several areas; foramina very minute, filled with OsO_4 precipitate. Note very thin foot layer in proportion to endexine.

Fig. 292. Ifloga seriphioicles. Mesocolpial section including spine. x16,900. Similar to Figs. 290, 291 with equally delicate columellar patterns. Note channel through spine tip.

Fig. 293. Pterothrix flaccida. Mesocolpial section. x27,200. Many circular foramina present in the columellae, more sparse in the tectum. Note thin foot layer in proportion to endexine as in Fig. 291.

Fig. 294. Petalacte coronata. Mesocolpial section. x26,350. Many large circular to irregular foramina throughout columellae and tectum; foot layer: endexine ratio not so magnified as above.

Fig. 295. Stylocline filaginea. Mesocolpial section. x20,800. Circular foramina common throughout entire exine; basal columellae fused (arrows).

Fig. 296. Ixodia schilleoides. Mesocolpial section. x23,300. Note thin, somewhat perforate tectum, foramina filled with OsO_4 precipitate. Foot layer and endexine not shown.

Fig. 297. Gnaphalium cheiranthifolium. Mesocolpial section. x20,800. As above, with foramina clearly visible throughout the tectum and columellae.

Fig. 298. Stoebe capitata. Mesocolpial section. x20,800. Note greater intensity of foramina in basal columellae and tectum, as opposed to upper columellar projections; basal columellae loosely fused; very disrupted endexine.

Fig. 299. Syncephalum candida. Mesocolpial section including spine. x14,300. Foramina present throughout columellae, tectum and lower spine; all filled with OsO_4 precipitate; endixine disrupted.

Fig. 300. Millotia myostidifolia. Mesocolpial section. x25,500. Foramina most predominant in basal columellae and tectum; foot layer: endexine ratio approximates 1:2.

Staining procedures. All species except Figs. 291, 293 were not prestained. Figs. 291, 293 were prestained in 1-2% OsO_4 followed by 0.5% UA. Fig. 297 was post-stained with OsO_4, UA and PbCit. All others were post-stained with UA followed by PbCit.

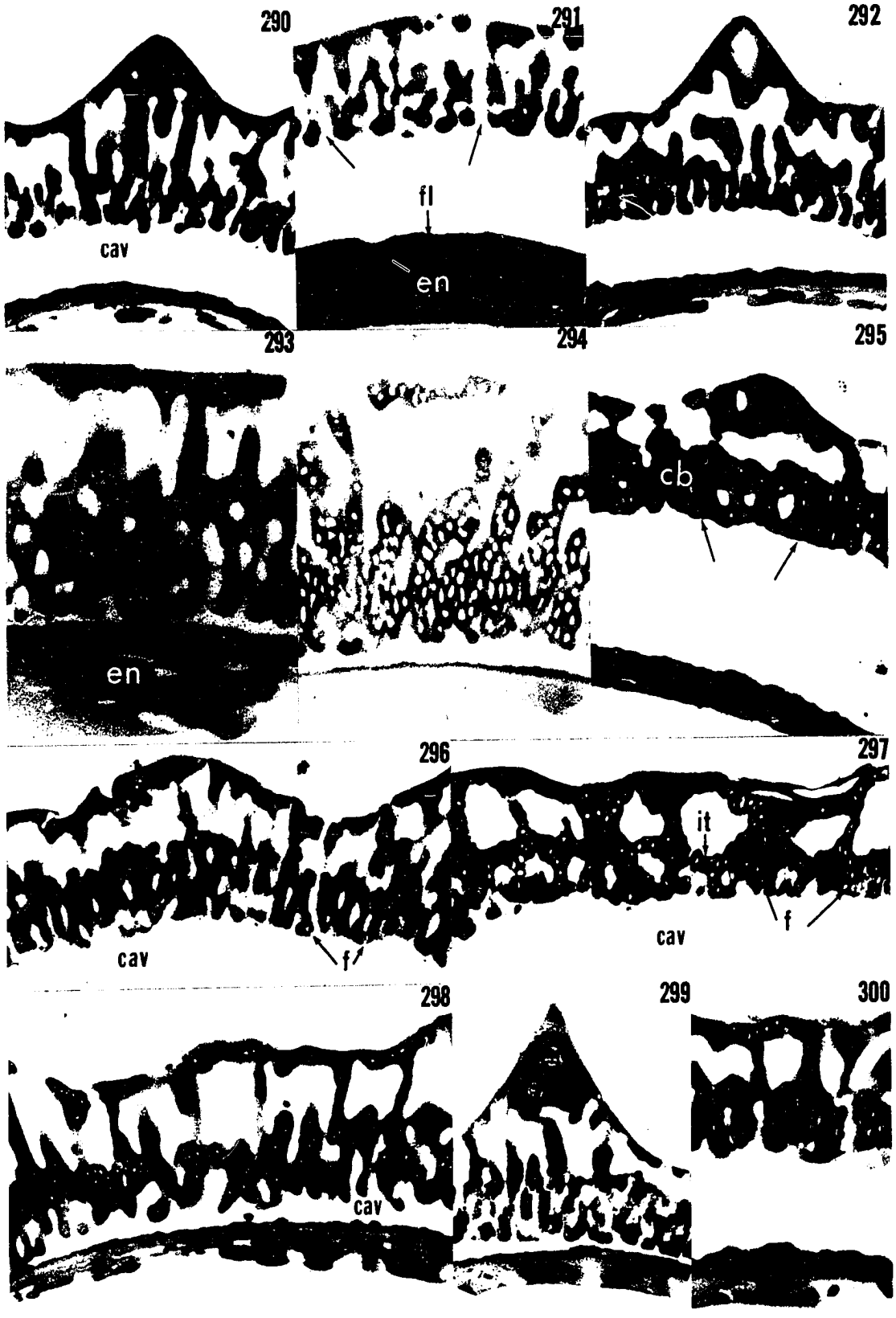
290
291
292
fl
cav
en
293
294
295
cb
en
296
297
it
cav
f
cav
f
298
299
300
cav

Fig. 301. Phagnalon saxatile. Mesocolpial section. x18,900. Small, circular foramina permeate the columellae and tectum; the foot layer is very thin in proportion to the endexine.

Fig. 302. Stuartina muelleri. Mesocolpial section. x20,800. Note double columellae layers with an obvious internal tectum; foot layer is very thin.

Fig. 303. Athrixia oblonga. Mesocolpial section. x42,560. Note variation in total exine thickness between this species and that of Fig. 302, this being twice the magnification. Note also the sub-basal extensions, the minute, if present, foramina, and the thickened foot layer.

Fig. 304. Facelis apiculata. Mesocolpial section. x25,500. Large circular to irregular foramina are present; internal tectum is one layer only; foot layer is thickened, as compared with Figs. 301-302, and foot layer: endexine ratio approximates 1:2.

Fig. 305. Sphaeranthus sp. Mesocolpial section. x25,500. Note irregular appearance of the tectum; small foramina are scattered throughout columellae and tectum; foot layer and ektexine are not well differentiated.

Fig. 306. Antennaria plantaginifolia. Mesocolpial section. x19,500. Foramina filled with OsO_4 precipitate.

Fig. 307. Antennaria campestris. Mesocolpial section including spinule. x19,500. As above, with highly disrupted endexine.

Fig. 308. Syncephalum candidum. Mesocolpial section including

spine. x22,750. Compare with Fig. 299. Similar except spine tip appears rounded in a more oblique section.

Staining procedures. All figures are of pollen prestained with 1-2% OsO_4 followed by 0.5% UA. All also were post-stained with UA followed by PbCit.

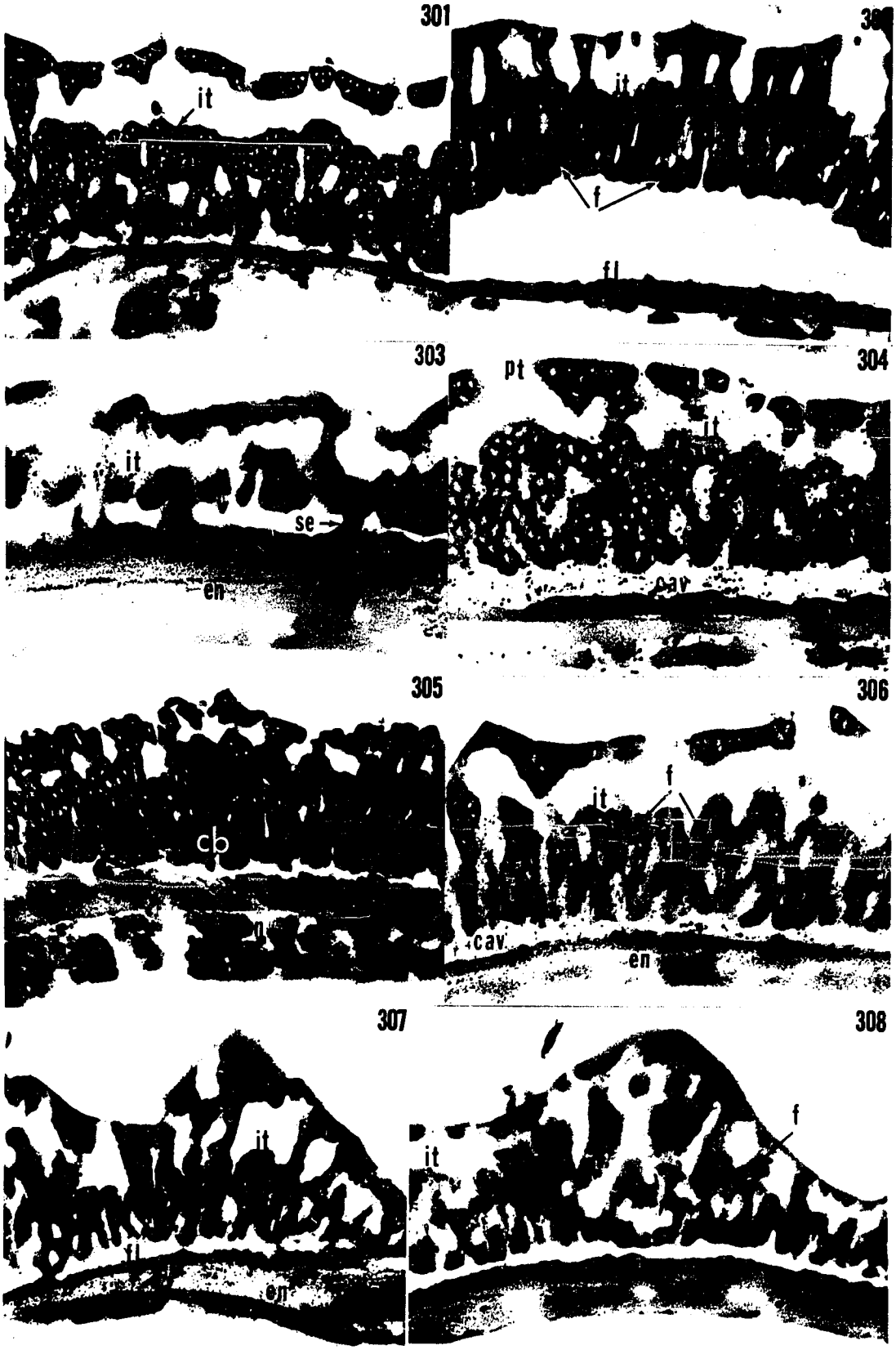
301
it
f
fl
303
it
se
en
pt
304
it
cav
305
cb
n
306
it
f
cav
en
307
it
fl
en
308
it
f

Fig. 309. Helichrysum davenportii. Mesocolpial section including spines. x11,600. Note thin foot layer; solid-tipped spines.

Fig. 310. Raoulia monroi. Mesocolpial section including spine. x14,300. Note foramina extending far into the spine area.

Fig. 311. Helichrysum davenportii. Enlarged section of Fig. 309 as indicated by arrow. x21,600. Note elongate foramina in basal columellae, with more rounded to irregular foramina in the tectum, which is thin and perforate. Also note the formation of a second internal tectum (arrows). Foot layer and endexine are not shown.

Fig. 312. Schoenia cassiniana. Mesocolpial section. x17,280. Foramina are filled with precipitate.

Fig. 313. Helipterum splendidum. Mesocolpial section through spines. x9,280. Note columellar pattern at spine bases, and the thin solid tips with the exception of single channels at the apex.

Fig. 314. Athrixia athrixioides. Mesocolpial section. x33,600. Tectum is imperforate; foramina as in Fig. 311; foot layer and endexine are not shown.

Fig. 315. Cephalipterum drummondii. Mesocolpial section through spinule. x22,400. Note columellar pattern throughout the spinule; foot layer and endexine are not well differentiated.

Fig. 316. Athrixia athrixioides. Mesocolpial section. x19,500. Description as in Fig. 314.

Staining procedures. Figures 310 and 312 are of pollen prestained

with 1-2% OsO_4 followed by 0.5% UA. Figures 313, 314, 316 are of pollen walls post-stained with OsO_4, UA and PbCit. In the others, the OsO_4 was omitted.

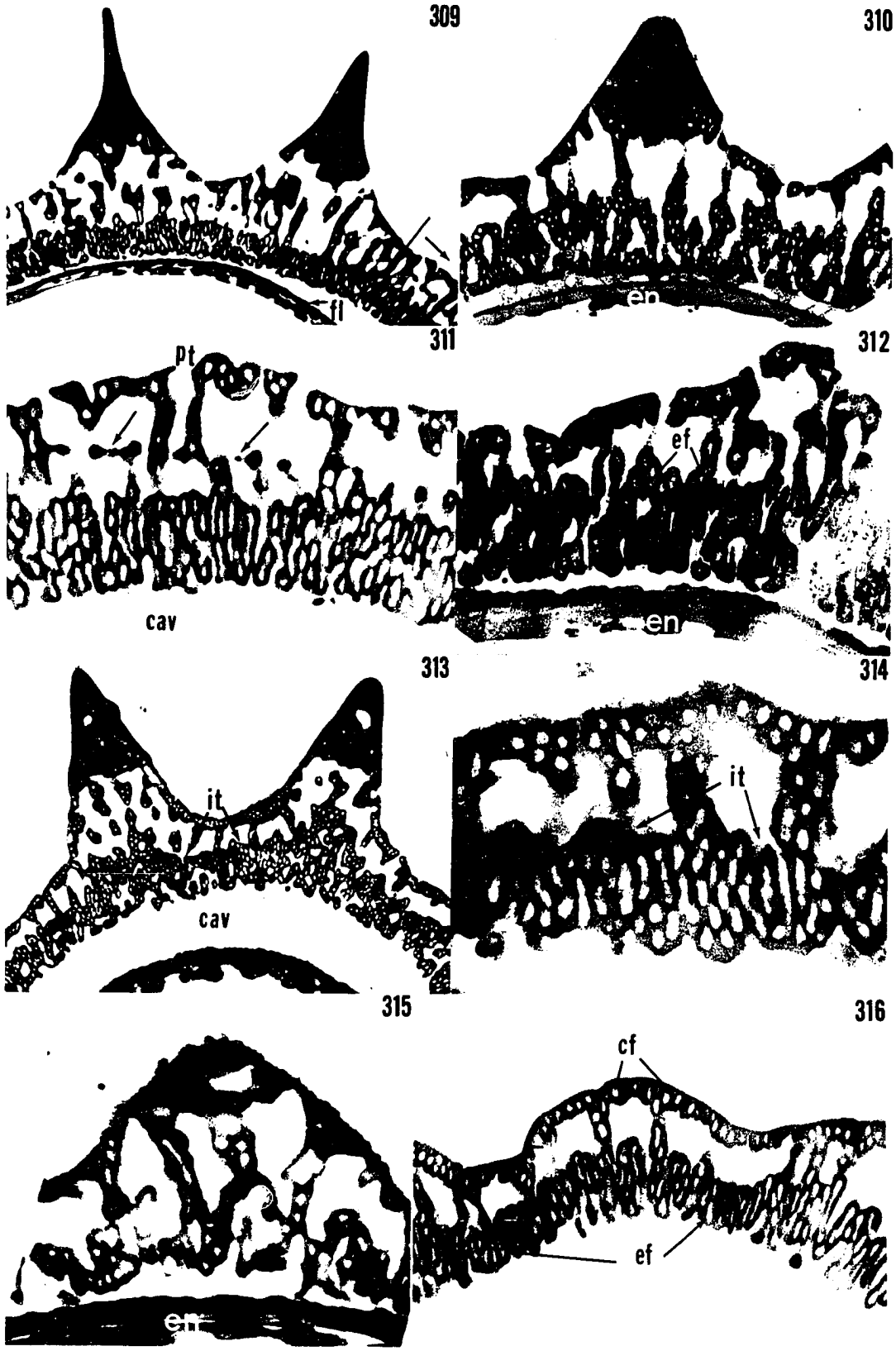
309
fl
310
en
311
pt
cav
312
ef
en
313
it
cav
314
it
315
en
316
cf
ef

Fig. 317-319. Helichrysum davenportii. Fig. 317. Mesocolpial midsection through spine. x17,280. Compare this slightly oblique cut with Fig. 309. Note formation of a second inner tectum. Fig. 318. Mesocolpial section. x13,500. Note very thin, perforate tectum with thin upper extensions. Fig. 319. Enlarged area of Fig. 318 as indicated by parallel lines. x24,300. Note elongate foramina in basal columellae, and more circular to irregular foramina in upper columellae and tectum.

Fig. 320. Pithocarpa corymbulosa. Mesocolpial section. x21,250. Note thin foot layer in relation to the thickened endexine, which is highly disrupted.

Fig. 321. Gilruthia osbornii. Mesocolpial section. x25,500. Tectum is thin, but imperforate. Note that foot layer is thicker than in other species depicted, and nearly equal in thickness to the endexine.

Figs. 322-323. Leptorhynchus ambiguus. Fig. 322. Mesocolpial section. x14,040. Thickened, imperforate tectum; very disrupted foot layer and endexine, which are not well differentiated. Fig. 323. Enlarged section of Fig. 322 as indicated by parallel lines. x20,520. Note elongate foramina in the basal columellae and circular to irregular foramina in the tectum. Foot layer and endexine are not shown.

Staining procedures. None of the species depicted here were prestained. Figures 320, 321 were post-stained with OsO_4, UA and PbCit. The others were post-stained with UA followed by PbCit.

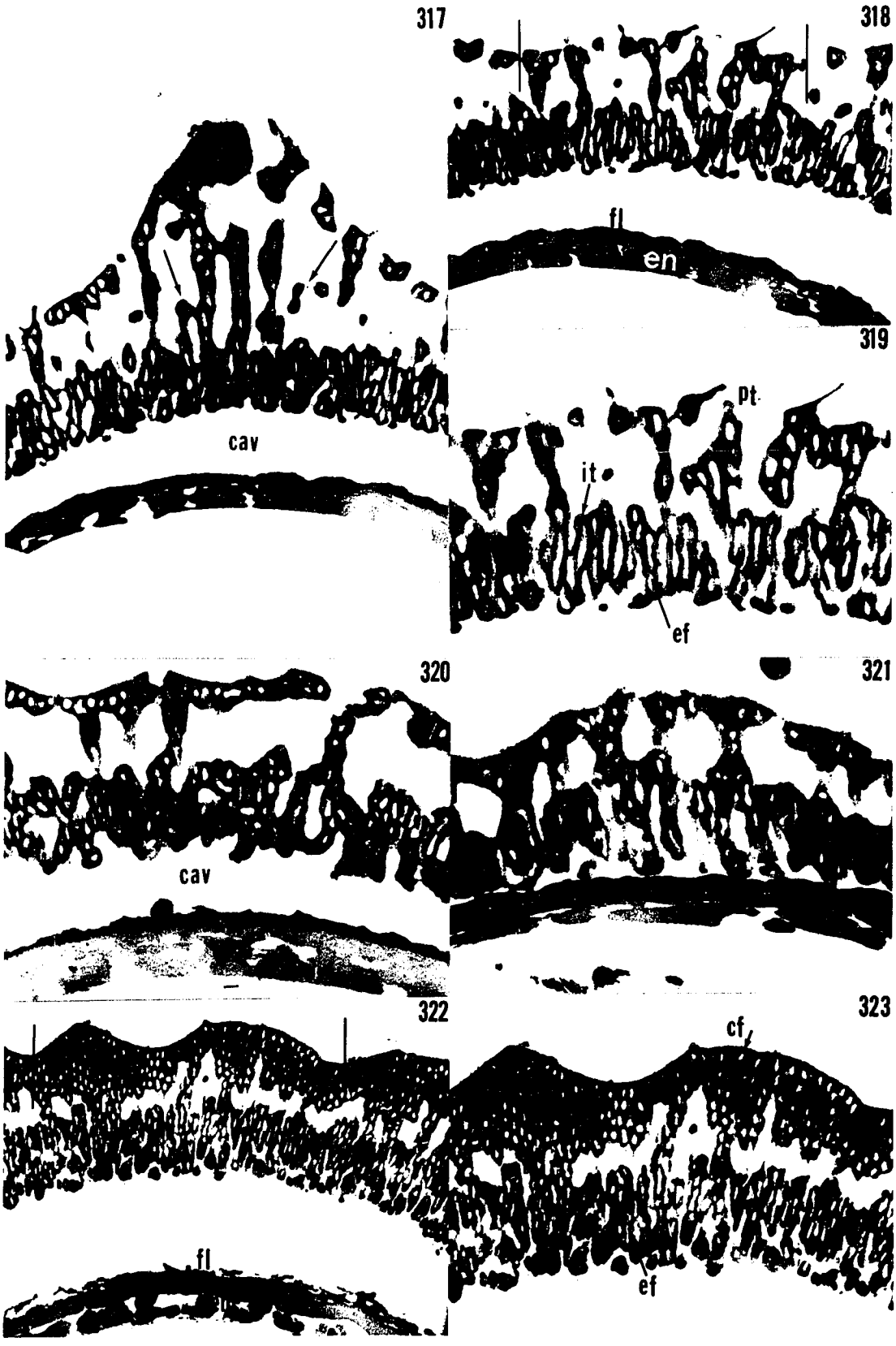
317
318
fl
en
319
pt
it
cav
ef
320
321
cav
322
323
cf
fl
ef

Fig. 324. Elytropappus adpressus. Mesocolpial section. x20,520. Note the complexly ramified and fused columellar pattern forming layers of internal tecta; foramina are absent; ektexine and endexine are not differentiated.

Fig. 325. Antithrixia angustifolia. Mesocolpial section. x16,200. Note lack of basal fusions; scattered traces of foramina can be seen; foot layer is very irregular with a large extension noted at the left of the picture; endexine is thoroughly disrupted and much thicker than the foot layer.

Fig. 326. Phagnalon rupestre. Mesocolpial section. x27,000. Note thickened columellar bases with traces (?) of internal foramina throughout the internal tectum and the tectum.

Fig. 327. Stenachenium riedelii. Mesocolpial section including spinule. x13,000. Note complex columellar pattern as in Fig. 324; traces of foramina are present.

Fig. 328. Antithrixia abyssinica. Mesocolpial section. x28,000. Note that this is a section through an imperforate region of the tectum; very long columellae form a complex pattern at the base; the ektexine, which has a very smooth surface, and the endexine, which is somewhat disrupted, are clearly differentiated.

Fig. 329. Elytropappus adpressus. Mesocolpial section including spinule. x19,500. Similar to Fig. 324.

Fig. 330. Phagnalon rupestre. Mesocolpial section including spine.

x19,500. Similar to Fig. 326, showing long upper columellae projecting into the spine tip, and depicting a more intensely differentiated foot layer.

Fig. 331. Myriocephalus stuartii. Mesocolpial oblique section including spines. Compare with Fig. 239. The columellae in the spine area appear more complex. Foramina are prevalent throughout columellae and tectum.

Staining procedures. All pollen walls except those shown in Fig. 327 were prestained with 1-2% OsO_4 followed by 0.5% UA. All were poststained with UA followed by PbCit.

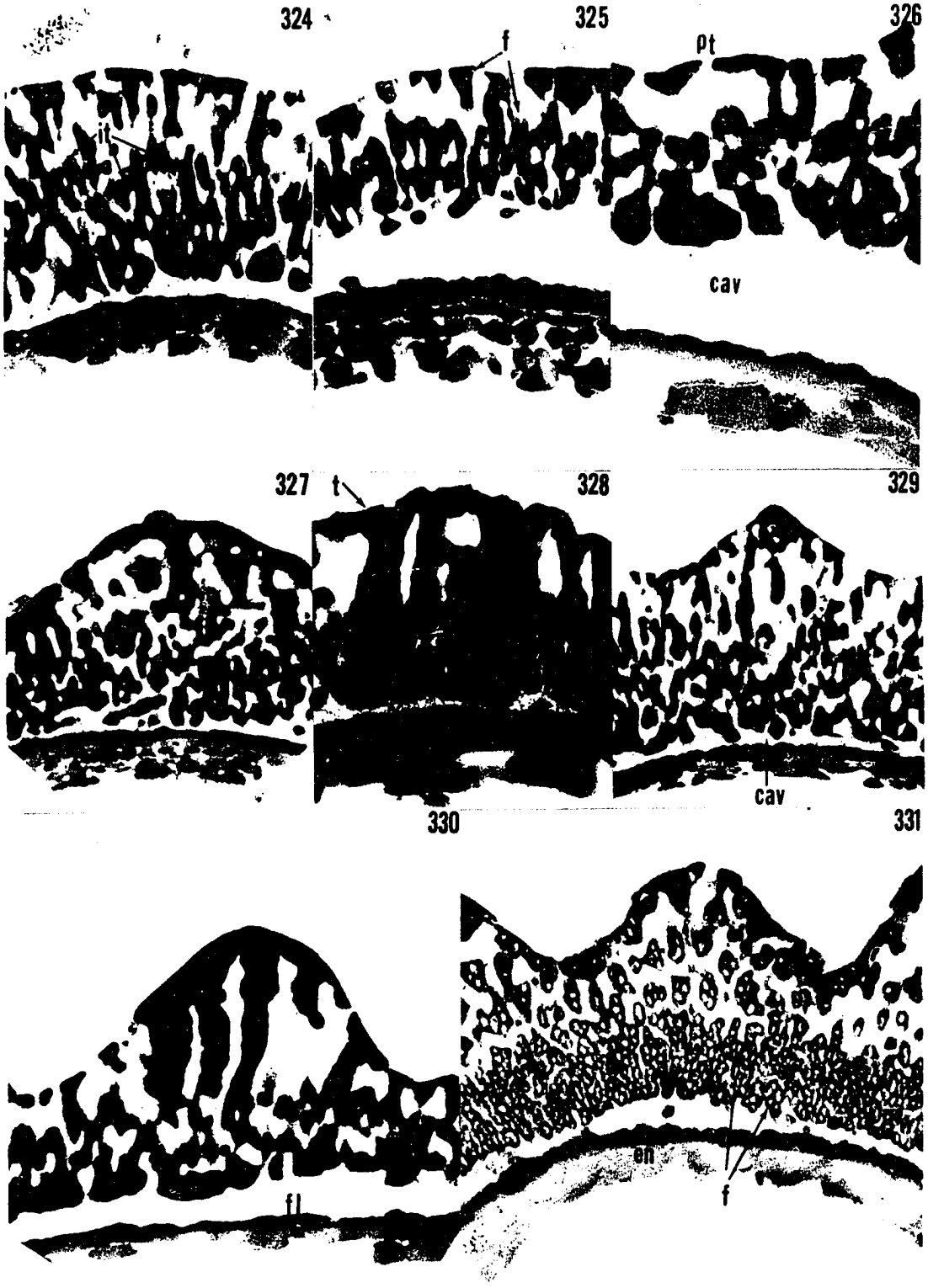
324
325
f
pt
326
cav
327
t
328
329
cav
330
331
fl
en
f

CHAPTER IV

DISCUSSION

Light Microscopy

Within the Inuleae, as presently studied, there is an impressive array of individually distinct combinations of characters including variations pertaining to the exine and to the germinal apertures. A profusion of variations was noted in: (1) pores 3-4 in number, with lateral extensions or congruent with colpi, and ranging from 2-7u in width, 3-5u in length, or being inconspicuous; (2) colpi width ranging from narrow to wide, running the full length of the polar axis or being reduced to pore size; (3) total pollen grain diameter varying from 18u to 50u; (4) spines ranging from 6u long to a spineless condition, the spines present in dense masses or being widely space; (5) cavus presence or absence. With few exceptions (i.e., Tarchonantheae) there is uniformity only with respect to pollen shape. Although this character has been utilized as a rough index of phylogeny in the Ambrosieae (Wodehouse, 1935), there is not sufficient variation in Inuleae pollen to indicate any phylogenetic or taxonomic trend. The other characters are discussed below.

Variations in Ora and Colpi

Due to the wide range of variations in the ora (pores) and colpi these characters are of limited taxonomic value at the generic and subtribal levels. Pores of every basic shape appear throughout the Inuleae, and the various shapes cannot be correlated with grain size. For example, a small grain may have a wide pore (Fig. 77, 79), or a large grain may have a small one (Fig. 95. 167). Pores may be thick or thin margined (Fig. 146-148). Pores with lateral extensions, while present in every subtribe, appear to be restricted to specific genera, and in future studies this may be a characteristic of important diagnostic value. These extensions are in general symmetrically extended, but on occasion (Fig. 66) are confined to one side only, with thickened margins. The former are either faintly delimited (Fig. 19, 24, 125, 145, 190) or are with thickened margins (Fig. 163; 225, 255). These extensions are found in most of the Compositae tribes and some other families as well, and reach their best development in the Cynareae, although their phylogenetic significance is not established (Wodehouse, 1929). Wagenitz' (1955) detailed examination of 350 species of the Centaurea (Cynareae) depicted these lateral extensions in each of the 8 pollen types he established for this genus. Although he presented a detailed phylogenetic scheme, this apertural characteristic was not considered of prime taxonomic importance because of its uniformity.

A "lip-patterned" pore (Fig. 128, 157, 160, 205, 217, 220, 222, 258), present as a result of the lateral extensions, is confined to

12 genera in 7 subtribes. This pattern, most prevalent in the Inulinae and Buphthalmeae, is an obvious delimiting characteristic that would merit further study to determine its full taxonomic or phylogenetic significance to the Inuleae. Leins' (1969) study of the Inulineae and Buphthalmeae did not recognize this characteristic as an important pollen morphological feature.

The narrow colpus with lolongate pore (Fig. 53-55) appears most frequently in the Filagineae. Constrictions of the colpus (Fig. 74, 238) at a wide pore region can also result in a narrow colpus type. Generally, wide colpi accompany wide ora (Fig. 68), but many extended pores are accompanied by narrow colpi (Fig. 217, 220, 222). Colpi may appear deeply sunken (Fig. 202, 233) or almost superficial (Fig. 44-48, 105), so thin-margined that they are barely visible in polar view. In certain grains (Fig. 154, 156, 158, 162, 195, 196, 198, 202, 204, 252) the colpi seem distinguishable only as a space between spines.

Although the colpus length is nearly that of the entire polar axis (Fig. 17, 24, 29, 55) in many grains, there is some evidence that the colpus is reduced in length in about 45 genera. Some colpi are only slightly shorter than the axis (Fig. 18, 20, 142, 175, 250), but others are much reduced (Fig. 28, 37, 41, 43, 193, 201, 204, 208, 225, 227, 259), to the extent that the pore and the colpus in a few grains appear as one.

Significant in the pore-colpus relationship is the appearance of the tetracolporate form in two species of Brachylaena in the Tarchonantheae,

This characteristic is a distinctive feature and appears to be a fairly constant delimiting factor in any consideration of these species. The tetracolporate form is unusual in the Compositae, although Wodehouse (1935) states that it is encountered from time to time in nearly all groups of the family as a result, perhaps, of the irregular distribution of chromosomes in the maturation divisions or as the result of hybridity. Nonetheless, studies of two separate collections of Brachylaena hutchinsii have demonstrated the consistency of this characteristic. Erdtman's (1964) suggestion that an increase in aperture numbers may accompany increased pollen size during polyploidy is not borne out in B. hutchinsii, since there is no significant size variation apparent between the tetracolporate and the tricolporate forms. In view of this, the Tarchonantheae might represent a very worthwhile subtribe for cytological study.

Size Range

Despite the evidence of wide size range within the Inuleae (notable in the light microscopy plates), this characteristic has not been used as a primary factor for the delimitation of pollen types. Reasons for this decision are based on the work of investigators (Wodehouse, 1935; Stebbins, 1950; Gould, 1957; Duigan, 1961; Powell, 1965; King and Robinson, 1967) who have found that the size of mature pollen can be indicative of the general effect of polyploidy within a species. Powell's work, for example, showed progressive diameter increases with larger

chromosome numbers. The recent investigation of Gifford and Larson (1969) with Tridax coronipfolia statistically correlated variation in grain diameter with increasing chromosome numbers. It might be pointed out here that none of the above studies have incorporated the Inuleae.

In addition, grain size variation has also been recognized as resulting from environmental or nutritional influences (Kurtz and Liverman, 1958), normal genetic variation within a population (Clausen, 1960), ecotypic variation (Bragg and McMillan, 1962; Ehrlich and Holm, 1963), developmental or positional variations within a single plant (Clausen, 1962; Graham et al, 1968), and, as previously noted, procedures of mounting media (Faegri-Iversen, 1964), and harmomegathi (Wodehouse, 1935).

Significance of Spine and Cavus

Wodehouse (1928, 1935) considered spine length and density (frequency per unit area) as stable morphological characters for generic differentiation because they are independent of total grain size. Although Gifford and Larson (1969) demonstrated variation in spine length and aperture width with chromosomal variation, and indicate that tetraploids of Dyssodia are differentiated from diploids not only on the basis of pollen size and length, but on spine distribution as well, the present study has tentatively included Wodehouse's suggestion as a valid criterion for the establishment of pollen types within the Inuleae. Patterns depicting spine

density are outlined in Fig. 3. Data for spine length are summarized in Table 1.

The cavus is included as a primary feature in the establishment of pollen types. If it is wide, it is an obvious characteristic, although it also may be a very narrow separation in the wall layer (Skvarla and Turner, 1966b). A series of detailed generic studies will be needed before the significance of its width can be determined. While the term "cavus" is not used in the studies of Wagenitz (1955), Stix (1960), and Leins (1969), these authors recognize this structural feature.

These characters make it possible to construct a simple key. This is not intended to be a scheme for ready identification, since there is much overlapping of types amongst Compositae genera, and throughout subtribes and tribes (Stix, 1960). Its purpose is to determine the type of pollen grain, along with the percentage of that type within specific groupings, i.e., the subtribes of the Inuleae. Thus, the genera studied have been assigned to divisions in the key with little concern for previously established generic relationships. It is not intended to deny established taxonomic divisions, but rather to demonstrate that pollen trends within subtribes may be significant. The terms "dense" and "not dense" as used below are defined as follows: (1) dense: more than 3-6 spines in the mesocolpial area, commonly present in more than one layer, as seen in polar optical section (Fig. 3A, 3C); (2) not dense: less than 3-6 spines in the mesocolpial area in polar optical section, clearly observable as a

single layer (Fig. 3B, 3D). Only generic names are listed unless the genus is divided by this arrangement.

Key to Light Microscope Surface Features

	Subtribe
I. Exines not caveate	
A. Surface smooth to subspinulose	
1. Tarchonanthus	Tarchonantheae
2. Brachylaena	
B. Spines reduced, ca. 2u in length	
1. Gymnarrhena	Buphthalmeae
2. Adenocaulon	Inulineae
C. Spines long, 3u in length or longer	
1. Osmites	Buphthalmeae
2. Osmitopsis	
II. Caveate exines	
A. Spines lacking	
1. Humea elegans	Gnaphalieae: Series 2
2. Helipterum battii	
3. Elytropappus	Relhanieae
B. Spines 1.5u or less, densely massed.	
1. Blepharispermum	Filagineae
2. Evax	
3. Filago, except F. montana	
4. Ifloga	
5. Micropsis	
6. Psilocarphus	
7. Stylocline	
8. Anaphalis briscus	Gnaphalieae: Series 1
9. Artemisiopsis	

10.	Chevreulia	Gnaphalieae: Series 1 (cont.)
11.	Desmidium	
12.	Facelis apiculata; F. retusa	
13.	Gnaphalium palustre; G. purpureum; G. stachydifolium	
14.	Lasiopogon	
15.	Loricaria	
16.	Raoulia australis	
17.	Stuartina	
18.	Leontonyx bicolor; L. glomeratus	Gnaphalieae: Series 2
19.	Cephalipterum drummondii (2 collections)	Angiantheae
20.	Craspedia chrysantha	
21.	Gnephosis cyathoppa; G. skirrophora	
22.	Relhania genistaefolia	Relhanieae
23.	Stoebe spiralis	
24.	Leyssera tenella	Athrixinae

C. Spines 1.5 to 3.0u, densely massed

1.	Blumea ambigua	Plucheineae
2.	Thespidium	
3.	Symphyllocarpus	Filagineae
4.	Filago montana	
5.	Achyrocline	Gnaphalieae: Series 1
6.	Anaphalis margaritica	
7.	Antennaria	
8.	Chiliocephalum	
9.	Chionolaena isabellae	
10.	Facelis apiculata	
11.	Gnaphalium americanum; G. uliginosum	
12.	Leontopodium	
13.	Luciliopsis	Gnaphalieae: Series 1
14.	Oligandra lycopodioides	
15.	Raoulia glabra; R. monroi; R. parkii	
16.	Stuchertiella	
17.	Ammobium	Gnaphalieae: Series 2
18.	Anaxeton	
19.	Cassinia	
20.	Eriochlamys	

21.	Helichrysum ambiguus	Gnaphalieae: Series 2 (cont.)
22.	Helipterum spicatum	
23.	Humea cassiniana	
24.	Ixiolaena	
25.	Leontonyx spathulatus	
26.	Leucopholis	
27.	Petalactella	
28.	Quinetia	
29.	Rutidosis multiflorum	
30.	Angianthus brachypappus; A. tomentosus	Angiantheae
31.	Calocephalus knappii	
32.	Chthonocephalus	
33.	Gnephosis eriocarpa; G. gynotricha	
34.	Disparago anomala; D. ericoides; D. hoffmanniana	Relhanieae
35.	Nestlera	
36.	Pterothrix	
37.	Syncephalum	
38.	Printzia densifolia	Inulinae

D. Spines 1.5 to 3.0u, not densely massed.

1.	Epaltes	Plucheineae
2.	Pterocaulon interruptum; P. sphacelatum	
3.	Psila	Gnaphalieae: Series 1
4.	Petalacte	Gnaphalieae: Series 2
5.	Phaenocoma	
6.	Stenocline chionaea	
7.	Waitzia acuminata	
8.	Zoutpansbergia	Relhanieae
9.	Antithrixia	Athrixieae
10.	Leyssera capillifolia	
11.	Anisopappus	Buphthalmeae
12.	Callilepis	
13.	Philyrophyllum	

E. Spines 3.1 to 4.5u, densely massed

1.	Pterocaulon virgatum	Plucheineae
2.	Denekia	
3.	Stenachenium campestre	

4.	Athroisma	Filagineae
5.	Cylindrocline	
6.	Amphidoxa	Gnaphalieae: Series 1
7.	Chionolaena lychnophoroides	
8.	Gnaphalium cheiranthifolium; G. luteoalbum; G. macounii; G. obtusifolium; G. polycephalum	
9.	Phagnalon	
10.	Acomis	Gnaphalieae: Series 2
11.	Anaxeton aspenum	
12.	Gilruthia	
13.	Helipterum australe; H. manglesii; H. roseum; H. splendidum	
14.	Leptorhynchus	
15.	Millotia	
16.	Phacellothrix	
17.	Pithocarpa	
18.	Rutidosis helichrysoides	
19.	Stenocline ericoides	
20.	Waitzia citrina; W. suaveolens	
21.	Actinobole	Angiantheae
22.	Angianthus cunninghamii; A. strictus	
23.	Calocephalus brownii; C. skirrophora	
24.	Cephalipterum drummondii (two collections)	
25.	Craspedia uniflora	
26.	Arrowsmithia	Athrixieae
27.	Athrixia athrixioides	
28.	Leyssera gnaphalioides	
29.	Macowania revoluta	
30.	Podolepis cupulata	
31.	Allagopappus	Inulineae
32.	Calostephane	
33.	Carpesium abrotanoides	
34.	Codonocephalum peacockianum	
35.	Inula, all species except I. candida	
36.	Iphiona	
37.	Perralderia	
38.	Pulicaria dysenterica	
39.	Varthemia iphionoides	
40.	Anvillea	Buphthalmeae
41.	Buphthalmum	
42.	Ondetia	

43.	Pallenis	Buphthalmeae (cont.)

F. Spines 3.1u to 4.5u, not densely massed

1.	Blumea laciniata; B. mollis	Plucheineae
2.	Laggera	
3.	Pluchea	
4.	Sachsia	
5.	Sphaeranthus	
6.	Tessaria	
7.	Triplocephalum	
8.	Ixodia	Gnaphalieae: Series 2
9.	Angianthus sp.	Angiantheae
10.	Caesulia	
11.	Gnaphalodes	
12.	Myriocephalus	
13.	Polycline	
14.	Disparago lasiocarpa	Relhanieae
15.	Metalasia	
16.	Relhania quinquinervis	
17.	Stoebe capitata; S. sphaerocephala	
18.	Athrixia australis; A. oblonga	Athrixieae
19.	Podolepis capillaris	
20.	Amblyocarpum	Inulineae
21.	Grantia	
22.	Inula candida	
23.	Pegolettia	
24.	Printzia pyrifolia	
25.	Geigeria vigintisquamea	Buphthalmeae
26.	Odontospermum	
27.	Chrysophthalmum sternutatorium	

G. Spines 4.6u to 6.0u, densely massed

1.	Helichrysum davenportii	Gnaphalieae: Series 2
2.	Podosperma gnaphalioides	
3.	Schoenia cassiniana	
4.	Calocephalus drummondii	Angiantheae
5.	Podolepis rugata	Athrixieae
6.	Jasonia	Inuleae
7.	Pulicaria sicula	
8.	Geigeria aspera; G. brevifolia	Buphthalmeae

H. Spines 4.6u to 6.0u, not densely massed

1.	Pterigeron liatroides	Plucheineae
2.	Pterocaulon undulatum	
3.	Rhodogeron coronopifolius	
4.	Stenachenium riedelii	
5.	Dimeresia howellii	Angiantheae
6.	Heterolepis aliena	Athrixieae
7.	Carpesium cernuum	Inulineae

I. Spines 6.1u or longer

1.	Nanothamnus sericeus	Plucheineae
2.	Helichrysum bracteatum	Gnaphalieae: Series 2

It is immediately obvious that most subtribes comprise a variety of pollen types and the following table clarifies this general conclusion.

Table 2. A summary of types within subtribes as elucidated by light microscopy

Subtribe	% Species	# Species	Pollen type (from key, pp. 186-191)
Tarchonantheae	100	15	I-A
Plucheineae	8	2	II-C
	16	4	II-D
	12	3	II-E
	44	11	II-F
	16	4	II-H
	4	1	II-I
Filagineae	82	19	II-B
	9	2	II-C
	9	2	II-E
Gnaphalieae: Series 1	4	2	II-A
	4	2	II-B
	33	15	II-C

Table 2 (cont.)

Gnaphalieae: Series 1	8	4	II-D
	40	18	II-E
	7	3	II-G
	4	2	II-I
Angiantheae	14	4	II-B
	22	6	II-C
	28	8	II-E
	28	8	II-F
	4	1	II-G
	4	1	II-H
Relhanieae	10	2	II-A
	10	2	II-B
	38	8	II-C
	4	1	II-D
	38	8	II-F
Athrixieae	7	1	II-B
	21	3	II-D
	37	5	II-E
	21	3	II-F
	7	1	II-G
	7	1	II-H
Inulinae	4	1	I-B
	4	1	II-C
	60	15	II-E
	20	5	II-F
	8	2	II-G
	4	1	II-H
Buphthalmeae	5	1	I-B
	15	3	I-C
	25	5	II-D
	30	6	II-E
	15	3	II-F
	10	2	II-G

Data Conclusions

1. No one type characterizes the Inuleae.

2. It is not possible to segregate the subtribes, except the Tarchonantheae, on the basis of pollen surface characters.

3. The non-caveate condition occurs in three subtribes (Tarchonantheae, Inulineae, Buphthalmeae).

4. The spineless exine occurs rarely both in non-caveate and caveate types; in the caveate types it occurs in one species of each of two genera.

5. A single pollen type may be observed in several subtribes.

6. The Plucheineae, Filagineae, and Inulineae possess one predominant pollen type; the Gnaphalieae, Relhanieae, and Athrixieae possess two predominant types, while the Angiantheae and Buphthalmeae commonly contain several pollen types.

7. The largest subtribe, Gnaphalieae, includes species representing every pollen type.

Total species counts for each pollen type are as follows:

I-A - 15	II-A - 4	II-D - 19	II-G - 9
I-B - 2	II-B - 43	II-E - 6	II-H - 7
I-C - 3	II-C - 56	II-F - 39	II-I - 2

These figures point out that the Inuleae are most often represented by caveate pollen, with variable densities of spines 1.5u-4.5u long.

Of the 61 genera considered, in which more than one species was studied, 29 had one pollen type. This suggests that a type may cross both generic and specific lines. Of the genera in which more than one collection of the same species was studied, 4 species had more than one

pollen type.

It is impossible to establish a single pollen type for the Inuleae; it is nearly impossible to establish valid, separating types for the subtribes. The one exception is the Tarchonantheae which have a distinctive non-caveate, and spineless exine. Species within genera may be separated from each other and genera within specific subtribes can be separated from each other, but this in no way implies that these same genera or species are isolated from taxa in other subtribes or even in other tribes, a conclusion in agreement with less comprehensive studies of composite pollen (Stix, 1960; Leins, 1969).

Correlations with Other Investigations

In contrast to the varied gross morphology of the Inuleae reported in this study, Wodehouse (1935) stated that little variation exists in pollen throughout the Astereae, and that the pollen of the Anthemideae, Cichorieae, and Vernonieae, although possessing variations which distinguish certain genera and species within the respective tribes, also possess distinctive tribal characteristics. He further noted that the Ambrosieae have pollen characters which can be found in other composite tribes, although they also have specific characters which identify them as Ambrosieae. An instance of extreme variation, the Mutisieae, was used by Wodehouse (1929) to suggest polyphyletic origin of the tribe. Stix's (1960) studies, however, indicated that only similarities exist in the Mutisieae,

and she stated that pollen wall differentiation suggested generic and specific separations in all tribes except the Mutisieae. In her work, the presence of a single delimiting pollen type was demonstrated only for the Cichorieae. It was not possible, in that study, to support Wodehouse's original contention that individual tribes of Compositae could be distinguished, almost without exception by pollen grains.

Electron Microscopy

Although the fine structure of Inuleae pollen is diverse, it is possible to characterize it by a few basic patterns which have been established from other investigations in the Compositae (Skvarla and Turner, 1966a, b). It is notable that Inuleae incorporate pollen forms observed in the Heliantheae, Astereae, Ambrosieae, Senecioneae, Helenieae and Anthemideae, in addition to displaying distinctive intrinsic patterns.

The morphological characters of greatest value in analysis of Inuleae pollen walls are: (1) cavus presence or absence, (2) columellar diversity, (3) internal foramina presence or absence and their diverse morphology, and (4) foot layer and endexine relationships. It should be emphasized here that these patterns have been established, as in the light microscopy section, as an attempt to relate similar morphologies. While they are recognized as being artificial, they are effective in pointing out subtribal relationships. Accordingly, a simple key identifying these wall patterns can be constructed from the electron microscope

data. Text figure numbers (Figs. 5, 6) are given to aid in clarification. Complete descriptions are given with the text figures. Only generic names are listed unless the genus is separated by these divisions.

Key to Wall Patterns as Interpreted with Electron Microscopy

	Subtribe
5. Exines not caveate	
A. Columellae thickened, branching at mid length	
1. Brachylaena	Tarchonantheae
2. Tarchonanthus	
B. Columellae elongate, branching at upper extremities	
1. Osmites	Buphthalmeae
2. Osmitopsis	
C. Columellae elongate, forming multiple layers of internal tecta	
1. Adenocaulon	Inulineae
2. Gymnarrhena	Buphthalmeae
6. Exines caveate	
A. Columellae single-layered, lacking, or with traces of, internal foramina	
1. Blumea	Plucheineae
2. Denekia	
3. Epaltes	
4. Laggera	
5. Nanothamnus	
6. Pluchea	
7. Pterigeron	
8. Pterocaulon	
9. Rhodogeron	

10.	Sachsia	Plucheineae (cont.)
11.	Tessaria	
12.	Thespidium	
13.	Symphyllocarpus	Filagineae
14.	Artemisiopsis	Gnaphalieae: Series 1
15.	Zoutpansbergia	Relhanieae
16.	Heterolepis	Athrixieae
17.	Allagopappus	Inulineae
18.	Amblyocarpum	
19.	Calostephane	
20.	Codonocephalum	
21.	Inula	
22.	Iphiona	
23.	Jasonia	
24.	Perralderia	
25.	Pulicaria	
26.	Varthemia	
27.	Anvillea	Buphthalmeae
28.	Buphthalmum	
29.	Odontospermum	
30.	Philyrophyllum	
31.	Rhanterium	

B. Columellae single-layered, obvious foramina

1.	Athroisma	Filagineae
2.	Blepharispermum	
3.	Evax	
4.	Psilocarphus	
5.	Anaphalis	Gnaphalieae: Series 1
6.	Chiliocephalum	
7.	Chionolaena	
8.	Leontopodium	
9.	Loricaria	
10.	Psila	
11.	Ammobium	Gnaphalieae: Series 2
12.	Anaxeton	
13.	Podosperma	
14.	Caesulia	Angiantheae
15.	Calocephalus	
16.	Craspedia	
17.	Dimeresia	
18.	Gnaphalodes	
19.	Gnephosis	

20.	Myriocephalus	Angiantheae (cont.)
21.	Polycline	
22.	Disparago	Relhanieae
23.	Nestlera	
24.	Leyssera	
25.	Macowania	Athrixieae
26.	Podolepis	
27.	Grantia	Inulineae
28.	Anisopappus	Buphthalmeae
29.	Geigeria	

C. Columellae double-layered, complexly ramified

1.	Stenachenium	Plucheineae
2.	Phagnalon rupestre	Gnaphalieae: Series 1
3.	Elytropappus	Relhanieae
4.	Stoebe	
5.	Antithrixia	Athrixieae

D. Columellae double-layered, circular foramina

1.	Sphaeranthus	Plucheineae
2.	Ifloga	Filagineae
3.	Stylocline	
4.	Antennaria	Gnaphalieae: Series 1
5.	Facelis	
6.	Gnaphalium	
7.	Phagnalon saxatile; P. sordidum	
8.	Stuartina	
9.	Stuchertiella	
10.	Ixodia	Gnaphalieae: Series 2
11.	Leontonyx	
12.	Leucopholis	
13.	Millotia	
14.	Petalacte	
15.	Petalactella	
16.	Stenocline	
17.	Waitzia	
18.	Chtonocephalus	Angiantheae
19.	Pterothrix	Relhanieae
20.	Relhania	
21.	Syncephalum	
22.	Arrowsmithia	

23.	Athrixia oblonga	Relhanieae (cont.)
24.	Pegolettia	Inulineae
25.	Printzia	
26.	Callilepis	Buphthalmeae
27.	Chrysophthalmum	

E. Columellae double-layered, elongate foramina

1.	Raoulia	Gnaphalieae: Series 1
2.	Acomis	Gnaphalieae: Series 2
3.	Gilruthia	
4.	Helichrysum	
5.	Helipterum	
6.	Ixiolaena	
7.	Leptorhynchus	
8.	Pithocarpa	
9.	Schoenia	
10.	Cephalipterum	Angiantheae
11.	Athrixia athrixioides	Relhanieae
12.	Geigeria	Buphthalmeae

Most subtribes comprise a variety of pollen types. However, a summarizing table will give evidence that the distribution is not quite as widespread as noted by light microscopy, if only because of the lack of variation.

Table 3. A summary of types within subtribes as indicated by electron microscopy

Subtribe	% Species	# Species	Pollen type (from key, pp. 196-199)
Tarchonantheae	100	6	5-A
Plucheineae	86	13	6-A

Plucheineae (cont.)	7	1	6-C
	7	1	6-D
Filagineae	14	1	6-A
	57	4	6-B
	29	2	6-D
Gnaphalieae: Series 1	5	1	6-A
	37	7	6-B
	5	1	6-C
	48	9	6-D
	5	1	6-E
Gnaphalieae: Series 2	14	3	6-B
	43	9	6-D
	43	9	6-E
Angiantheae	84	11	6-B
	8	1	6-D
	8	1	6-E
Relhanieae	11	1	6-A
	22	2	6-B
	22	2	6-C
	45	4	6-D
Athrixieae	11	1	6-A
	34	3	6-B
	22	2	6-C
	22	2	6-D
	11	1	6-E
Inulineae	7	1	5-C
	73	11	6-A
	7	1	6-B
	13	2	6-D
Bupthalmeae	21	3	5-B
	7	1	5-C
	37	5	6-A
	14	2	6-B
	14	2	6-D
	7	1	6-E

Data Conclusions

1. No one wall pattern characterizes the Inuleae.

2. One wall pattern appears to characterize the Tarchonantheae.

3. A predominant pattern of fine structure is present in 5 subtribes (Plucheineae, 6-A; Filagineae, 6-B; Gnaphalieae, 6-D; Angiantheae, 6-B; Inulineae, 6-A).

4. Three subtribes (Relhanieae, Athrixieae, Buphthalmeae) are more evenly distributed throughout the range of differentiation.

5. In those genera (14) in which more than one species was studied, 12 exhibited similar wall patterns.

6. Wall variation crosses subtribal and generic but, perhaps, not specific boundaries.

Total species count for each pollen variation is as follows:

5-A - 6	6-A - 33	6-D - 32
5-B - 2	6-B - 33	6-E - 13
5-C - 2	6-C - 6	

These figures point out that the Inuleae are most often represented by a fine structure which is caveate, with: (1) non-foraminate single level columellae; (2) foraminate single level columellae; or (3) double level columellae with circular foramina.

Non-Caveate Exines

Type 5-A. The non-caveate exines representative of the Tarchonantheae (Fig. 260-265) generally correspond with descriptions given for

representatives of the Anthemideae (Skvarla and Larson, 1965a) and designated as Anthemoid (Skvarla and Turner, 1966a). Briefly, this type is distinguished by a complex ektexine, lack of internal foramina, and possession of a thickened endexine. The principal variation within the Tarchonantheae is that the internal tectum separates columellar levels of equal length. Interspecific variation is also noted: (1) in Brachylaena (Fig. 260-262, 264) the columellae are wide, the tectum is thickened and imperforate, and the internal tectum is thickened, complex and difficult to interpret; (2) in Tarchonanthus (Fig. 263, 265), the columellae are narrow, the tectum is thin and imperforate and the internal tectum is much finer, though still complex in formation.

The fine structure of these genera appears to set them apart from the rest of the Inuleae, as the surface features do. It is pertinent that Carlquist (1961), employing wood anatomy studies, noted a very close relationship between Brachylaena and Tarchonanthus and recognized differences between these genera and the rest of the Inuleae.

Types 5-B and 5-C. Osmites parvifolia (Fig. 266), Osmitopsis asteriscoides (Figs. 267, 269) and Gymnarrhena micrantha (Fig. 268), all from the Buphthalmeae, and Adenocaulon bicolor (Fig. 270), from the Inulineae, while separable from the Tarchonantheae by longer basal columellae and multiple layers of internal foramina, exhibit patterns strikingly similar to published electron micrographs of pollen walls of Anthemideae (Skvarla and Larson, 1965a, Skvarla and Turner, 1966a).

These taxa are also similar to published electron micrographs of Liabum caducifolium Robl. et Bartl. (Senecioneae) and Cacosmia rugosa H. B. K. var. arachnoides Hier. (Helenieae) (Skvarla and Turner, 1966b). It is of interest to note that Liabum and Cacosmia are thought to have other characteristics in common with the Anthemideae and might possibly be placed in that tribe (Turner, personal communication).

Stix's (1960) study of several genera of the Anthemideae, along with Osmites and Osmitopsis (Inuleae) influenced her to propose the transfer of the latter species from the Inuleae to the Anthemideae. Leins (1969) concurred with this conclusion. Analysis of fine structure, as noted, supports these observations, with one significant addition: recognition of the endexine, which Stix said was absent in many Anthemideae, as well as in Osmites and Osmitopsis.

Adenocaulon, placed in the Senecioneae by Bentham (1873), in the Inuleae by Hoffman (1897, and in the Senecioneae by Cronquist (1955b) has, as shown in this study, Anthemid-like characteristics. The Senecioneae also exhibit Anthemid-like pollen, and the position of Adenocaulon within the Senecioneae is not disputed by this study (Skvarla and Turner, 1966b).

Gymnarrhena was placed in the Inuleae by both Hoffman (1897) and Bentham (1873), although Hoffman placed it in the Filagineae and Bentham in the Buphthalmeae. Bentham's decision was based on the natural affinities of Gymnarrhena to Geigeria, although it lacked most of the essential

characters of the tribe. The pollen is different from Geigeria (Fig. 287), and is not closely related to the fine structure of pollen in the Astereae, Bentham's alternate choice for this genus.

It should be reiterated that, although the Tarchonantheae and other above named taxa in this study are described as possessing an Anthemoid pattern, the variations, as shown in the Results section, are principally of degree, for example, a thickening or thinning of an exine component rather than an alteration in pattern, and are considered as reflecting the plasticity of the morphological parameters of this pollen type. Only after more studies are done in the Compositae, will it be possible to consider the Anthemoid pattern as an aggregate of variable characters or to subdivide it into several pollen wall types.

Caveate Exines

Type 6-A. The exine illustrated in Figs. 271-280, has presented difficulties in interpretation because of the apparent absence of internal foramina. As noted in this study and elsewhere (Payne and Skvarla, Grana, in press) it is possible to observe minute holes in the exine which could be interpreted as vestiges of internal foramina (Figs. 275, 280). Furthermore, exines stained in OsO_4 commonly incorporate "dots" of reduced osmium or perhaps heavy metal section stains, (i.e., lead), and past studies (Skvarla and Turner, 1966b), as well as the present one, have shown these artifacts to fill the internal foramina.

While this study has not definitely excluded the complete absence of internal foramina from the exine, it is certainly obvious that a group of exines in the Inuleae at least is characterized by a paucity of such features which stands in marked contrast to other tribal members. Although a name for this pattern has not been adopted, it appears to come closest to that described as Senecioid by Skvarla and Turner (1966a). Until the question of internal foramina is resolved it seems appropriate to reserve final decision.

In some members of the Inuleae described above there is close correspondence with published electron micrographs of other taxa: (1) Calostephane divaricata (Fig. 275) and Ambrosia tomentosa Nutt., (2) Blumea mollis (Fig. 273) and Ambrosia camphorata Greene, (3) Cylindrocline commersoni (Figs. 271, 272) and Ambrosia divaricata (Brandeg.) Payne (Payne and Skvarla, Grana, in press); (4) C. commersoni and Amblyopappus pusillus H. et A. and Blennosperma nanum (Hook.) Blake (Helenieae) (Skvarla and Turner, 1966a, b).

Type 6-B. The ability to differentiate type 6-A and type 6-B depends solely on the capacity to resolve the presence of internal foramina. Figure 285 (Dimeresia howellii) clearly depicts this as well as the presence of OsO_4 precipitate within the foramina. Figure 289 (Myriocephalus gracilis) and Fig. 287 (Geigeria vigintisquamea) also demonstrate the presence of many foramina, but without OsO_4 precipitate. In Athroisma laciniata (Fig. 281), Polycline proteiformis (Figs. 282, 286) and

Blepharispermum zanquebaricum (Fig. 283) the foramina are assumed to be filled with OsO_4 precipitate. This assumption is based on the ordered presence of the precipitate throughout the columellae and tectum, rather than a random scattering around exine units. Additionally, its frequent presence in the foot layer and endexine also supports the above assumption, since these units are commonly disrupted and should be capable of their incorporation.

Type 6-B has previously been termed Helianthoid (Skvarla and Turner (1966a) because of its widespread occurrence in the Heliantheae, but it also occurs with equal frequency in the Helenieae, Ambrosieae, Astereae, and, less frequently, in the Senecioneae (Skvarla and Larson, 1965a; Skvarla and Turner, 1966a, b; 1969).

Type 6-C. Type 6-C depicts a complexity of columellar ramifications which is less ordered than the other patterns. Lateral fusions establish variable layers of internal tecta which are very difficult to interpret. Internal foramina appear to be absent in Elytropappus adpressus (Fig. 324, 329), Phagnalon rupestre (Fig. 326, 330) and Stenachenium rupestri (Fig. 327) although they are obvious in Antithrixia angustifolia (Fig. 325). This pattern is limited to four subtribes: Plucheineae, Gnaphalieae, Relhanieae, and Athrixieae. Exact correlations of type 6-C with electron micrographs are lacking in the present literature, and it appears to be unique to the Inuleae.

Type 6-D. The double columellar wall pattern characterized in

Fig. 6-D, and illustrated in Fig. 290-308, contains a variety of basal columellar fusions and lengths, and internal foramina are either not present, sparsely scattered, or densely interspersed throughout columellae and tectum. Callilepis laureola (Fig. 291) appears to lack foramina, and may be compared with the exine patterns described for Parthenice mollis Gray (Heliantheae) and Iva axillaris Pursh (Ambrosieae), both of which are also characterized by a loose, discontinuous tectum (Skvarla and Larson, 2965a). The pattern described for most taxa of the section Iva (Ambrosieae), i.e., with the columellae subtending internal tecta longer than those above it, and with these basal columellae loosely fused, corresponds to several Inuleae genera (Pterothrix flaccida, Fig. 293; Petalacte coronata, Fig. 294; Phagnalon saxatile, Fig. 301), with the exception that internal foramina are present. This same pattern, with the basal columellae more tightly fused (Fig. 302, 305-306) can also be seen. Other species show the columellae above and below the internal tecta to be of equal length (Fig. 292, 295-298, 300). Variation of thick (Fig. 304) versus thin (Fig. 298) columellae should also be noted. This foraminate, double-layered columellar exine is found in 27 genera, in every subtribe except the Tarchonantheae and the Athrixieae, and appears unique to the Inuleae.

Type 6-E. The presence of elongate foramina in the basal columellae is the most striking feature of type 6-E, illustrated by Fig. 309-323. The pattern of smaller circular foramina throughout a very thin, perforate

tectum (Fig. 316, 317, 320) is also important. The internal tecta are either continuous (Fig. 314, 315, 321) at midlengths between the columellae or somewhat discontinuous (Fig. 310, 320). Interestingly, Helichrysum davenportii (Fig. 311, 317, note arrows) a second, distinct internal tectum appears to be present. Leptorhynchus ambiguus (Fig. 322, 323) is differentiated from the other species in this type by its very thick tectum, in which are scattered circular to irregularly shaped foramina.

An elongate type of foramina was previously noted by Skvarla and Turner (1966b) with reference to Anaphalis margaritacea var. occidentalis (Inuleae), a single-layered columellar form with elongated openings in the columellae and columellar bases. This type is common to 12 genera in four subtribes: Gnaphalieae, Relhanieae, Athrixieae, and Buphthalmeae.

Significance of Tectum, Foot Layer and Endexine Units

Tectum. When considering tectum morphology, thickness and contiguity, (i. e., perforations in the tectum), are major criteria. As noted in the plates of electron micrographs the tectum indicates a spectrum of thicknesses from exceptionally thin (Fig. 317-320) to markedly thick (Fig. 233, 232). While thickness appears uniform for a given species it has not been found to be restricted to any of the pollen types established. Perforations in the tectum are also highly variable. This character has not been specifically analyzed in relation to pollen types, but it is likely that detail-

ed studies at generic or specific levels, done by thin sectioning and scanning electron microscopy (Heslop-Harrison, 1969; Ridgway and Skvarla, 1969) could effectively utilize this character. In a recent scanning electron microscope study by J. R. Wells, unpublished, species of Polymnia appear to be differentiated by the variability of tectum perforations at the base of the spines.

Foot layer. The foot layer is most prominently developed in exines lacking caveae (Tarchonanthus, Brachylaena, Osmites, Osmitopsis, Adenocaulon, Gymnarrhena) and in contrast to caveate exines, it is always consistently uniform, and either equal in thickness to the underlying endexine or, usually, considerably thicker. In caveate exines the foot layer displays a nearly consistent thickness (variation no greater than that depicted in Fig. 292, 295) and is always thinner than the endexine. While a few caveate exines depict smooth foot layer surfaces (Fig. 276, 280, 281, 283, 287), most have slightly undulating (Fig. 271, 282) to somewhat irregular (Fig. 302, 304-308, 312, 317) to disrupted, jagged surfaces (Fig. 322, 320, 325, 331). This character is stable at the tribal level and appears to be equally stable at the species level.

The occasional difficulty in recognizing the foot layer (e.g., Fig. 283, 284, 287) in electron micrographs may be the result of oxidative or other chemical influences on the pollen both prior to and during processing for electron microscopy. However, close observations in this region of the exine, particularly where columellae join the foot layer at colpial mar-

gins, indicate a stain density similar to that of the other ektexine units (i.e., columellae and tectum). While the foot layer occasionally shows disruptions, internal structure of diagnostic significance has not been noted.

Endexine. The remaining exine unit, the endexine, is also a stable morphological character. Because of this, thickness ratios with the foot layer have been readily established (Skvarla and Turner, 1966b), and Inuleae pollen does not dispute this. As was noted in the discussion of the foot layer in the non-caveate exines, the endexine is either equal to the foot layer in thickness (Fig. 263, 268) or much thinner (Fig. 268, 270). This position is reversed in the caveate forms where the endexine is never equal to the foot layer in thickness. It is always thicker, and the foot layer: endexine ratios approximate ranges from 1:2 to 1:8. The total range can be seen by a close examination of several Figures: (1) Fig. 281, 321; (2) Fig. 304; (3) Fig. 318, 320, 325: (4) Fig. 276, 291, 293, 301, 305, 307. There is also considerable variation in the amount of variation in the amount of disruption that can be observed in the endexine of both caveate and non-caveate exines. The range is from nearly smooth, i.e., homogeneous in composition (Fig. 265, 270, 280) to slightly torn (Fig. 265, 268, 276, 283) to severely disrupted (Fig. 298, 305, 322, 325).

There appears to be no correlation of endexine thickness with amount of disruption present, nor does either characteristic correspond to pollen types described, although they may be generically significant. In all

grains examined, the endexine is heavily thickened at the apertural region (Fig. 261), as noted by Skvarla and Larson, 1965a. All endexines also appear lamellate (Skvarla and Larson, 1965a,b; Skvarla and Turner, 1966a, b), although no new data have been obtained from this tribe which add to an understanding of its taxonomic significance.

Correlations with Other Investigations

Several of the Inuleae genera examined in this study have also been examined by Stix (1960) and Leins (1969). Relationships between these contrasting investigations are discussed below.

1. Fifteen genera of the Inulineae and Buphthalmeae are placed in type 6-A (see key, pp. 196-199); Leins included 7 of these same genera (Inula, Amblyocarpum, Calostephane, Codonocephalum, Perralderia, Pulicaria, Varthemia) in an "Inula candida type" (i.e., the exine pattern is simply baculate, with simple rods in the wall between the spines), along with four other genera which were not included in the present study. Stix inserted Inula, along with Bupthalmum and Odontospermum into an "Inula type", defined, essentially, the same as the "Inula candida type."

2. Three genera (Allagopappus, Grantia, Geigeria) which Leins assigned to this "Inula candida type" are put into type 6-B on the basis of the presence of internal foramina, a characteristic below the resolution of light microscopy. Stix's evaluation of Geigeria was similar to Leins'.

3. The genera Iphiona, Jasonia and Philyrophyllum (type 6-A) were

placed by Leins in individual type groupings, not on the basis of the exine pattern, which is similar to the "Inula candida type," but on the variation in development of spine tip and number of spines present.

4. Printzia, Callilepis, Chrysophthalmum and Pegolettia (type 6-D) were placed by Leins in separate divisions which appear morphologically equivalent to type 6-D, that is, with an inner, irregular, thickened part of the sexine a detail revealed by electron microscopy, as a thick basal layer of a double-columellar pattern.

5. Pegolettia (6-D) was placed by Stix in the classification corresponding here with type 6-A. The validity of this is questioned on the basis of this work as well as that of Leins.

6. In Stix's investigation of the Compositae, 6 species (Amphidoxa, Angianthus, Elytropappus, Filago, Gnaphalium, Relhania) were examined in addition to those belonging to the Inulineae and Buphthalmeae, and all were assigned to the "Gnaphalium type" (i.e., the outer part of the ektexine is twice as thick or thicker than the length of the supporting bacula or columellae). Of these, Gnaphalium and Relhania are here placed in type 6-D, while Elytropappus is placed in 6-C. There is no correlation evident between these species and the above description of the type into which they were originally placed. The remaining 3 genera were not examined in the present study.

7. Certain surface characteristics in agreement with Leins are:

   a. Anvillea, with smaller spine tips can be separated

from Geigeria, with larger spine tips.

b. Inula graveolens can be separated from Inula candida on the basis of spine length and density.

c. Iphiona, with narrower spine bases, can be distinguished from Pegolettia, with wide spine bases.

d. Iphiona, with long (4.0u) spines, can be distinguished from Philyrophyllum, with spines less than 3.0u long.

It should be pointed out here that although there are several correlations that can be made in these studies between the surface characters of spine length and density, this investigation considers neither Leins' nor Stix's explanation of the wall pattern of the spine alone as valid in the separation of pollen types. Angles of sectioning of spines may depict very different shapes (Fig. 309, 317) or delineate several columellar variations (Fig. 290, 292; 313; 279; 263, 265) within the same grain. An even more germaine illustration of this is found in Leins' statement that the spine tip of the Printzia type appears solid. Electron micrographs of Printzia (not illustrated in the present study) clearly illustrate the presence of several, small, subapical channels within the spine tip. This problem of analyzing the morphological variations of spines has been noted by Skvarla and Turner, 1966b. In their discussion it was revealed that spine characters once thought significant in the structure of two tribes (Heliantheae and Anthemideae) were, upon further investigation, shown to

be so variable as not expected to have taxonomic significance.

This study supports Leins' suggestion that mutual relationships exist between the Inulineae and the Buphthalmeae at the palynological level, but takes issue with his suggestion that a new division based on pollen morphology would be significant at the subtribal level. Leins' contention is that the system of Compositae appears unnatural from several points of view, particularly with regard to interpretation of floral characteristics. The position taken in the present study is that pollen characters, considered apart from floral characteristics, would support an equally unnatural system. The present study would indicate that consequent upon the establishment of taxa at the megamorphic level, pollen data may be found to contribute significantly to the phylogenetic relations within that same taxa, a position also affirmed by Wagenitz (1955).

Both Stix (1960) and Leins (1969) referred to the presence of the foot layer and endexine, respectively, as nexine 1 and nexine 2. Leins' drawings of pollen types indicated variations in thickness of the foot layer as well as a certain amount of disruption in the endexine. No mention was made, however, of their significance to the types outline.

Stix's consideration of nexine 1 and nexine 2 is more fully explained as an integral part of each type established. The general observations are: (1) the footlayer is, as a rule, thinner than the endexine; (2) the structural differences are trivial; the outer part (foot layer) seems to be compact, the inner one (endexine) somewhat looser; (3) this division of

the nexine (i.e., into foot layer and endexine) can be assumed to occur in all grains, if the material has been especially fixed and stained for this purpose; (4) although specific measurements for nexine 1 (foot layer) and nexine 2 (endexine) are given for several pollen types, none are given for the Inuleae, and the nexine 2, as was mentioned previously, is not recognized as being a part of some genera.

Techniques

Apart from discussing Inuleae pollen in relation to the systematics of the Compositae, this study has provided interesting data concerning sample preparation. Of primary concern in all electron microscope studies is that of staining the exine to a degree where differential absorption, and, hence, contrast is obtained under the electron beam. For this reason OsO_4 is commonly used as a stain following acetolysis, while uranyl acetate and lead citrate are used as section stains immediately prior to examination with the electron microscope. Uranyl acetate can also be used after OsO_4 but does not contribute to exine contrast if OsO_4 is omitted. The principal drawback to using OsO_4, aside from extending the processing schedule, is that it appears to react in some way, as yet unknown, to create reduction products in the form of opaque precipitates, around and within the exine. Although this reaction occurs inconsistently and appears to be related to the original state of preservation of the pollen (e.g., pollen from herbarium sheets reacts less favorably to OsO_4 than

pollen preserved in liquid fixatives) it often causes some difficulty when interpreting exine fine structure. When OsO_4 stain is omitted after acetolysis the intrinsic density of the exine is usually of too low a contrast to be photographed. Figures 288, 317, of acetolyzed, unstained pollen show excellent contrast and detail. However, these electron micrographs have been selected with a prejudice since it is more often observed that such pollen is of too low contrast to be adequately photographed. The application of uranyl acetate and lead citrate section stains (Larson, 1964) provided too great an inconsistency to be of practical use. Therefore, a group of Inuleae pollen walls were prepared without osmication and appropriate sections obtained. If after section stains were applied the exines were still of inadequate contrast, a second group of sections was placed on a drop of OsO_4 for a few minutes prior to normal section staining. The results, as indicated in Figures 270, 320,appear to be highly satisfactory. Although this technique was not commonly used throughout the study, it does appear to offer an alternative to pre-embedding staining with OsO_4.

Phylogenetic Implications

Introduction

Interest in phylogenetic relationships within the Compositae has absorbed the attention of taxonomists for several decades (Cronquist, 1955a). A number of investigations involving megamorphology, chemo-

taxonomy, and cytotaxonomy (see Cronquist, 1955a, for a complete review; Carlquist, 1966; Drury and Watson, 1966), have attempted to analyze the interrelationships of the various tribes. Numerous pollen morphologists have also pursued this problem, incorporating the basic concepts cited by Wodehouse (1928) and summarized as follows: (1) pollen-grain characters within specifically outlined groups are useful for the determination of phylogenetic relationships; (2) in most families the pollen-grains bear a general similarity throughout, proportional in amount to the closeness of interrelationship within the group; (3) this general similarity is the composite of a limited number of more or less independent characters, which occur individually in varying degrees of similarity throughout somewhat restricted groups of plants; (4) these similarities have a strong tendency to recur in similar or different associations within a family or order, or even in entirely unrelated groups, as to the phylogenetic characters of multicellular plant organs.

In view of the above considerations, the purpose of this section is to discuss the phylogenetic significance of the wide range of pollen variability within the Inuleae, and attempt to relate it to the other Compositae tribes.

Review of Other Studies Based on Pollen Morphology

Wodehouse (1928) pointed out that the majority of authors agreed with Bentham that the most primitive Compositae are to be found among

the Heliantheae, and added that whatever the primitive Composite may be, the Heliantheae can be regarded as fairly generalized or central in position. He later (1935) described the pollen grains of Helianthus annuus Linn. (Heliantheae) as provided with long, sharp spines, and three broad short germinal furrows, and considered these characteristics indicative of such a central phylogenetic position, if not primitive. Other studies of Heliantheae pollen (Carlquist, 1957a, 1963) described surface features which did not differ appreciably from Wodehouse's description of H. annuus.

An electron microscope survey of the tribe Heliantheae (Skvarla and Larson, 1965a) provided data consistent with the light microscope findings of Carlquist (1957a, b, 1963) and Stix (1960),although it clarified in detail the concept of the structure of these exines. Skvarla and Larson (1965a) also examined pollen of Wyethia and Rudbeckia, genera considered to be the most primitive representatives of the Heliantheae (Weber, 1946; Battaglia, 1946; Stebbins, in Cronquist, 1955a). Their conclusion was that the genera did not differ from other exine morphologies in the Heliantheae.

Wodehouse (1935) and Wagenitz (1955), in investigations of other tribes, established a series of phylogenetic relationships which recognized the presence of the Helianthoid grain, but assigned it different phyletic positions.

In his study of the Ambrosieae Wodehouse (1935) considered the

primitive pollen grain as thick-walled, echinate and with long furrows. These progressed gradually to a thin-walled, smooth form with short furrows, accompanied by a tendency toward increased grain size.

At the fine structural level, it was postulated (Skvarla and Larson, 1965a) that the advance was from pollen grains with a weakly developed cavus, long spines, single-layered columellae and abundant internal foramina, to pollen grains which are more distinctly caveate, with the beginnings of an internal tectum. This line, in turn, gave rise to the multiple-layered exines, with or without internal foramina.

Wagenitz (1955) outlined a detailed system in which he presented both surface features and wall patterns depicting the phylogenetic relationships within 350 species of Centaurea (Cynareae). The basis for this system is a spherical, non-caveate spiny exine type which is predominant throughout the genus. From this, pollen morphology radiated in three directions: (1) retention of the non-caveate wall pattern, with a reduction in spines and with the formation of an ellipsoidal shape; (2) retention of a few columellae, thus establishing a cavus with interspersed columellae, and from thence to either a caveate type which is subspinulose or to a caveate form which has no spines, both of which are ellipsoidal; (3) retention of a few columellae interspersed throughout the caveate region, with a reduction in length of spines, but with the addition of small wart-like structures between the spines. In this series the progression is from a short colpus to a long one, and from a wide pore with lateral

extensions to a narrow pore with lateral extensions. It is to be noted that while the essential evolutionary steps were considered to be reductions, i.e., in spine length and in number of columellae, it was admitted that all the "progressions" could also be in the opposite direction.

In the Mutisieae Wodehouse (1929) suggested that short furrows and a spinose exine were primitive. Carlquist (1957b) questioned this from evidence that most of the genera he had studied had very long furrows. He also found that both long and short furrows occurred in both putatively primitive and advanced Mutisieae, and questioned the phylogenetic importance of this character. He, similarly, questioned the reliability of spine reduction as a phylogenetic indicator since, while the Mutisieae are mostly spinose, reduction to the spineless condition may occur within a single genus.

Of further interest is the presence in this tribe of a two-layered ektexine. To Carlquist (1957b) it seemed apparent that the types of exine stratification found in primitive Heliantheae and Mutisieae represented two lines of development. Electron microscopy (Skvarla and Larson, 1965a) has demonstrated the presence of this two-layered ektexine in Parthenice mollis Gray. This taxon was also noted as having the greatest structural variation in the essentially palynologically uniform tribe Heliantheae.

Studies with other families (Punt and Leenhouts, 1967; Smit and Punt, 1969) pointed out possible evolutionary trends involving types of

reduction. They suggested that such trends (i.e., reduction) are not necessarily correlated with genera or species. For example, a specific reduction may occur within certain members, but not all members, of a taxon. There have been, then, various interpretations of the significance of palynology in phylogeny.

Relationship of these Studies to the Inuleae

In the above schematic proposals, possible evolution is from very long spines to none. This character can be easily correlated with the present study (refer to key). The contrasting interpretation, however, relative to the position of the short or long colpus, makes it difficult to suggest any correlation of this character in the present study, since total colpus variation in the Inuleae is from very long to very reduced.

The Helianthoid wall pattern is found in many of the genera of the Buphthalmeae (6-A and 6-B) with the exception that in the majority of these types the internal foramina appear to be absent. This same Helianth-pattern is found throughout other subtribes within the Inuleae. Progression through the development of discontinuous layers of internal tecta would include type 6-C, and formation of distinctive double layers of columellae can be seen in types 6-D and 6-E. In accord with this is a tendency for the development of elongate internal foramina.

The presence of a spineless, caveate type is considered by Wagenitz (1955) to be most advanced in two of his lines of development,

although he admitted that different phylogenetic postulations could have been made, one of which would have progressed from the caveate, spineless type in the opposite direction. It is notable that both types are present in the Inuleae.

The presence or absence of caveae and internal foramina are difficult to assess. It is also difficult to postulate whether the adherence of the columellae-foot layer and internal foramina presence are signs of reduction or developments that have not yet occurred. Nonetheless, if the Helianth type, as found in the Buphthalmeae, is primitive, and assuming that types 6-D and 6-E represent progressions, it can readily be seen (from checking the key) that the progressions arise in different subtribes and genera. This substantiates Cronquist's (1955a) hypothesis that striking parallel features develop in the Compositae in diverse species, genera, and tribes.

Phylogenetic Studies Based on Other Characters

By the use of floral characteristics Cronquist (1955a) outlined a phyletic scheme wherein he concluded that the Heliantheae come the nearest to matching the hypothetical progenitor of the Compositae. Using the Heliantheae as a base, he placed the Inuleae next to the Heliantheae, along with the Astereae, the Senecioneae, and the Anthemideae, inferring, in essence, that the Inuleae has its closest morphological affinities with the Heliantheae, and that each of the four tribes: Anthemideae, Astereae,

Senecioneae, and Inuleae, in fact, seem to be related to each other only through the Heliantheae--each presenting different groups or series of phyletic advances.

Specific advances noted with reference to the Inuleae were: (1) the inuleous style is derivable from the primitive heliantheous type; (2) the Inuleae and Senecioneae have similar forms of style-branches; (3) elongation of the tube of the ray corolla marks genera or groups of genera in the Astereae, Inuleae and Senecioneae; and (4) both the Inuleae and Anthemideae appear to have inherited the chaffy receptacles of their more primitive members from the Heliantheae.

Other generalized relationships given were:

1. The Inuleae are related through the inuleous subtribe Bupthalmeae, and an individual taxon which combined all the primitive characters found in the Inuleae would scarcely be separable from the Heliantheae. The similarity of Anisopappus africanus (Bupthalmeae) to some species of Verbesina (Heliantheae) was given as an example.

2. There is sometimes a strong similarity in habit and general structure of the heads between members of the Inuleae-Plucheineae and genera of the Conyza-Baccharis group of the Astereae, due either to a close relationship between the genera of the two tribes or to parallelism.

Carlquist's (1960) preliminary observations of the position of the Inuleae was that it did not seem to be a natural group. From studies of wood anatomy, however, he made generalizations that suggested that

many inuloid genera have affinities to the Vernonieae and are thus referable to that portion of the family which includes Vernonieae, Eupatorieae, Mutisieae, Cynareae and Cichorieae. He also cited common floral characteristics within these tribes. Nevertheless, he concluded that individual genera in the Inuleae may have affinities elsewhere, and suggested opportunities for study of phylogenetic problems in Inuleae. He concluded that until such problems have been given a satisfactory solution, one cannot speak with any certainty about the relationships of the Inuleae or even of the limits of the tribe itself.

Turner (1970) reported in a cytotaxonomic study that whatever the explanation for the base numbers, it is clear that there exists a wide assemblage of karyotypes in the Inuleae.

Phylogenetic Relationships of the Inuleae

The wide variety of surface characteristics of Inuleae pollen has already been pointed out. There is evidence of the presence of the Helianth surface, as well as similarities to the Anthemideae, the Senecioneae, the Astereae, the Ambrosieae, and the Mutisieae, for there is a multiplicity of spine and furrow lengths, in both the caveate and the non-caveate grains.

However, it is significant to point out that phylogenetic characters at the light microscope level are not easily correlated with those at the electron microscope level. Although both types of characters must be

assumed to be influenced by environmental factors, polyploidy, chromosome number, etc., it seems obvious that the least amount of variation is apparent in the wall fine structure, and, consequently, that wall patterns are more significant to the determination of phylogenetic relationships.

Conclusions

Carlquist's (1960) phylogenetic suggestions are borne out in this study only in recognition of pollen wall forms similar to those of the Mutisieae.

The present study relates much more concretely to the hypothesis formulated by Cronquist (1955a). There are many wall patterns similar to those depicted for the Heliantheae, yet there are representative patterns of the other closely related tribes, as well as wall patterns that may be considered unique to the Inuleae.

The wide range of variability in this tribe, however, as opposed to the great palynological uniformity in some of the other tribes, provokes questions relative to a monophyletic origin of the Compositae. It seems plausible that there might either have been more than one ancestral type, from which this variety of characteristics arose in a direct line, or that the present types might have arisen, through introgression, from a combination of ancestral types. Answers to these questions must await more extensive analysis of the many tribes of the Compositae.

CHAPTER V

CONCLUSIONS AND SUMMARY

1. A detailed survey of 132 genera and 266 species of the tribe Inuleae by light and electron microscopy has revealed an impressive assortment of pollen characters.

2. These characters have been used in an attempt to broadly delineate the pollen morphology of this tribe, which, heretofore, has been little studied.

3. In contrast to other tribes which are generally characterized as possessing a fairly homogeneous pollen morphology, Inuleae pollen exhibits a wide diversity, and includes pollen types found in most other composite tribes.

4. With the exception of the Tarchonantheae, all subtribes have a variety of pollen types.

5. In contrast to the great variability at the light microscope level, fewer patterns are noted by electron microscopy.

6. This study suggests that the Inuleae have their closest pollen affinities with the Ambrosieae, Astereae, Senecioneae, and Heliantheae, and to a lesser degree with the Anthemideae.

LITERATURE CITED

Battaglia, E. 1946. Ricerche cariologiche e embriologiche in genere Rudbeckia (Astereae). Nuov. Giorn. Bot. Ital. 53: 1-69.

Bell, C. R. 1959. Mineral nutrition and flower pollen size variation. Am. J. Bot. 46: 621-624.

Bentham, G. 1873. Notes on the classification, history and geographical distribution of Compositae. J. Linn. Soc. Bot. 13: 335-557.

_____, and J. D. Hooker. 1873. Genera Plantarum 2: 166-533. London.

Bragg, L. H., and C. McMillan. 1962. Morpho-geography of four grass taxa in Texas. Amer. Midl. Nat. 67: 321-333.

Carlquist, S. 1957a. The genus Fitchia (Compositae). Univ. Calif. Publ. Bot. 29: 1-144.

_____. 1957b. Anatomy of Guayana Mutisieae. Mem. N. Y. Bot. Gard. 9: 441-476.

_____. 1961. Wood anatomy of Inuleae (Compositae). Aliso 5: 21-37.

_____. 1966. Wood anatomy of Compositae: a summary, with comments on factors controlling wood evolution. Aliso 6: 25-44.

_____, and M. Grant. 1963. Studies in Fitchia (Compositae): Novelties from the Society Islands; anatomical studies. Pacific Science 17: 282-298.

Cronquist, A. 1955a. Phylogeny and taxonomy of the Compositae. Am. Midl. Nat. 53: 478-551.

_____. 1955b. Compositae. In: C. L. Hitchcock, A. Cronquist, M. Ownbey, and J. W. Thompson, Vascular Plants of the Pacific Northwest. Univ. of Washington Publ. Biol. 17: 1-343.

Clausen, K. E. 1960. A survey of variations in pollen size within individual plants and catkins of three taxa of Betula. Pollen et Spores 2: 299-304.

_____. 1962. Size variation in pollen of three taxa of Betula. Pollen et Spores 4: 169-174.

Cushing, E. J. 1961. Size increases in pollen grains mounted in thin slides. Pollen et Spores 3 : 265-274.

Dahl, A. O. 1952. The comparative morphology of the Icacinaceae. VI. The pollen. Jour. Arnold Arb. 32: 252-295.

deDalle Torre, C. G., and H. Harms. 1907. Embryophyta Siphonogama. Berlin.

Drury, D. G., and L. Watson. 1966. Taxonomic implications of a comparative anatomical study of Inuloideae--Compositae. Am. J. Bot. 53: 828-833.

Duigan, S. L. 1961. Studies of the pollen grains native to Victoria, Australia. Royal Soc. Victoria, Proc. 74: 89-109.

Ehrlich, Paul R., and R. W. Holm. 1963. The process of evolution. McGraw-Hill, New York.

Erdtman, G. 1952. Pollen morphology and plant taxonomy. I. Angiosperms. Chronica Botanica, Waltham, Massachusetts.

_____. 1960. The acetolysis method. A revised description. Svensk Bot. Tidskr. 54: 561-564.

_____. 1964. Palynology, pp. 23-54. In Turrill, W. B. (ed.) Vistas in botany. McMillan Co., New York.

Faegri, K. 1956. Recent trends in palynology. Bot. Rev. 22: 639-664.

_____, and J. Iversen. 1964. Textbook of modern pollen analysis. Hafner Publ. Co., New York.

Fischer, Hugo. 1890. Beitrage zur vergleichenden Morphologia der Pollen-korener, p. 72. Berlin.

Gifford, K. L., and D. A. Larson. 1970. Effects of polyploidy on pollen grain diameter and other exomorphic exine features in

Tridax coronipfolia. Pollen et Spores 11: 203-221.

Gould, F. W. 1957. Pollen size as related to polyploidy and speciation in Andropogon saccharoides. A. barbinoides complex. Brittonia 9: 71-75.

Graham, A., S. A. Graham, and D. Geer. 1968. Palynology and systematics of Cuphea (Lythraceae). I. Morphology and ultrastructure of the pollen wall. Am. J. Bot. 55: 1080-1088.

Heslop-Harrison, J. 1969. Scanning electron microscope observations on the wall of the pollen grain of Cosmos bipinnatus Compositae. pp. 89 96. In Proc. 2nd Stereoscan Colloquium. Engis Equipment Co., Merton Grove, Ill.

Hoffman, O. 1897. Compositae. In Engler and Prantl. Nat. Pflanzenf. 4: 87-387.

Humbert, H. 1923. Les Composees de Madagascar. E. Lanier. Caen.

Iversen, J., and J. Troels-Smith. 1950. Pollenmorfologiske Definitioner og Typer. Danmarks geol. Unders. 4. 4k. 3,8.

King, R. M., and H. Robinson. 1967. Multiple pollen forms in two species of the genus Stevia (Compositae) SIDA. 3: 165-169.

Kurtz, E. B., and J. L. Liverman. 1958. Some effects of temperature on pollen characts. Bull. Torrey Club 85: 136-138.

Larson, D. A. 1964. Processing pollen and spore exines for electron microscopy. Stain Tech. 39: 237-243.

Leins, P. 1969. Versuch einer Gliederung der Inulinae and Buphthalminae nach der Pollenkorntypen. Ber. Dtsch. Bot. Ges. Bd. 81: 498-504.

Pausinger-Frankenburg, F. 1951. Vom Blutenstaub der Wegwarten. (Die Pollengestaltung der Cichorieae). Carinthia II. 13: 3-47.

Peachey, L. D. 1958. Thin sections. I. A study of section thickness and physical distortion produced during microtomy. J. Biophys. Biochem. Cytol. 4: 233-243.

Powell, A. M. 1965. Taxonomy of Tridax (Compositae). Brittonia 17: 47-96.

Punt, W., and P. W. Leenhouts. 1967. Pollen morphology and taxonomy in the Loganiaceae. Grana Palyn. 7: 369-516.

Ridgway, J. E., and J. J. Skvarla. 1969. Scanning electron microscopy as an aid to pollen taxonomy. Ann. Mo. Bot. Gard. 56: 121-124.

Skvarla, J. J. 1966. Techniques of pollen and electron microscopy. Part I. Staining, dehydration and embedding. Okla. Geol. Notes 26: 179-186.

_____, and A. G. Kelley. 1968. Rapid preparation of pollen and spore exines for electron microscopy. Stain Tech. 43: 139-144.

_____, and D. A. Larson. 1965a. An electron microscope study of pollen morphology in the Compositae with special reference to the Ambrosieae. Grana Palyn. 6: 210-169.

_____, and _____. 1965b. Interbedded exine components in some Compositae. Southwestern Naturalist 10: 65-68.

_____, and C. C. Pyle. 1968. Techniques of pollen and spore electron microscopy. Part II. Ultramicrotomy and associated techniques. Grana Palyn. 8: 255-270.

_____, and B. L. Turner. 1966a. Systematic implications from electron microscopic studies of Compositae pollen--a review. Ann. Mo. Bot. Gard. 53: 220-256.

_____, and _____. 1966b. Pollen wall ultrastructure and its bearing on the systematic position of Blennosperma and Crocidium (Compositae). Am. J. Bot. 53: 555-563.

_____, and _____. 1969. Fine structure of Petrobinae (Compositae-Heliantheae) pollen walls. Am. J. Bot. 56: 418-419.

Stebbins, G. L. 1950. Variation and evolution in plants. Columbia Univ. Press. New York.

Stix, E. 1960. Pollenmorphologische untersuchungen an Compositen. Grana Palyn. 2: 41-114.

Stuchlik, L. 1969. Pollen morphology in the Polemoniaceae. Grana Palyn. 7: 146-240.

Smit, P. G., and W. Punt. 1969. Taxonomy and pollen morphology of the Caltha leptosepala complex. Proc. Roy. Neth. Acad. Sci. Ser. 72: 16-27.

Turner, B. L. 1970. Chromosome numbers in the Compositae. XII. Australian species. Am. J. Bot. 57: 382-389.

Venable, J. H., and R. Coggeshall. 1965. A simplified lead citrate stain for use in electron microscopy. J. Cell Biol. 24: 407.

Wagenitz, G. 1955. Pollen morphologie und Systematik in der Gattung Centaurea L. s. l. Flora 142: 213-279.

Weber, W. A. 1946. A taxonomic and cytological study of the genus Wyethia, etc. Am. Midl. Nat. 35: 400-452.

Willis, J. C. 1957. A dictionary of the flowering plants and ferns. Sixth edition. Cambridge Univ. Press.

_____. 1966. A dictionary of the flowering plants and ferns. Seventh edition. Revised by H. K. Airy Shaw. Cambridge Univ. Press.

Wilson, L. R., and G. J. Goodman. 1964. Techniques of palynology--Part II. Microscope-slide preparation of modern spores and pollen. Okla. Geol. Notes 24: 277-280.

Wodehouse, R. P. 1928. The phylogenetic value of pollen-grain characters. Ann. Bot. 42: 891-934.

_____. 1929. Pollen grains in the identification and classification of plants. IV. The Mutisieae. Am. J. Bot. 16: 297-313.

_____. 1935. Pollen grains. McGraw Hill. New York.

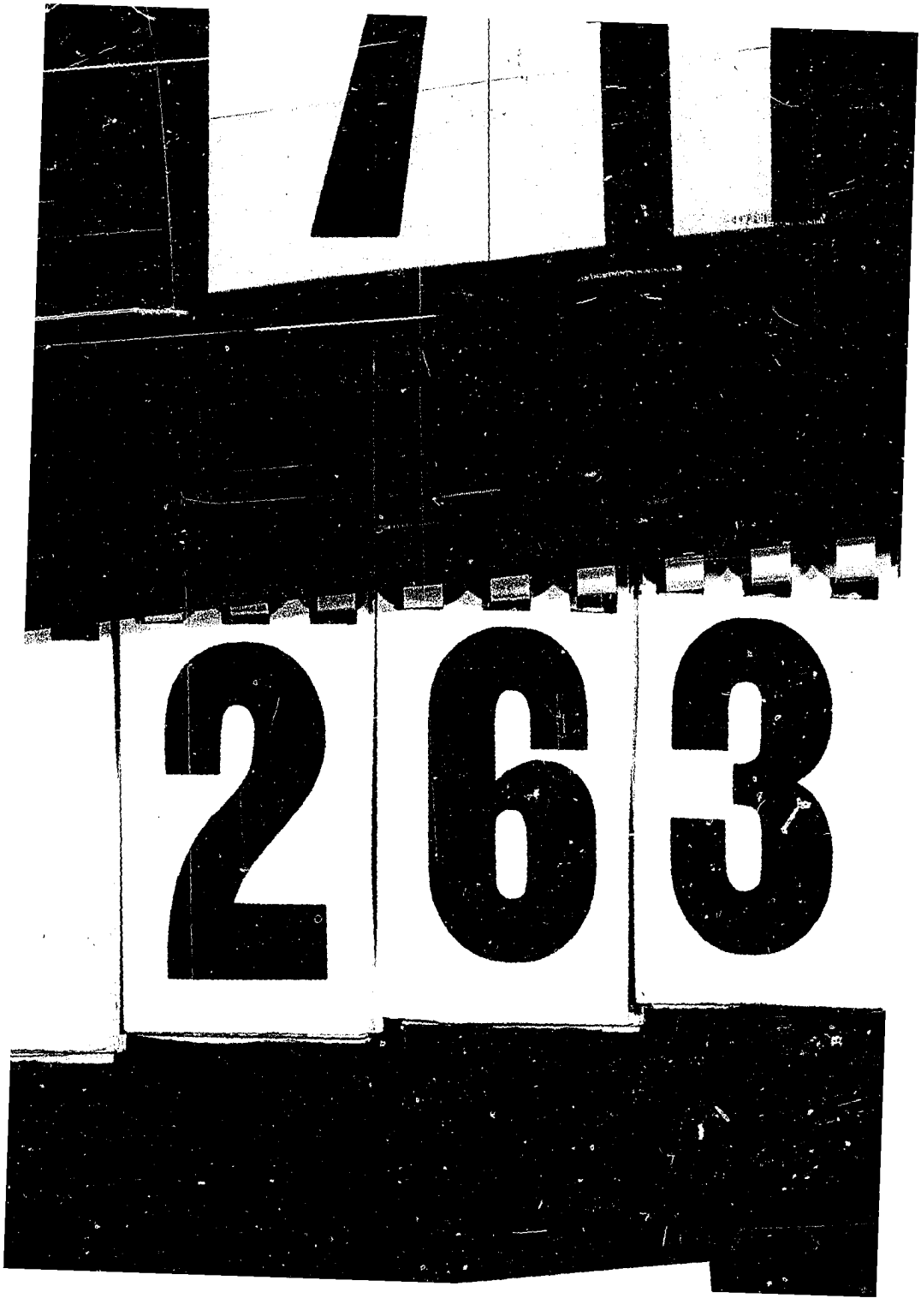
263



